universität wien

MASTERARBEIT | MASTER'S THESIS

Titel | Title

Tailor-made Ubiquitin Chains

verfasst von | submitted by

Dominik Appel BSc

angestrebter akademischer Grad | in partial fulfilment of the requirements for the degree of

Master of Science (MSc)

Wien | Vienna, 2024

Studienkennzahl lt. Studienblatt | Degree programme code as it appears on the student record sheet:	UA 066 862
Studienrichtung lt. Studienblatt | Degree programme as it appears on the student record sheet:	Masterstudium Chemie
Betreut von | Supervisor:	Univ.-Prof. Dr. Christian Friedrich Wilhelm Becker

Acknowledgement

I want to thank Professor Christian Becker for giving me the opportunity to participate in his research group. As well as his support and supervision during my master's thesis.

I would also like to thank my supervisor Dr. Susanne Huhmann, who taught me the relevant molecular biology methods and practical aspects needed for my thesis and always had an open ear for questions during my research.

I extend my appreciation to everybody at the Becker group for their tips and lunchbreaks.

As last I want to thank my family and friends for their support during my studies.

Abstract

Ubiquitin is a small, highly conserved protein that plays a crucial role in a variety of cellular processes by tagging other proteins for degradation. Composed of 76 amino acids, ubiquitin is found in all eukaryotic cells. The process of ubiquitylation involves the attachment of one or more ubiquitin molecules to a substrate protein, marking it for recognition by the proteasome, a large protein complex responsible for degrading unneeded or damaged proteins. Since ubiquitin itself has 8 possible reaction sites for ubiquitylation, there are many possible poly-ubiquitin chains with different functions. The (patho-)physiological role of ubiquitin chains is not completely understood yet. The aim of this master's thesis was to generate different ubiquitin mutants containing a Cys instead of Lys at the following positions: K11, K29, K48, K63 and with C-terminal modifications that allow to form covalent bonds between ubiquitin and target proteins. The latter was achieved by using ubiquitin-intein fusion constructs. To provide greater synthetic flexibility, the free thiol group of the ubiquitin mutants were transiently protected with phenacyl. During this work the removal conditions for phenacyl were improved. By thiol-ene coupling between the thiols in Cys mutants and C-terminal allylamide modifications of Ub, a series of diubiquitins with different likage types and selected tri- and tetraubiquitins were generated.

Zusammenfassung

Ubiquitin ist ein kleines, hochkonserviertes Protein, das bei einer Vielzahl von zellulären Prozessen eine entscheidende Rolle spielt, indem es andere Proteine zum Abbau markiert. Ubiquitin besteht aus 76 Aminosäuren und ist in allen eukaryontischen Zellen zu finden. Bei der Ubiquitylierung werden ein oder mehrere Ubiquitinmoleküle an ein Substratprotein angehängt, um es für die Erkennung durch das Proteasom zu markieren, einen großen Proteinkomplex, der für den Abbau nicht benötigter oder beschädigter Proteine zuständig ist. Da Ubiquitin selbst 8 mögliche Reaktionsstellen für die Ubiquitylierung hat, gibt es viele mögliche Poly-Ubiquitin-Ketten mit unterschiedlichen Funktionen. Die (patho-)physiologische Rolle von Ubiquitin-Ketten ist noch nicht vollständig geklärt. Ziel dieser Masterarbeit war es, verschiedene Ubiquitin-Mutanten zu erzeugen, die an den folgenden Positionen ein Cys anstelle von Lys enthalten: K11, K29, K48, K63 und mit C-terminalen Modifikationen, die die Bildung kovalenter Bindungen zwischen Ubiquitin und Zielproteinen ermöglichen. Letzteres wurde durch die Verwendung von Ubiquitin-Intein-Fusionskonstrukten erreicht. Um eine größere synthetische Flexibilität zu erreichen, wurde die freie Thiolgruppe der Ubiquitinmutanten vorübergehend mit Phenacyl geschützt. Während dieser Arbeit wurden die Bedingungen für die Entfernung von Phenacyl verbessert. Durch Thiol-Ene-Kopplung zwischen den Thiolen in den Cys-Mutanten und C-terminalen Allylaminde-Modifikationen von Ub wurden eine Reihe von Diubiquitinen mit unterschiedlichen Lagen und ausgewählte Tri- und Tetraubiquitine erzeugt.

List of abbreviations

AA	Allylamide
ACN	Acetonitrile
APS	Ammonium persulfate
AMP	Ampicillin
CAM	Chloramphenicol
CBD	Chitin binding domain
DTT	Dithiothreitol
DI	Direct injection
E. coli	Escherichia coli
ESI-MS	Electrospray Ionisation – mass spectrometry
IPTG	Isopropyl β-D-1-thiogalactopyranoside
KxC	Lysine to cysteine mutation at position x
LAP	Lithium phenyl-2,4,6 trimethylbenzoylphosphinate
MESNa	2-Mercaptoethane sulfonate
MPAA	4-Mercaptophenylacetic acid
NaOAc	Sodium acetate
NCL	Native chemical ligation
PAc	Phenacyl
PAGE	Polyacrylamide gel electrophoresis
PBS	Phosphate-buffered saline
PTM	Post-translational modification
RP-HPLC	Reverses phase – High performance liquid chromatography
SDS	Sodium dodecyl sulfate
SPPS	Solid phase peptide synthesis
TCEP	Tris(2-carboxyethyl)phosphine
TEMED	Tetramethylethylendiamine
TFA	Trifluoroacetic acid
TBS	Tris-buffered saline
Tris	Tris(hydroxymethyl)aminomethane
Ub	Ubiquitin
Wt	Wildtype

Table of contents

Table of contents

1. Introduction

Proteins, in their native or modified form, play an important role in many cellular processes. Examples for modifications are post-translational modifications (PTMs) such as phosphorylation, acetylation, methylation, glycosylation and ubiquitylation which can significantly change the properties of the original proteins in terms of structure and function.[1]

Ubiquitylation is one of the best studied PTMs which regulates important cellular processes. The development of diseases such as neurodegeneration, immune disorders and cancer are connected to dysfunction in ubiquitin signalling.[2,3]

1.1 Ubiquitin

Ubiquitin consists of 76 amino acids and occurs ubiquitously in cells. The exact sequence is highly conserved.[4] In ubiquitylation, ubiquitin or a polyubiquitin chain is attached to a Lys or the N-terminus of a substrate protein by the means of three enzymes (E1, E2 and E3) via the C-terminal glycine, thereby acting as a versatile signal regulating protein-based communication in and between eukaryotic cells. It is assumed that this system contains over 1000 proteins in the human body.[5] Namely 2 E1s (activating), 30-49 E2s (conjugating) and >600 E3s (ligating) are encoded in the human genome, leading to a large number of combinatorial possibilities.[4] During ubiquitylation, ubiquitin is first activated at the C-terminal glycine by E1 as a thioester intermediate to a cysteine of the enzyme. This step consumes ATP. Ubiquitin is then transferred to an E2 ubiquitin-conjugating enzyme as a further thioester-intermediate and finally an isopeptide bond between the C-terminus of the glycine and an ε-amine of a Lys of the substrate protein is catalyzed via an E3 ligase (Figure *1*).[6] Nowadays, ubiquitylation is mainly studied in relation to the ubiquitin proteasome system (UPS), where it is significantly involved in the degradation of proteins by 26S proteasomes. However, recent studies have shown that there are also non-proteolytic signals that play a role in chromatin remodeling, DNA repair, protein homeostasis, cell cycle control and viral infections.[7,8,9,10]

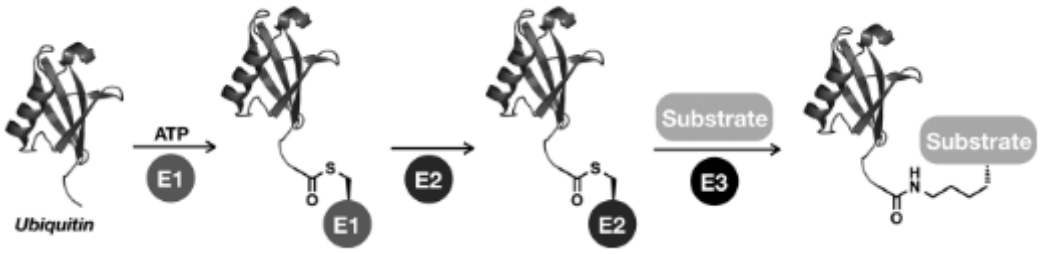

Figure 1 Enzymatic pathway of ubiquityation. (retrieved from[6])

Since ubiquitin itself can be ubiquitylated at seven lysines (K6, K11, K27, K29, K33, K48, K63) and the N-terminus via the above-mentioned process, a large number of possible products exist. Furthermore, ubiquitin can be additionally modified with other PTMs such as Ub-like proteins (UBIs), acetylation and phosphorylation[11,12] - the first ubiquitylated protein to be discovered was the histone protein H2A.[13]

It is now known that a different number and linkage of individual ubiquitins within a chain has a different cellular effect. A principal distinction is made between homotypic and heterotypic

chains (mixed or branched). In homotypic chains, one linkage is dominant in the connection of the individual ubiquitins.[14] Mono-ubiquitylation is associated with DNA repair, receptor endocytosis and regulation of neuronal proteins.[15] K48-linked homotypic chains act in conjunction with the ubiquitin proteasome system (UPS) in the proteosomal degradation of proteins.[16] K63-linked chains are associated with non-proteolytic functions like NF-κB6 signaling, DNA damage response and protein kinase activation.[17,18] Heterotypic chains are more focused on controlling cellular processes but have also been implicated to play a part in the degradation of aggregation-prone proteins.[19,20,21] K11/K48-, K29/K48-, K48/K63- and M1/K63-branched conjugates are each associated with a different cellular function.[20] The complexity is further increased by so-called hybrid chains such as Ub-SUMO (small ubiquitin modifier), where a ubiquitin-like modifier is linked to ubiquitin.[14]

Despite all efforts to date, the physiological role of most ubiquitin chains is still poorly understood, since generating homogeneous Ub based conjugates in high purity and large quantities is a major challenge.[14,22]

The methods used so far to obtain ubiquitin chains or conjugates work by the means of enzyme-based systems, transpeptidation and total chemical synthesis. In the enzymatic synthesis of ubiquitin, the availability of E2/E3 enzymes represents a major challenge, since these are not yet known for all possible chains and substrate proteins. Furthermore, it is difficult to control the length and exact position on the target protein of the obtained chain.[22]

Recent developments in chemical protein synthesis and semisynthesis have helped to overcome some of the challenges with enzymatic synthesis and one can now generate Ub conjugates with almost complete control over its molecular structure. These improvements contribute to a better understanding of Ub signaling at the molecular level.[23]

1.2 Strategies to modify Ub

1.2.1 SPPS

Solid Phase Peptide Synthesis (SPPS) is a technique for the chemical synthesis of peptides, which was introduced by Merrifield in 1963.[24] In this method, the C-terminal amino acid of the desired target protein is covalently linked to an insoluble polymer. The N-terminal protecting group of this amino acid is then removed, the polymer is washed and the next amino acid of the sequence is linked in protected form. After linking, the polymer is washed again and the procedure is repeated until the desired peptide is formed. Finally, all remaining protective groups and the linkage to the polymer are dissolved to obtain the crude peptide product. The advantage of this method is that the solid phase simplifies purification after each synthesis step. This makes it possible to use a significant excess of activated amino acid, which allows the reactions to proceed quickly and almost quantitatively. Furthermore, handling losses are minimized. For this reason, it is possible to obtain peptides up to 50 amino acids in high yields.[25]

1.2.2 NCL

Native chemical ligation (NCL) is a method to efficiently and chemoselectively link unprotected peptides. Therefore, it is possible to incorporate non-proteinogenic amino acids, post-translational modifications and non-proteinogenic modifications such as fluorescent tags or NMR tags into proteins. For the coupling reaction, one peptide fragment must be present as a C-terminal thioester and the other with an N-terminal cysteine. Under aqueous conditions with a chaotropic salt (e.g. guanidine) and at neutral pH, trans-thioesterification first takes place by the nucleophilic thiol of the Cys attacking the carbonyl group of the thioester and forming an intermolecular thioester intermediate. This intermediate is then rearranged by an S-N acyl shift in which the terminal amine of the thioester attacks the newly formed thioester and forms a native amide bond (Figure 2).[26]

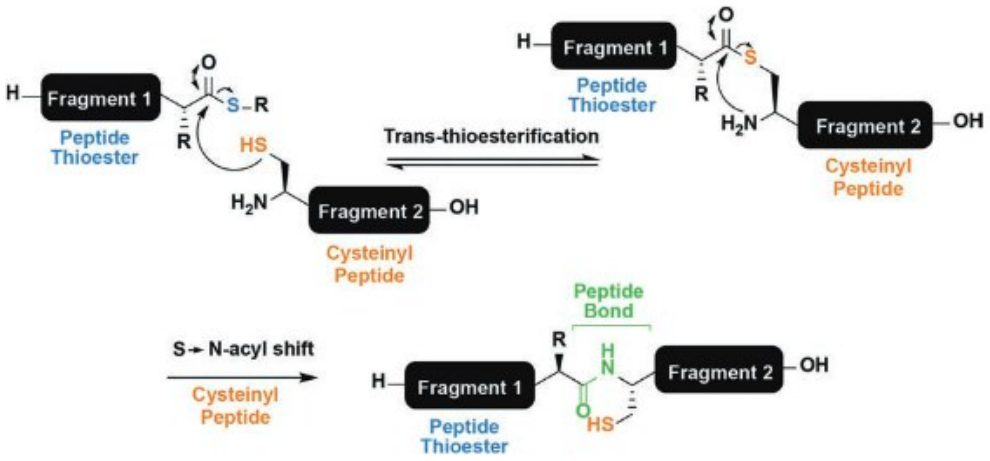

Figure 2 Reaction scheme for NCL (retrieved from[26]).

Expressed protein ligation (EPL) is an extension of NCL in which recombinantly expressed polypeptide fragments are used for ligation.[26]

1.2.3 Expression in E. coli

Expression of recombinant proteins has made a significant contribution to increase the number of accessible proteins for biochemical and structural experiments. As a result, the method has revolutionized many aspects of the biological sciences. This is due to the fact that expression in hosts is simple, fast, inexpensive and robust. Furthermore, it is possible for the desired protein to make up to 50 % of the total cellular protein. Due to these advantages and newly developed protein purification techniques, 31 recombinant proteins were approved as therapeutics in biopharmaceutical research between 2003 and 2006. Although other, non-bacterial expression systems have been researched over the last 30 years, E. coli is still preferred because it is easy to genetically manipulate and expression is particularly quickly.[27]

Despite all the advantages mentioned so far, expression in E. coli also has disadvantages. Due to the particular speed and the lack of chaperones, it is possible for proteins to end up unfolded or misfolded. Furthermore, E. coli cannot carry out some eukaryotic posttranslational modifications and the highly reductive environment in the cytosol of the bacterium can result in insoluble proteins which accumulate in inclusion bodies.[28] Due to new strategies, some of these problems have now been solved for a large number of proteins. In addition, protocols for

the isotopic labeling of proteins for NMR spectroscopy and the incorporation of selenomethionine for X-ray crystallography are currently available. It is also possible to co-express chaperones with the desired protein.[27]

Depending on the protein of interest, it is important to choose an appropriate strategy. If it's planned to yield antibodies against a recombinant protein, it is not necessary to express it in soluble form, since the sequence and not the fold is relevant.[29] For this reason, expression and accumulation in inclusion bodies is even proposed here in order to protect them from proteases.[30]

The basic requirements for the expression of proteins in E. coli are the desired protein, a bacterial expression vector, an expression cell line and the necessary materials and equipment for cell culture.[27]

Some heterologous proteins cannot be expressed in E. coli due to a higher rate of "rare" codons in the target mRNA. These codons are rare in E. coli but occur more frequently in human proteins.[31] If proteins with a higher number of rare codons are expressed, these genes may be mistranslated and lysine may be inserted instead of arginine.[32] Nowadays, this problem can easily be overcome with online tools such as the rare codon calculator, RaCC (http://nihserver.mbi.ucla.edu/RACC/). To express a target protein with an increased number of rare codons, either the gene can be "codon optimized" by site-directed mutagenesis by adapting the codon to E. coli, or an already "codon-optimized" gene can be purchased. The latter has the advantage that the mRNA secondary structure is also optimized, which has a positive effect on translation efficiency.[33] It is also possible to co-express the genes encoding the rare tRNAs with the wild-type target gene.[34] Today, E. coli strains already are available which contain plasmids coding for rare tRNAs such as BL21 (DE3)-RIL/RP/RILP cells from Stratagene or Rosetta cells from Novagen.[27,35]

1.3 Building PolyUb Chains

Various strategies generate Ub chains via either native or non-native isopeptide bonds.[14]

1.3.1 Enzyme-mediated coupling (native)

Early methods to obtain polyubiquitin chains with native linkage are based on the use of enzymes E1-E3, similar to the natural mechanism of UPS. The availability of conjugating enzymes specific for a particular linkage is crucial for enzyme-mediated coupling of ubiquitin. Those enzymes are not available for every possible ubiquitin chain.[36] In some cases, linkage in vitro is possible without E3.[37]

1.3.2 Chemical Strategies for Protein Ubiquityation

Various chemical strategies have been described in literature for selectively coupling a ubiquitin to a target protein using isopeptide linkage. These methods include glycyl-auxiliary strategy, δ-mercaptolysin strategy and orthogonal protection with SPPS isopeptide bond construction.[38]

1.3.2.1 Glycyl-auxiliary strategy

In this strategy, a photo-cleavable thiol-containing glycyl auxiliary is introduced as an orthogonal protection group of a lysin from the substrate protein in SPPS (section 1.2.1). After subsequent NCL with a Ub (1-75) thioester and selective removal of the auxiliary from the protein photolytically, the desired ubiquitinated protein is generated. In the product, the Gly linker between the auxiliary and Lys serves as Gly 76 of the Ub. (Figure 3) [38,39]

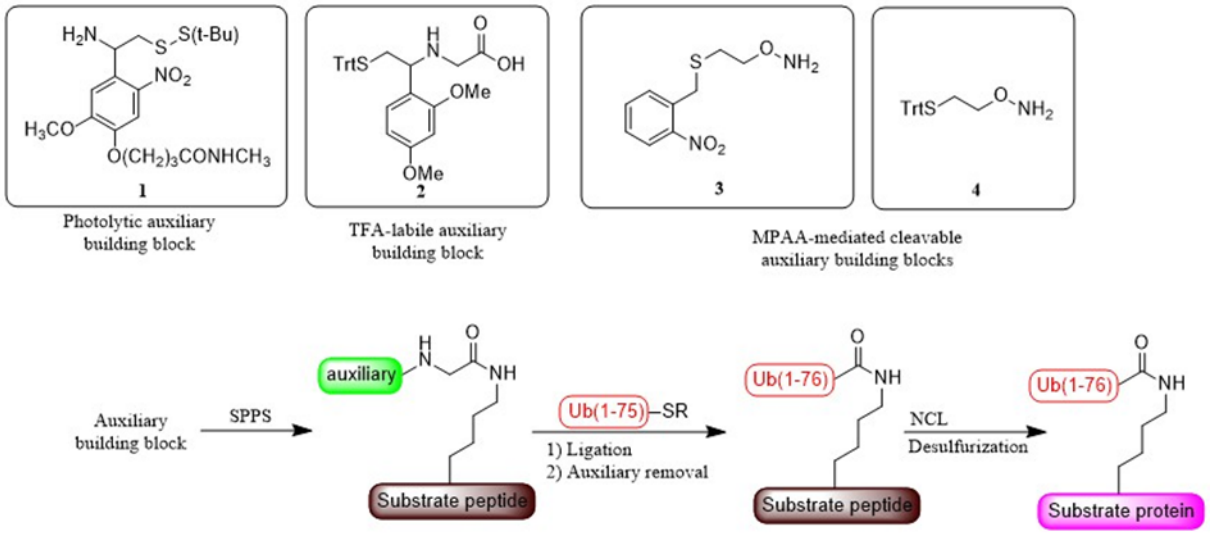

Figure 3 Reaction scheme of Glycyl-auxiliary strategy (based on[38]).

Since cleavage of the auxiliary is crucial to prevent undesirable modifications in this method, various strategies have been developed to carry out this cleavage under mild conditions. Photolytic cleavages are of great importance here, as they do not damage the peptide backbone or side chains.[38] This strategy has also been used to release proteins in living cells for functional control.[40] Furthermore, ubiquitinated proteins with native isopeptide binding[41], as well as a full-length H2B-K120Ub have been successfully generated.[42]

By using 2-(aminooxy)-ethanethiol as an auxiliary, this strategy could be further improved to achieve ubiquitinated peptides and sumoylated histones H4 and H2B.[43,44] This auxiliary can be removed by 4-mercaptophenylacetic acid (MPAA) and used under denaturing and folding conditions, allowing it to be used with cysteine-containing natively folded proteins.[38] Since the glycyl-auxiliary strategy does not require a desulfurization step to form a native isopeptide bond, the preservation of cysteine side chains with a thiol group provides greater flexibility to selectively modify the resulting protein, e.g. with fluorophores.[45]

Recently, a series of poly-Ub conjugates such as DiUb, TriUb and TetraUb chains could be generated using a TFA-labile auxiliary.[46,47] The method can also be used for the generation of specifically phosphorylated ubiquitin chains and mono- and diubiquitylation of histones which are modified at Lys.[48]

1.3.2.2 δ-Mercaptolysine strategy

In this strategy, δ-mercaptolysine, a cysteine-like system, is generated directly at the δ-carbon of a Lys side chain and subsequently linked to a Ub thioester by isopeptide chemical ligation[49] (ICL, Figure 4) After free radical desulfurization[50], native Ub conjugates with peptides and proteins are obtained.

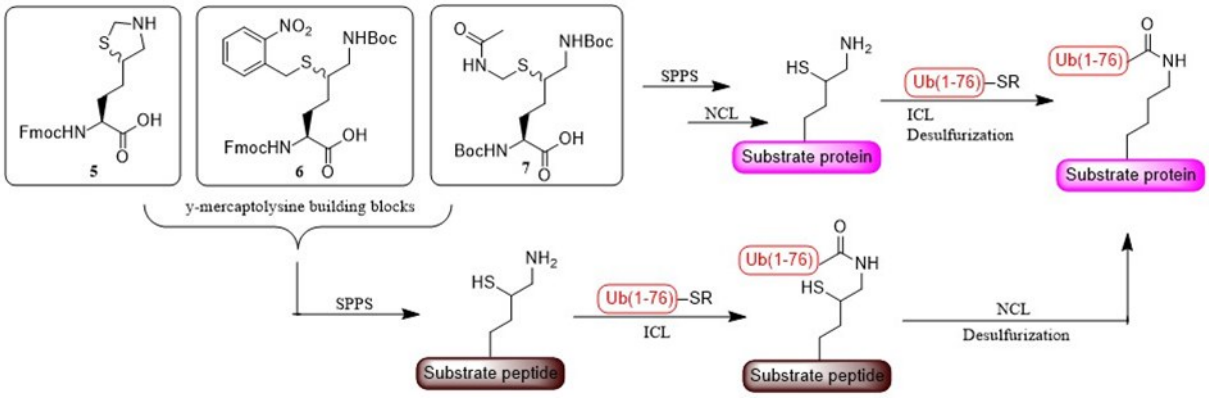

Figure 4 Reaction scheme of δ-mercaptolysin strategy (based on[38]).

In order for the generated δ-mercaptolysin to withstand the conditions of SPPS, specific protecting groups were developed for the building blocks.[51] This method showed higher efficiencies in the ubiquitylation of proteins than the glycyl-auxiliary strategy. In the latter, the secondary amine in S-N acyl transfer leads to a significantly lower ligation rate.[52] This method was used to synthesize a number of Ub conjugates such as large poly Ub chains and polyubiquitylated proteins and peptides.[49,53,54,55] Limitations of this strategy lie in the extensive organic synthesis of the building blocks, which requires more than 10 steps.[52,51]

1.3.2.3 Orthogonal protection and SPPS isopeptide bond construction

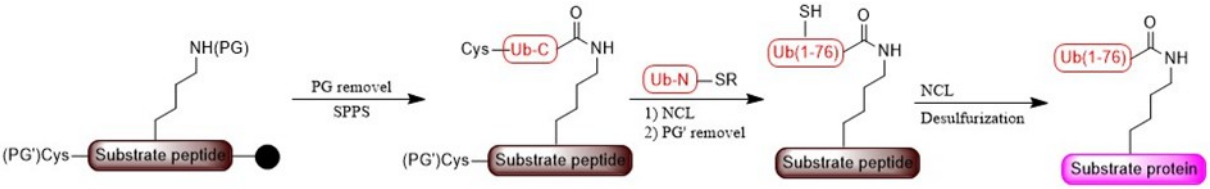

Figure 5 Reaction scheme of Orthogonal protection and SPPS isopeptide bond construction (based on[38]).

In comparison to this strategy, both the glycyl-auxiliary strategy and the δ-mercaptolysin strategy have the disadvantage that a multi-stage organic synthesis is required to generate the building blocks. Therefore, this method was developed to rapidly synthesize ubiquitinated peptides and proteins with native isopeptide bonds using only SPPS and NCL.[56,57]

First, an orthogonally protected Lys is incorporated into the desired peptide using SPPS. The ε-amine is then selectively deprotected and an isopeptide bond is generated between Ub and the desired Lys during SPPS. The resulting ubiquitinated peptide can now be further reacted to the desired ubiquitinated protein by NCL and desulfurization. (Figure 5) [38]

Various ubiquitinated proteins, such as histone H2B67 and α-globin, have already been produced in this way.[58] Furthermore, this strategy was recently further developed and a series of ubiquitin chains such as Di-Ub[59], K29 linked TetraUb and K11/K48 branched Tri-, Tetra-, Penta- and HexaUb were generated.[60]

Since this strategy does not require complex organic syntheses, it is particularly suitable for generating ubiquitin chains and ubiquitinated proteins.[38]

1.3.3 Thiol-ene Coupling

One method of coupling proteins or peptides to each other is thiol-ene coupling (TEC). This involves linking a cysteine-containing protein to a C-terminal alkene of another protein via a thiyl radical.[61] This method, among many others, is classified as a so-called click reaction. These include simple orthogonal reactions that can generate heteroatom-linked molecular systems selectively, efficiently and without by-products under mild conditions.[62] Reactions between thiols and carbon-carbon double bonds were already described as effective in an article in 1905.[63]

The basic characteristics of Click reactions also include quantitative conversions even at low concentrations, the use of low levels of benign catalysts, high reaction rates, environmentally friendly solvents, no clean-up and insensitivity to oxygen or water. Due to all these advantages, thiol-ene chemistry plays a major role in the production of high-performance polymer protection networks, as well as in the fields of biomedicine, sensor technology and bioinorganics. Nowadays, both Michael addition reactions and thiol-ene radical reactions are counted as click reactions in literature.[62]

A general distinction is made between radical-mediated and catalyst-mediated thiols. Which of the two types of chemistry is effective for a specific thiol strongly depends on the basic structure of the thiol, although both work very efficiently in principle.[62]

The thiol-ene coupling has great potential in the modification of proteins.[61] The addition of thiyl radicals to alkenes has a bimolecular rate of 10^6 M^{-1} s^{-1}, which enables a reaction in the µM range. A further advantage is the possibility of using recombinant proteins, whereby this method is prioritized for direct modification of Cys.[61]

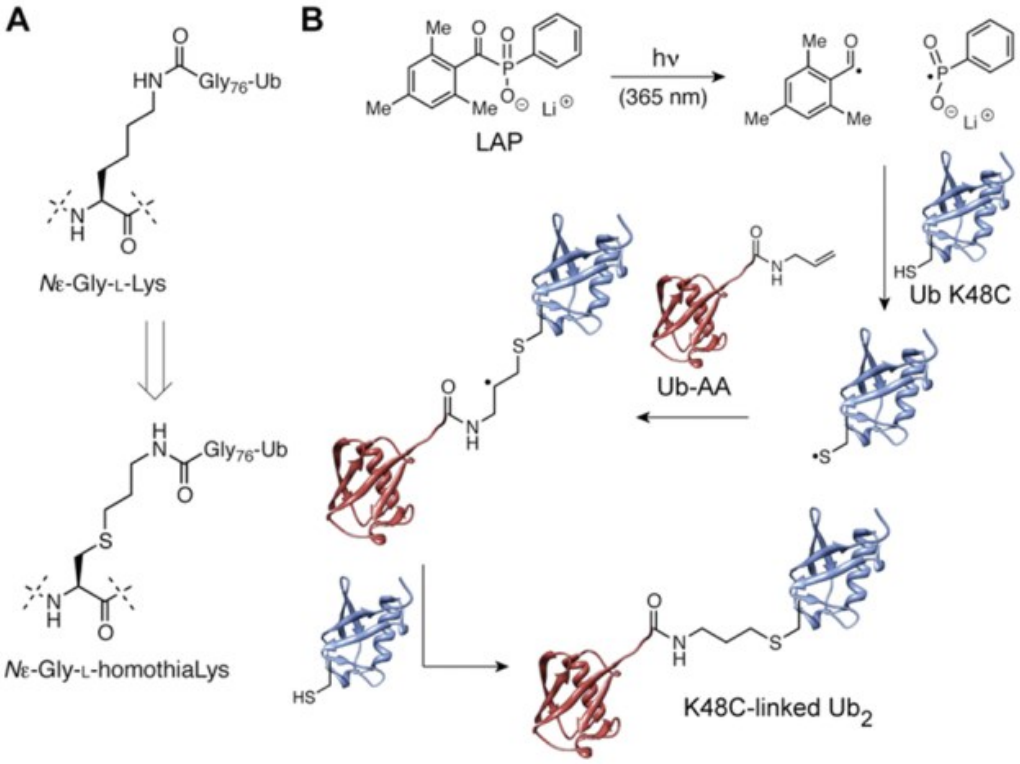

Figure 6 Reaction scheme of TEC. (retrieved from[61])

Using thio-ene coupling, it is possible to use standard proteins with minimal synthetic effort. For the coupling of ubiquitin to a target protein with a Cys residue instead of a Lys a small alkene (e.g. allylamide) at the C-terminal end of the ubiquitin is used. (Figure 6) The exchange of amino acids can be carried out by site-directed mutagenesis. The resulting Nε-Gly- L -HomothiaLys isopeptide bond is one bond longer than the natural one, which should not change its function. Di- and triubiquitins have already been successfully generated using this chemical approach.[61]

As a photoinitiator, lithium acylphosphinate (LAP) was found in studies to be effective for the formation of diubiquitins, obtaining functional dimers at a concentration of 0.5 mM.[61]

2. The Outline of the project

The goal of this master's thesis was to generate polyubiquitin chains of different linkage types by TEC. Therefore, different building blocks of Ub were produced via recombinant expression of ubiquitin-intein fusion constructs. Upon intein cleavage and C-terminal modifications to both hydrazide and allylamide functional groups were introduced. For coupling of two Ub chains, each containing a cysteine mutant (Ub^{KxC}), a thiol selective protecting group (PAc) was envisioned to transiently protect one cysteine and to allow fully controlled Ub chain assembly. These approaches were aimed at producting the following DiUbs: wt/K11C, wt/K29C, wt/K48C, wt/K63C, K29C/K63C, K48C/K48C, K63C/K29C. These DiUbs could be employed to obtain homotypical and heterotypical tri- and tetraubiquitin chains (such as $TriUb^{wt\text{-}K48C\text{-}K48C}NHNH_2$, $TriUb^{wt\text{-}K29C\text{-}K63C}NHNH_2$ und $TetraUb^{wt\text{-}K48C\text{-}K48C\text{-}K48C}NHNH_2$).

3. Methods

3.1 Instruments

A Shimadzu HPLC system (FCV-200AL prep quaternary valve, CMB-20ACL communication bus module, LC-20AP prominence preparative liquid chromatograph, SPD-10A UV-Vis detector, FRC-10A fraction collector) or Varian ProStar HPLC system with either Kromasil C4 reversed-phase semipreparative columns (300-10-C4/C18, 10 x 250 mm, 10 µm particle diameter, 300 Å pore size), or Kromasil C4 reversed-phase preparative columns (300-10-C4/C18, 21.2 x 250 mm, 10 µm particle diameter, 300 Å pore size) were used.

For LCMS and ESI-MS a system from Waters Corporation (2826 Sample Manager, 2545 Binary Gradient Modul, 515 HPLC Pump, 2489 UV/VIS Detector, 3100 Mass Detector) was used. Separation was performed on a Kromasil C4 reverse-phase column (300-5-C4, 140 x 4.6 mm, 5 µm particle diameter) with a gradient from 5% solvent B (ACN + 0.08 % TFA) in solvent A (H_2O + 0.1 % TFA) to 65% solvent B in 10 min at a flowrate of 1 mL/min. The mass spectrometer was run in positive mode.

For Analytical HPLC either a Vanquish Flex UHPLC System or a Dionex Ultimate 3000 HPLC system (Thermo Fischer Scientific) on a Kromasil C4 reverse-phase column (300-5-C4, 150 x 4.6 mm, 5 µm particle diameter) was used. The linear gradient ranged from 5 to 65 % B in 30 min at a flow rate of 1mL/min and was monitored at 214 and 280 nm. For PAc-protected diubiquitins, a longer gradient of 5-65 %B in 40 min was chosen.

A NanoDrop UV/VIS spectrophotometer from Thermo Scientific was used to calculate optical densities and concentrations.

3.2 Chemicals

All chemicals and solvents, unless explicitly stated, were obtained from commercial sources and not further treated. If not further specified, deionized water (Milli-Q Reference A+) was always used.

Site directed mutagenesis primers were obtained from Microsynth and the origin of all kits used are explicitly stated in the respective paragraph.

All chemicals used for transformation and expression were purchased from PanReac AppliChem, GERBU, ROTH and Sigma-Aldrich.

All chemicals used for the cleavage reactions and conversions of the mono-ubiquitins were purchased from ROTH, Sigma-Aldrich and fluorochem.

All chemicals used for the coupling reactions were purchased from Sigma-Aldrich.

3.3 Media, Buffers, Stock Solutions and Gels

LB-medium	10 g/L Tryptone, 5 g/L Yeast extract, 10 g/L NaCl
2YT-medium	16 g/L Tryptone, 10 g/L Yeast extract, 5 g/LNaCl
TBS buffer	150 mM NaCl, 50 mM Tris, pH 8.0
PBS buffer	140 mM NaCl, 2.7 mM KCl, 10 mM Na_2HPO_4, 1.8 mM KH_2PO_4, pH 5.5
2x SDS buffer	500 mM Tris, pH 6.8, 6% /w/v) SDS, 35% (v/v) Glycerol, 3.55% (v/v) β-mercaptoethanol, 0.05% bromophenol blue
Coomassie-Staining solution	0.1% (w/v) Coomassie R250, 10% (v/v) acetic acid, 45% (v/v) methanol
Separating gel buffer	1.5 M TrisHCl, 0.4 % (w/v) SDS, pH 8.8
Stacking gel buffer	0.5 M TrisHCl, 0.4 % (w/v) SDS, pH 6.8
Laemmli buffer	25 mM Tris, 200 mM Glycine, 0.1% w/v SDS
AMP-stock	100 mg/mL AMP
CAM-stock	30 mg/mL CAM
Hydrazine Cleavage solution	5% hydrazine, 50 mM DTT in TBS-buffer
MESNa Cleavage solution	500 mM MESNa in PBS-buffer
TEC buffer	250 mM NaOAc, 6M Gnd HCl, pH 5.4
Protection buffer	0.4 M phosphate buffer, 6M Gnd HCl, pH 7.2
Conversion buffer	0.2 M phosphate buffer, 6M Gnd HCl, pH 3.0

3.4 Site-directed mutagenesis Ub^{K11C}-Mxe-H7-CBD

Bought Primers (Microsynth) for mutagenesis of Ub^{K11C} were dissolved in H_2O and diluted to a final concentration of 10 µM. For amplification via PCR, a master mix (35 µL 5x Reaction Buffer, 3.5 µL 10 mM DNTPS, 8.75 µL 10 µM forward and reverse primer, 1.75 µL Q5 Polymerase, 35 µL 5x GC Enhancer, 75.25 µL H_2O) was prepared. 24 µL of this master mix was placed in each of 6 PCR tubes and 1 µL of template was added to (2x undiluted, 2x 1:10 diluted, 2x 1:100 diluted).

PCR started with an initial denaturation step (98 °C, 30 secs), followed by 35 cycles of denaturation (98 °C, 10 sec), annealing (60 °C, 30 sec) and extension (72 °C, 4.5 min). Finally, a final extension (72 °C, 2 min) step happened.

After completion of PCR, agarose gel electrophoresis was performed to check the results. For this, 0.5 g agarose in 50 mL 1x TAE was heated in a microwave and then allowed to harden in a designated facility to obtain a 1% agarose gel. 5µL of the PCR reaction mixture of each PCR tube was mixed with 3 µL of 6x loading dye for DNA samples and 12 µL of H_2O. 3 µL of a 1 kb DNA+ ladder was also mixed with 3 µL of 6x loading dye for DNA samples and 14 µL of H_2O. 20 µL of each reaction mixture and the DNA ladder were loaded onto the agarose gel and run at constant 100V for 1.5 h in 1x TAE. The gel was then stained in ethidium bromide for 30 min and washed 3x with 1x TAE.

All PCR samples were combined (120 µL) and purified using GeneJet PCR Purification Kit (Thermo Fisher Scientific). The PCR mixture was mixed with 120 µL binding buffer and transferred to GeneJET purification columns. It was incubated for 1 min at room temperature and then centrifuged for 1 min at 14 000 rpm (flow through discarded). Then 700 µL Wash Buffer was added and centrifuged again for 1 min at 14 000 rpm (flow through discarded). The empty column was additionally centrifuged for 1 min at 14 000 rpm and placed on a fresh 1.5 mL Eppendorf tube. 30 µL H_2O was pipetted onto the center of the column and centrifuged at 14 000 rpm for 1 min after 1 min incubation at room temperature. The PCR product contained in the flow through was stored at -20 °C.

To achieve ring closure of the amplicon, a kinase, ligase & DpnI (KLD) treatment (Q5 site directed mutagenesis kit, New England Biotabs) was performed. In this procedure, 1 µL of the purified PCR product was mixed with 5 µL of 2x KLD reaction buffer, 3 µL of H_2O and 1 µL of 10x KLD enzyme mix (added last) by gently pipetting up and down and incubated at room temperature for 30 min.

To amplify the plasmid obtained by KLD treatment, it was transformed by heat-shock technique into E. coli XL1-Blue competent cells. For this, an aliquot of XL-1 cells was thawed on ice for 30 min and then 10 µL of the KLD ligation reaction was added to them and mixed by gentle tapping. After 5 min on ice, the cells were incubated for 90 sec at 42 °C, 1 mL of sterile LB medium (10 g/L tryptone, 5 g/L yeast extract, 10 g/L NaCl) was added, and shaken for 45 min at 37 °C and 300 rpm. Subsequently, centrifugation was performed for 1 min at 8000 rpm and 850 µL of supernatant was removed. The pellet was resuspended in the remaining solution, spread on an agar plate and incubated overnight at 37 °C.

Two colonies from the agar plate were each added to 25 mL of sterile LB medium (10 g/L tryptone, 5 g/L yeast extract, 10 g/L NaCl) containing 100 mg/mL ampicilin and this was incubated overnight at 37 °C and 170 rpm. From each of the media, 1.5 mL was transferred to four Eppendorf tubes each, centrifuged for 30 s at 14 000 rpm, and the supernatant discarded. This step was performed for a total of three times for each of the Eppendorf tubes.

Plasmid purification using GeneJET Plasmid Miniprep Kit (Thermo Fisher Scientific) was performed. For this purpose, the cell pellet was dissolved in 250 µL resuspension buffer by gentle pipetting up and down. 250 µL of Lysis Solution was added and mixed by inverting the Eppendorf tube 4-6 times. Subsequently, 350 µL of neutralization buffer was added and inverted again 4-6 times. The Eppendorf tubes were centrifuged at 14 000 rpm for 10 min and the supernatant was transferred to spin columns. Centrifugation was performed for 1 min at 14 000 rpm and the flow through was discarded. Twice, 500 µL of wash solution were applied to the spin columns, centrifuged for 1 min at 14 000 rpm and the flow through discarded. The column was then placed on a fresh Eppendorf tube and 50 µL of H_2O was pipetted onto the center of the column. After 2 min incubation, the column was centrifuged for 2 min at 14 000 rpm and the concentration of the plasmid in the flow through was determined using Nanodrop (2 µL). Since the plasmid concentration of the solutions was only around 25 ng/L, they were combined and narrowed down by speedvac to obtain final concentrations of 58.5 (K1) and 73.6 ng/L (K2) for the clones. Subsequently, for each clone, two samples of 12 µL each were sent to Microsynth for sequencing.

3.5 Transformation and Expression of Ub^{K11C}-Mxe-H7-CBD

The plasmid encoding Ub^{K11C}-Mxe-H7-CBD was transformed into E. coli BL21 (DE3) Gold and E. coli BL21 (DE3) Rosetta 2 via heat shock method. Therefore, 5 µL of plasmid solution K1, as described in section 3.4, was kept on ice for 5 min with one stick each of E. coli Gold/Rosetta 2. Cells were then incubated at 42 °C for 90 sec. 1 mL of sterile LB medium (10 g/L tryptone, 5 g/L yeast extract, 10 g/L NaCl) was added and the mixture was left at 37 °C and 300 rpm for 45 min. The cell suspension was then spread on an agar plate in the same manner as XL1 cells and incubated overnight at 37 °C. The next day, 3 mL each of sterile LB medium was prepared for E. coli Gold (AMP) and Rosetta 2 (AMP + CAM) and each inoculated using a clone excised from the agar plate. Cultures were incubated overnight at 37 °C and 300 rpm and then stock was prepared by mixing 750 µL of culture with 750 µL of glycerol. This was frozen at -80 °C.

First, test expression of both glycerol stocks for Ub^{K11C} was performed. For this, 50 mL of sterile 2YT medium (16 g/L Tryptone, 10 g/L Yeast extract, 5 g/L NaCl) was mixed with the corresponding antibiotic (100 µg/mL AMP for Gold, 100 µg/mL AMP and 30 µg/mL CAM for Rosetta 2) and inoculated with the glycerol stock. This culture was incubated overnight at 37 °C and 160 rpm. The next day, the optical density (OD600) of the 1:10 diluted culture was measured at 600 nm using NanoDrop UV/VIS spectrometer. Depending on the OD600 value of the culture, enough was added to 500 mL of fresh, sterile 2YT medium (plus antibiotics) to achieve an OD600 of approximately 0.2. This second culture was then incubated again at 37°C and 160 rpm until it reached an OD600 value of approximately 0.6-0.7. After around 90 min,

protein expression was induced by adding 1 mM IPTG. Cells were then incubated at 37 °C and 160 rpm for 4 h, with gel samples taken before the addition of IPTG and hourly thereafter. The amount of sample was calculated using the following formula:

$$\mathrm{V}\ [\mu\mathrm{L}] = \frac{200\ [\mu\mathrm{L}]}{\mathrm{OD}_{\mathrm{measured}}}$$

Formula 1

Gel samples were stored at -20 °C until SDS PAGE.

After protein expression, the cell suspensions were centrifuged for 25 min at 4°C and 6300 rpm, the supernatant was discarded, and the pellet was stored at -80°C. The next day, the pellets were resuspended in 60 mL TBS (150 mM NaCl, 50 mM Tris, pH 8.0) and lysed on ice by ultrasonication (pulse 15 sec, pause 45 sec, amplitude 60%, pulse time 10 min). The lysate was centrifuged for 30 min at 4 °C and 20 000 rpm. The supernatant was transferred to a glass vial and stored at 4 °C, and the cell pellets were stored at -80 °C until lysis was confirmed by SDS PAGE. For this, a spatula tip of the pellet, as well as 20 µL of the supernatant were frozen at -20 °C.

For SDS PAGE, protein expression cell pellets were resuspended in 20 µL H_2O, mixed with 20 µL 2x SDS buffer (500 mM Tris, 6% SDS, 35% glycerol, 3.55% beta-mercaptoethanol, 0.05% bromophenol blue, pH 6.8), and boiled at 95 °C for 5 min. The cell pellet after lysis was washed twice with 100 µL TBS, centrifuged at 14 000 rpm for 1 min, and the supernatant was discarded. Both the sample of lysate and the washed cell pellet were also mixed with 20 µL of 2x SDS and boiled at 95 °C for 5 min. All samples were centrifuged at 14 000 rpm for 1 min and 10 µL of the supernatant was loaded onto the gel and allowed to run at a constant 250 V and a maximum current of 120 mA in Laemmli buffer (25 mM Tris, 200 mM Glycine, 0.1% w/v SDS) for 37 min. The gel was washed several times with H_2O and stained for 15 min in Coomassie staining solution (0.1% w/v Coomassie R250, 10% v/v acetic acid, 45% v/v methanol in H_2O). It was then destained in H_2O for several hours.

All subsequent protein expressions were performed on a 6 L (3 x 2 L) scale.

3.6 Expression of $Ub^{wt,\ K29C,\ K48C,\ K63C}$ – intein fusion construct

Since glycerol stocks were already available for the other ubiquitin mutants through my supervisor and previous master's students, protein expression was performed directly on these, analogous to that described in section 3.5, at a 6 L scale (3 x 2 L). The glycerol stocks with respective antibiotics are E. coli BL21 (DE3) Gold (AMP) for Ub^{Wt}, Ub^{K48C}, Ub^{K63C} and E. coli BL21 (DE3) Rosetta 2 (AMP + CAM) for Ub^{K29C}.

3.7 Cleavage of Ub^{K11C}- intein fusion construct

To obtain the protein in the different C-terminal modifications, they were purified via chitin resin (New England BioLabs Inc.) and then cleaved as the desired modification. For this purpose, 7.5 mL of the chitin resin was used for 35 mL of crude protein solution. The resin was washed 1x with H_2O and 2x with 1x TBS (150 mM NaCl, 50 mM Tris, pH 8.0) before loading with the protein mixture. The tubes were each left on a tuber roller for 1 min, centrifuged at 1300 rpm and 4°C for 2 min, and the supernatant discarded. Then, the protein mixture (after Lysis) was

added to the chitin resin and incubated for 2 h at room temperature on a tuberoller. Afterwards, centrifugation was performed for 2 min at 4 °C and 1300 rpm, and the supernatant was collected in an extra tube until SDS PAGE confirmed loading of the desired protein onto the resin.

For this, 20 µL of the supernatant and 50 µL of beads suspension were taken as samples for SDS PAGE.

3.7.1 MESNa-Cleavage

The resin was washed 1x with 1xTBS (150 mM NaCl, 50 mM Tris, pH 8.0) and 2x with 1x PBS (140 mM NaCl, 2.7 mM KCl, 10 mM Na_2HPO_4, 1.8 mM KH_2PO_4, pH 5.5). Then, 40 mL MESNa Cleavage Solution (500 mM MESNa, 140 mM NaCl, 2.7 mM KCl, 10 mM Na_2HPO_4, 1.8 mM KH_2PO_4, pH 5.5) was added to each tube and incubated for 2 days at 37 °C and 75 rpm. Since this did not work for the test expression, MESNa Cleavage for this mutant was performed at 25 °C for the following protein expressions. After 24 hours, 100 µL bead suspension and 20 µL supernatant were taken as sample for SDS PAGE. After 2 days, 100 µL bead suspension and 20 µL supernatant were taken as sample for SDS PAGE and the cleavage solution was centrifuged for 2 min at 4 °C and 1300 rpm. The supernatant containing the protein of interest was transferred to a tube and stored at 4 °C. The resin was washed with ~ 15 mL 1x PBS (140 mM NaCl, 2.7 mM KCl, 10 mM Na_2HPO_4, 1.8 mM KH_2PO_4, pH 5.5) per Falcon tube and this supernatant was added to the first supernatant.

3.7.2 Hydrazide-Cleavage

The resin was washed 2x with 1xTBS (150 mM NaCl, 50 mM Tris, pH 8.0). Then, 40 mL of Hydrazine Cleavage Solution (5% Hydrazine, 50 mM DTT, 150 mM NaCl, 50 mM Tris) was added to each tube and incubated at 37 °C and 75 rpm for 2 days. After 24 hours, 100 µL bead suspension and 20 µL supernatant were taken as sample for SDS PAGE. After 2 days, 100 µL bead suspension and 20 µL supernatant were taken as sample for SDS PAGE and the cleavage solution was centrifuged for 2 min at 4 °C and 1300 rpm. The supernatant containing the protein of interest was transferred to a tube and stored at 4 °C. The resin was washed with ~ 15 mL 1x TBS (150 mM NaCl, 50 mM Tris, pH 8.0) per Falcon tube and this supernatant was added to the first supernatant.

For SDS PAGE, beads suspension samples were centrifuged at 14 000 rpm for 1 min and then washed with 100 µL TBS (150 mM NaCl, 50 mM Tris, pH 8.0). SDS PAGE was performed analogously to protein expression as described in section 3.5. After SDS PAGE confirmed cleavage as successful, protein mixtures were purified by preparative HPLC, lyophilized, and frozen at -20 °C.

A Kromasil 300-10-C4, 21.2 x 250 mm with a flow of 9 mL/min and a gradient of 5-30% B in 5 min and 30-60% B in 40 min at 60°C was used to purify the protein mixture.

3.8 Cleavage of Ub^{Wt} - and Ub^{KxC}- intein fusion construct

MESNa and Hydrazine cleavage of the remaining ubiquitin mutants were performed analogously to that of Ub^{K11C} as described in sections 2.7.1 and 2.7.2, with temperature being 37 °C for all cleavages.

3.9 Synthesis of C-terminal Allylamide

In order to use the C-terminal MESNa thioester for thiol-ene coupling, it must first be converted to an allyl amide. For this purpose, the lyophilized protein was dissolved in H_2O (+0.1 % TFA) and then allylamide was added to obtain a final concentration of 1.5 mg/mL protein and 500 mM allylamide. This mixture was then placed under argon atmosphere and stirred on ice for 2 hours. Before the addition of allylamide and after 2 hours, 20 µL of the reaction mixture was taken as a time point. The pH of this solution was adjusted to 6-8 and LCMS was done to check the progress of the reaction.

After LCMS confirmed the reaction, the protein mixture was purified analogous to section 3.7, lyophilized and frozen at -20 °C.

3.10 Thiol-ene coupling of Ub^{wt} with Ub^{KxC}

Initially, all solutions such as 6M GndHCl, H_2O and buffer were degassed with argon for 15 min. The solutions LAP (75 mM in H_2O) and TCEP (50 mM in H_2O) were freshly prepared for each batch of reactions. All solutions were stored on ice before and during the coupling reaction. All additions, as well as the reaction, were performed under argon shower. Subsequently, the proteins to be coupled were dissolved by alternately freezing in liquid nitrogen and vortexing in 22.6 µL each of buffer (250 mM NaOAc, 6M Gnd HCl, pH 5.4) to give a concentration of 6 mM (allylamides) and 7.5 mM (hydrazide) in the final volume of 50 µL. To the dissolved hydrazide, 1.5 µL of the TCEP (50 mM) was added and stirred for 5-10 min. The allylamide was then added to the solution and a sample for SDS PAGE (1µL reaction solution in 39 µL H_2O) and LC-MS (1 µL reaction solution in 39 µL 6M Gnd HCl) were taken. Then, 3.3 µL LAP (75 mM) was added to the mixture and the reaction was started by irradiation (15 s irradiation, 15 s pause, 15 s irradiation). Samples were then taken for SDS PAGE and LCMS, analogous to before the reaction, and the reaction was stopped by adding 200 µL of 6m Gnd HCl. The reaction mixture was frozen in liquid nitrogen and stored at -80 °C until SDS PAGE and LCMS have taken place.

After LCMS confirmed the reaction, the protein mixture was purified using a Kromasil 300-10-C4, 10 x 250 mm with a flow rate of 3 mL/min and a gradient of 5-25 %B in 10 min and 25-40 %B in 40 min at 60°C.

3.11 Thiol-ene coupling of Ub^{KxC} with Ub^{KxC}

In the coupling of two ubiquitin mutants, the incorporated cysteine was first blocked with the aid of a protective group to prevent the formation of by-products.

3.11.1 PAc-Protection of $Ub^{KxC}SR$

The lyophilized MESNa thioesters of ubiquitin mutants were dissolved in degassed buffer (0.4 M phosphate buffer, 6M Gnd HCl, pH 7.2) to give a concentration of 0.52 mM. Subsequently, 2.5 eq of PAcBr (0.1 M in anhydrous DMF) was added to the solution, the flask was purged

with argon and sealed with a septum. For the first reaction, it was waited for 1h and then 20 µL of the reaction mixture was diluted with 20 µL of a mixture of 1:1 ACN:H_2O for an LCMS. Since the reaction was completed after a short time regardless of the mutant, only a few minutes were waited for the following reactions and after confirmation by LCMS, the conversion to allylamide was already performed in situ. For this, the mixture was diluted with H_2O and allylamide was added to give a protein concentration of 1.5 mg/mL and allylamide concentration of 500 mM. Subsequently, the transformation was performed analogously to that described in section 3.9.

After LCMS confirmed the reaction, the protein mixture was purified analogous to section 3.7, lyophilized and frozen at -20 °C.

3.11.2 PAc-Deprotection of DiUb

To remove the PAc protecting group from the diubiquitins obtained by the coupling reaction, zinc powder (180 mg/L) and 45% (v/v) acetic acid were added to the reaction mixture from the TEC reaction and stirred at room temperature. The completion of the reaction was determined by LCMS. The reaction mixture was then centrifuged at 14 000 rpm for 1 min and the supernatant transferred to a new Eppendorf tube. Then two times 300 µL of 6M Gnd HCl was added and the centrifugation step was repeated. Since the first deprotections took 2.5 hours and a by-product appeared in increasing amounts over time, the protein concentration was halved in the following deprotection reactions to speed up the process. This reduced the reaction time to 1 h. Furthermore, high-resolution LCMS measurements of a pool after purification containing the by-product were measured to identify that by-product.

3.12 Generation of DiUb$^{wt\text{-}K48C}$AA

To subsequently generate triubiquitin and tetraubiquitin chains from the generated diubiquitins, the diubiquitin Ub$^{wt\text{-}K48C}$ was converted to a C-terminal allyl amide. For this, 17.4 mg of the diubiquitin was first dissolved in 160 µL of degassed buffer (0.3M phosphate buffer, 6M Gnd HCl, pH 3.0) to obtain a concentration of 5 mM. The protein solution was stirred in an ice/saline bath at -15°C for 15 min, 16 µL of 0.5 M $NaNO_2$ (0.3M phosphate buffer, 6M Gnd HCl, pH 3.0) was added, followed by stirring for 20 min. At the beginning and end of this step, 1 µL of reaction solution was added in 39 µL of buffer A as a time point and LCMS was recorded to confirm the reaction.

To convert the obtained C-terminal azide to an allylamide, 10.978 mL of 6 M Gnd HCl and 434.7 µL of allylamide were added and the solution was further stirred in a normal ice bath for 2h. After 2h, an LCMS of 15 µL reaction solution in 15 µL 6 M Gnd HCl was measured to confirm the conversion.

Since the diubiquitin used was already pure, a faster gradient was chosen here for purification. The protein mixture was purified using Kromasil 300-10-C4, 10 x 250 mm with a flow rate of 3 mL/min and a gradient of 5-55 %B in 10 min at 60°C.

3.13 Thiol-ene coupling of DiUb$^{wt\text{-}K48C}$AA with Ub^{K48C}NHNH$_2$

All solutions were prepared as described in section 2.10 and the reaction was performed analogously. In this reaction, the DiUb$^{wt\text{-}K48C}$AA was used as allyl amide and the Ub^{K48C}-NHNH$_2$ as hydrazide to generate the corresponding triubiquitin.

After LCMS confirmed the reaction, the protein mixture was purified analogous to section 3.10, lyophilized and frozen at -20 °C.

3.14 Thiol-ene coupling of DiUb$^{K29C\text{-}K63C}$NHNH$_2$ with Ub^{wt}AA

All solutions were prepared as described in section 3.10 and the reaction was carried out analogously. In this reaction, Ub^{wt}AA was used as allyl amide and the DiUb$^{K29C\text{-}K63C}$NHNH2 was used as hydrazide to generate the corresponding triubiquitin. However, since it was not possible to obtain enough diubiquitin with the monoubiquitins originally obtained, the proteins used were in the same ratio but at lower concentrations (4.75 mM for the allylamide and 6.07 mM for the hydrazine).

After LCMS confirmed the reaction, the protein mixture was purified analogous to section 3.10, lyophilized and frozen at -20 °C.

3.15 Thiol-ene coupling of DiUb$^{wt\text{-}K48C}$AA with DiUb$^{K48C\text{-}K48C}$NHNH$_2$

All solutions were prepared as described in section 3.10 and the reaction was carried out analogously. In this reaction, Ub$^{wt\text{-}K48C}$AA was used as allyl amide and the DiUb$^{K48C\text{-}K48C}$NHNH$_2$ was used as hydrazide to generate the corresponding tetraubiquitin. However, since it was not possible to obtain enough diubiquitin with the monoubiquitins originally obtained, the proteins used were in the same ratio but at lower concentrations (3.70 mM for the allylamide and 4.66 mM for the hydrazine).

After LCMS confirmed the reaction, the protein mixture was purified analogous to section 3.10, lyophilized and frozen at -20 °C.

4. Results and discussion

4.1 Recombinant production of Ub^{wt}

4.1.1 Expression of Ub^{wt} fusion construct

A 6 L expression of Ub^{wt}-Mxe-H7-CBD fusion construct was performed, as described in section 3.6. The E. coli BL21 (DE3) Gold stock which was already available, was used for this purpose. A sample was taken every hour during expression, as well as of the supernatant and pellet after lysis, and the progress was visualized on an SDS-PAGE (Figure 7).

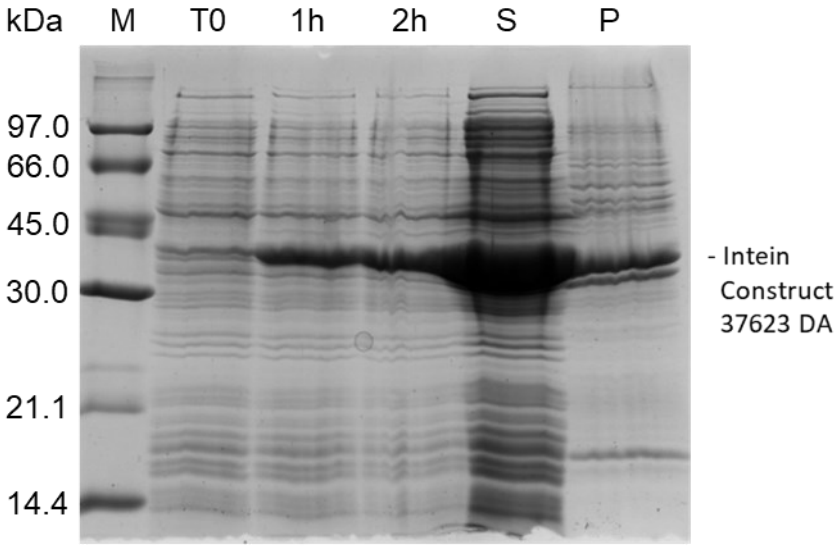

Figure 7 SDS PAGE of 6 L Expression and Lysis of Ub^{wt}. Lane 1 DNA ladder, Lane 2-5 before and every hour after induction, Lane 6 Supernatant (S) after lysis, Lane 7 Pellet (P) after lysis.

Since experiments by Dr. Susanne Huhmann showed that the optimal duration of protein expression for the wild type is 2 h, this was used there. A strong band between 30.000 and 45.000 kDa can be seen on the gels of both test expressions. This indicates the overexpressed fusion construct with a mass of 37.623 kDa. After cell lysis, the fusion construct was isolated from the supernatant by affinity purification on chitin beads.

4.1.2 Cleavage of Ub^{wt}-intein fusion construct

Cleavage of Ub^{wt}-intein fusion construct was performed as described in section 3.7. Since there is no cysteine in the wildtype of ubiquitin, only cleavage as MESNa thioester is necessary here.

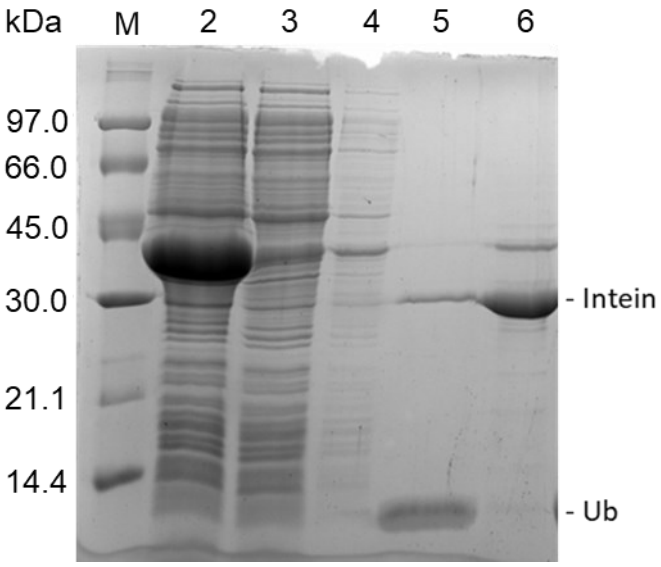

Figure 8 SDS PAGE of Loading and MESNa Cleavage of Ub^{wt}. Lane 1 Marker, Lane 2 Supernatant before loading, Lane 3 Supernatant after loading, Lane 4 Beads after loading, Lane 5 Supernatant after 72 h MESNa cleavage, Lane 6 Beads after 72 h MESNa cleavage.

As shown in the SDS-PAGE in Figure *8*, loading of the protein construct onto beads worked well. The large band at 37 kDa is clearly visible in the supernatant before loading and on the beads after loading. However, it is not present in the supernatant after loading. MESNa cleavage worked, indicated by the band at around 8.500 kDa in the supernatant (Ub).

The protein was purified by RP-HPLC as described in section 3.7.2, pure fractions were identified by direct ESI-MS, combined and lyophilized. The final product (17 mg per liter of expression medium for $Ub^{wt}SR$) was characterized by ESI-MS and RP-HPLC (Figure 9).

Ub^{wt}SR:

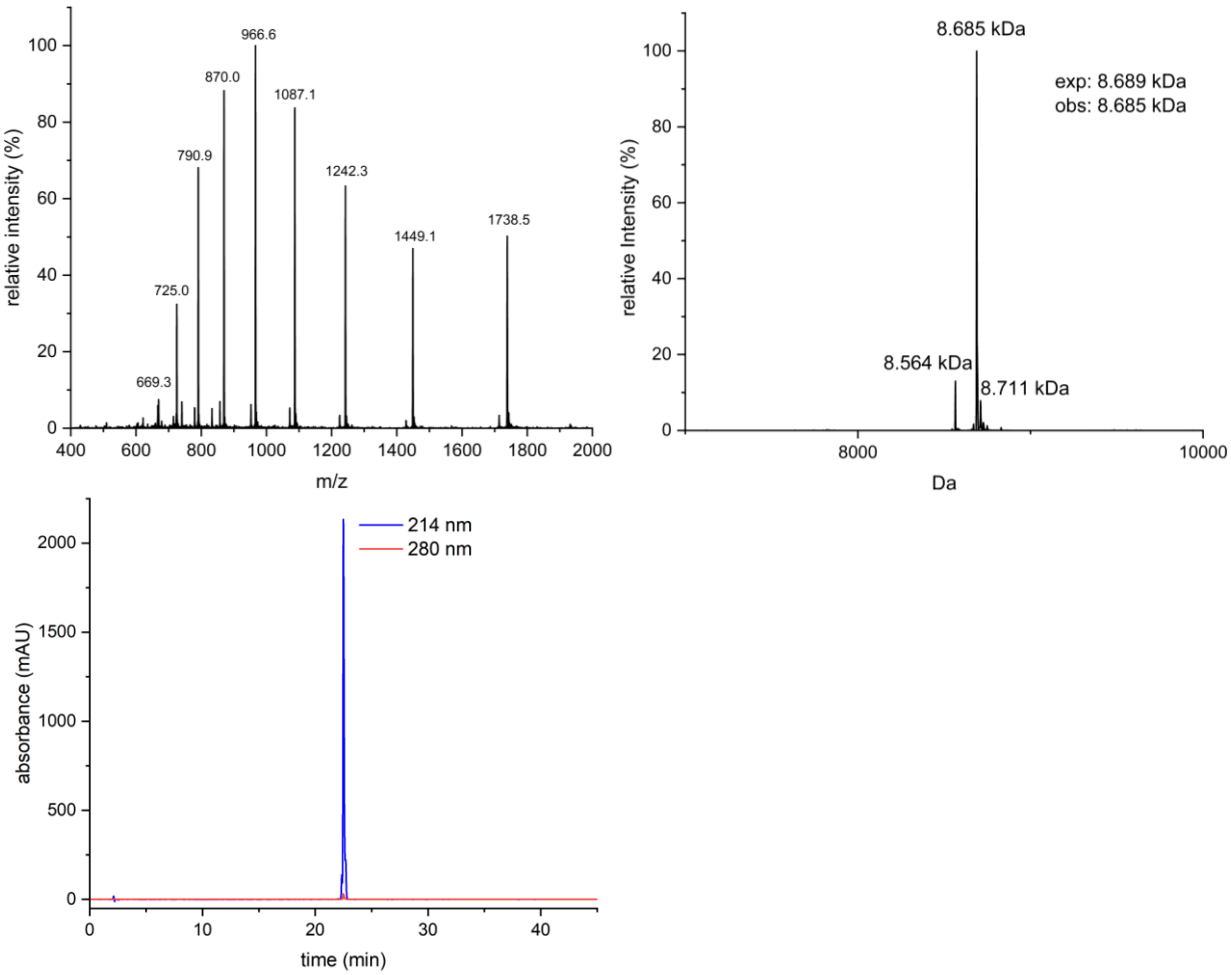

Figure 9 Characterization of isolated Ub^{wt}SR. ESI-MS (left), deconvoluted mass spectrum (right), analytical RP-HPLC (bottom).

Figure 9 shows ESI-MS, deconvoluted mass spectrum and analytical RP-HPLC of isolated Ub^{wt}SR. Minor impurity of 8.564 kDa in this spectrum refers to the hydrolyzed thioester of Ub^{wt}.

4.1.3 Generation of Ub^{wt}AA:

The conversion of the Ub^{wt}SR into a C-terminal allylamide was carried out as described in section 3.9. For this, the dissolved Ub^{wt}SR was stirred in 500 mM allylamine on ice for 2 h under argon. The reaction progress was followed by LCMS and the crude protein mixture was then purified using preparative RP-HPLC.

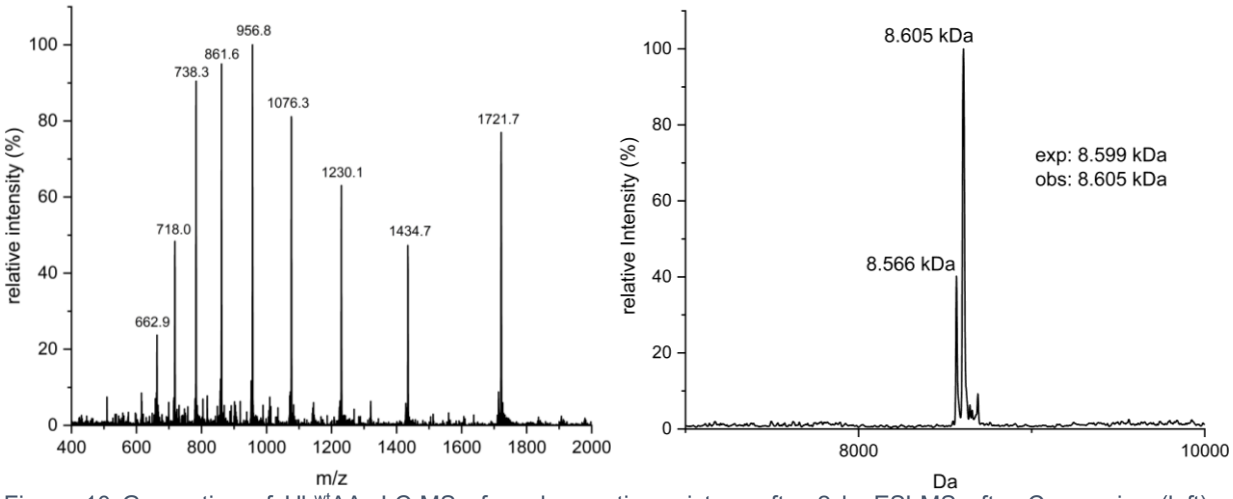

Figure 10 Generation of Ub^{wt}AA, LC-MS of crude reaction mixture after 2 h. ESI-MS after Conversion (left), deconvoluted mass spectrum (right).

As shown in Figure 10, the conversion of the thioester to a C-terminal allylamide was successful. The reaction mixture contained mostly Ub^{wt}AA according to the intensities of the ESI mass spectrum (Figure 10). The deconvoluted mass spectrum nicely illustrates that the intensity of the deconvolution results strongly depends on the deconvolution parameters and the algorithm. As a closer look, this spectrum is slightly different from all other deconvoluted mass spectra in this thesis, according to peak width and a low intensity over the whole background. This is because deconvolution with standard parameters used in this work delivered a spectrum that gives the correct product mass but changed intensities. (Figure 10, right). This occurred a few times during this master's thesis, although it mostly affected clean fractions during purification. Another method of deconvoluting could also be used to bypass this problem. Since the peaks corresponding to impurities in the spectrum (left) have rather low intensity, it can be assumed that the intensity of the mass 8.566 kDa in the spectrum is not representative for the actual impurity. This is also confirmed by the yield after purification with RP-HPLC. Since this spectrum shows an LC-MS of the crude reaction mixture, which was further purified, this was neglected.

The crude mixture was purified by RP-HPLC to yield 71.7 mg (71.6 %) of Ub^{wt}AA from 6 L of E. coli culture and characterized by ESI-MS and RP-HPLC (Figure 11).

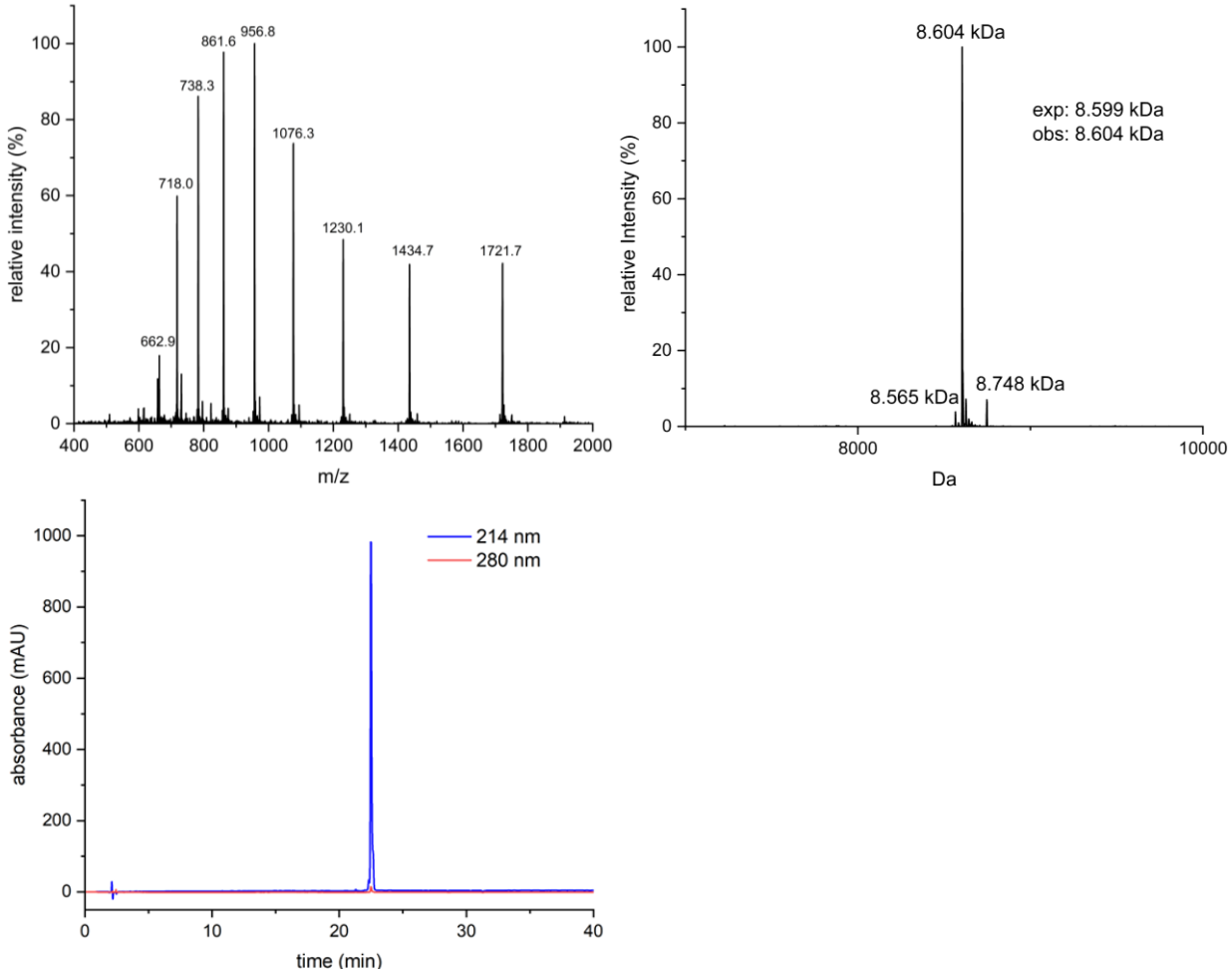

Figure 11 Characterization of isolated Ub^{wt}AA. ESI-MS (left), deconvoluted mass spectrum (right), analytical RP-HPLC (bottom).

Figure 11 shows ESI-MS, deconvoluted mass spectrum and analytical RP-HPLC of isolated Ub^{wt}AA. Little amount of hydrolyzed thioester of Ub^{wt} (8.565 kDa) are still visible in the spectrum.

4.2 Recombinant production of Ub^{K11C}

4.2.1 Site directed Mutagenesis

In order to obtain a ubiquitin with a thiol function at a specific point, a lysine was exchanged for a cysteine at this site. For this purpose, the vector pTXB1 encoding Ub^{K11C}-Mxe-H7-CBD fusion construct was produced by site-directed mutagenesis of the corresponding vector encoding a wildtype Ub fusion construct, which contained a codon change from AAA to TGC encoding for position 11 of ubiquitin. As described in section 3.4, a hot start PCR was performed with three different template concentrations (Primer shown in the appendix, Figure A 2). The products of the PCR were visualized by agarose gel electrophoresis and shown in Figure 12.

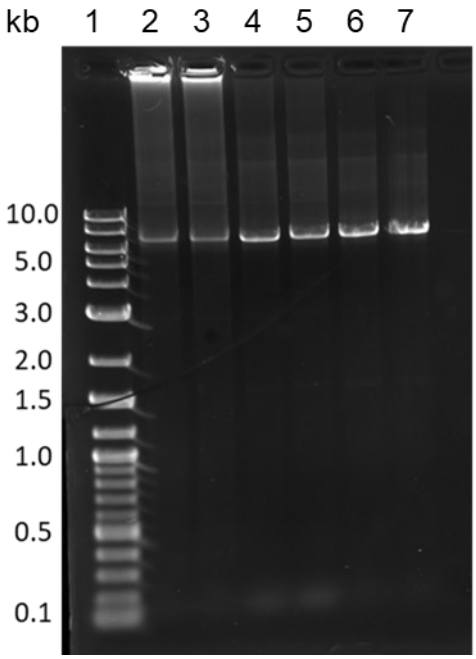

Figure 12 Agarose Gel of PCR Products. 1. Lane DNA ladder, Lane 2-3 product of Ub^{K11C} with undiluted template concentration, Lane 4-5 product of Ub^{K11C} with 1:10 diluted template concentration, Lane 6-7 with 1:100 diluted template concentration.

As shown on the gel, a bright band between 6000 and 8000 bp forms on all lanes with PCR product. Since the PCR product with the desired amino acid exchange has 6883 base pairs, this was seen as an indication that the PCR was successful.

All PCR products were combined, purified and ligated (section 3.4).

E. coli XL1-Blue competent cells were transformed with the plasmid generated with the kinase, ligase & DpnI (KLD) treatment, introduced via heat-shock technique and spread on an agar plate. Subsequently, two colonies were propagated in LB medium and the plasmid of both clones was purified (GeneJet Plasmid Kit). The plasmids were pre-concentrated in a Speedvac to a final concentration of 58.5 ng/L (Clone 1) and 73.6 ng/L (Clone 2). Samples of both clones were sequenced to confirm the intended mutation. The exact mode of operation is described in section 3.4. The result of the sequencing can be found in the appendix.

The plasmid encoding UbK11C-Mxe-H7-CBD was introduced via heat shock method in E. coli BL21 (DE3) Gold and Rosetta 2 and cultivated in LB medium. Subsequently, a glycerol stock was prepared for each of the two E. coli strains as described in section 3.5 and stored at -80 °C for later expression.

4.2.2 Test expression of Ub^{K11C} fusion construct

A test expression was performed with both glycerol stocks of Ub^{K11C}-Mxe-H7-CBD fusion construct as described in section 3.5. A sample was taken every hour during expression, as well as of the supernatant and pellet after lysis, and the progress was visualized on an SDS-PAGE (Figure 13).

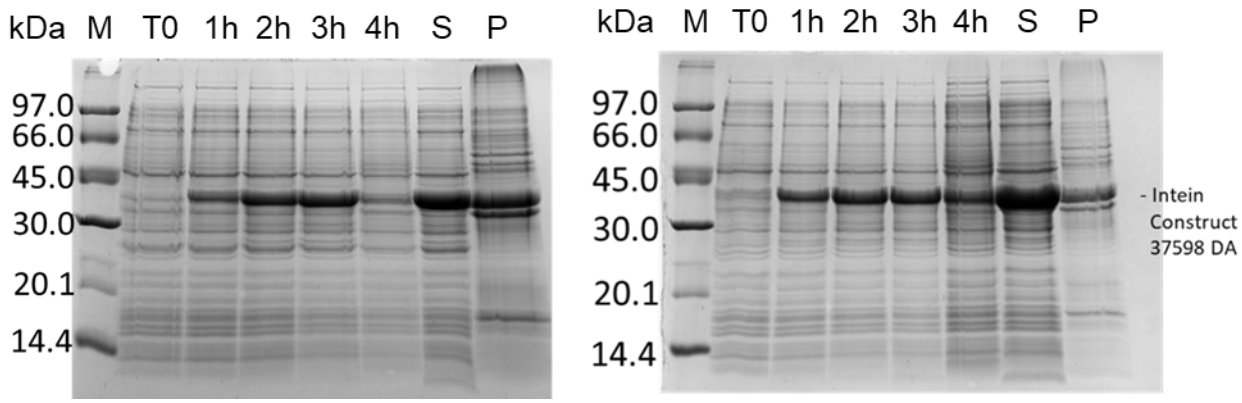

Figure 13 SDS PAGES for test expression and Lysis of Ub^{K11C} in E. coli BL21 (DE3) Rosetta 2 (left) and E. coli BL21 (DE3) Gold (right). Lane 1 marker, Lane 2-6 before and 1-4 hour after induction, Lane 7 Supernatant (S) after lysis, Lane 8 Pellet (P) after lysis.

A strong band between 30.000 and 45.000 kDa can be seen on the gels of both test expressions. This indicates the overexpressed fusion construct with a mass of 37.598 kDa. This band becomes stronger on both gels in the progress of expression, up to a maximum. When expressed in E. coli BL21 (DE3) Rosetta 2 (left), 3 h seems to be the optimal time for termination, since the band is most intense. In E. coli Gold (right) this is also at 3 h, as at 4 h the corresponding band is less and each band throughout the whole gel is significantly more intense, indicating protein degradation within the cell. After cell lysis, there is more construct in the supernatant than in the pellet. Since in the test expression of E. coli BL21 (DE3) Gold was proportionally more desired fusion construct in the supernatant than for Rosetta 2, it was decided to use this stock for the following expressions of Ub^{K11C}.

4.2.3 Cleavage of Ub^{K11C}-intein fusion construct

Since the test expression was successful, the fusion construct was isolated by affinity purification on chitin beads and half of the Ub^{K11C} fusion construct was cleaved by addition of hydrazine (50 %) and by addition of MESNa, leading to Ub^{K11C}-hydrazide ($Ub^{K11C}NHNH_2$) and Ub^{K11C}-thioester ($Ub^{K11C}SR$), respectively as described in section 3.7).

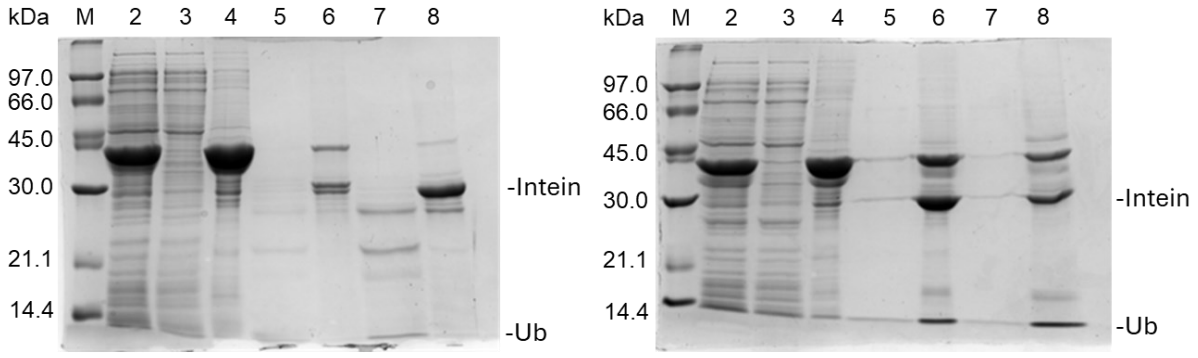

Figure 14 SDS PAGEs Hydrazine cleavage (left) and MESNa cleavage (right) of Ub^{K11C}. Lane 1 DNA ladder, Lane 2 Supernatant before loading onto chitin beads, Lane 3 Supernatant after loading, Lane 4 Beads after loading, Lane 5 Supernatant after 24 h cleavage, Lane 6 Beads after 24 h cleavage, Lane 7 Supernatant after 72 h cleavage, Lane 8 Beads after 72 h cleavage.

As shown in the SDS-PAGEs in Figure 14, the loading of the protein construct onto the beads worked well. The hydrazine cleavage (5 % hydrazine, 50 mM DTT, 37 °C), as shown on the left gel, also worked. Although the bands are weak, the ubiquitin as C-terminal hydrazide with

8.554 kDa is already weakly visible in lane 5 in the supernatant after 24 h cleavage and clearly recognizable in lane 7 after 72 h of cleavage. In addition, a strong protein band in lane 8 is noticeable under the protein fusion construct during expression. This band corresponds to the (Intein-H7-CBD part of the fusion construct) with a mass of 29.075 kDa.

For the MESNa-Cleavage, however, the associated ubiquitin-thioester band is only barely identifiable in the supernatant after 24h as well as after 72h. However, it is clearly recognizable in the lanes of the beads. Since the beads were already washed, when this result was obtained, it was not possible to obtain a C-terminal MESNa thioester of Ub^{K11C} from the test expression.

4.2.4 Full Expression of Ub^{K11C} fusion construct

Next, 6 L expression of Ub^{K11C}-Mxe-H7-CBD fusion construct was performed. The E. coli BL21 (DE3) Gold stock was used for this purpose.

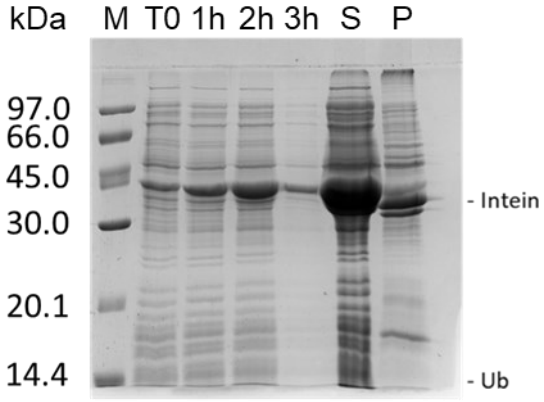

Figure 15 SDS PAGE of 6 L Expression and Lysis of Ub^{K11C}. Lane 1 DNA ladder, Lane 2-5 before and every hour after induction, Lane 6 Supernatant (S) after lysis, Lane 7 Pellet (P) after lysis.

Like the test expression, the desired fusion product was found in the supernatant after lysis.

4.2.5 Cleavage of Ub^{K11C}-intein fusion construct

Cleavage of Ub^{K11C}-intein fusion construct was performed as described in section 3.7.

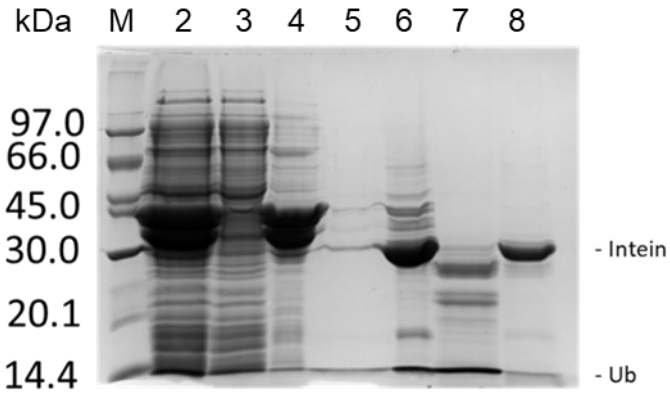

Figure 16 SDS PAGE of loading and cleavages for Ub^{K11C}. Lane 1 Marker, Lane 2 Supernatant before loading, Lane 3 Supernatant after loading, Lane 4 Beads after loading, Lane 5 Supernatant 24 h after MESNa cleavage, Lane 6 Beads 24 h after MESNa cleavage, Lane 7 Supernatant 2 72 h after hydrazine cleavage, Lane 8 Beads 72 h after hydrazine cleavage.

As shown in Figure 16, the 6 L expression of Ub^{K11C} gave the same result as the test expression. The loading of the chitin beads and the hydrazine cleavage worked without any

problems, but the thioester could only be found in the bead fraction, which indicates either that the cleaved Ub-thioester precipitates or adsorbes to chitin beads.

An attempt was made to extract the thioester from the bead fraction. For this purpose, an aqueos solution with 6 M GndHCl was added to the beads and samples were taken for SDS PAGE after 5 and 30 min on the shaker.

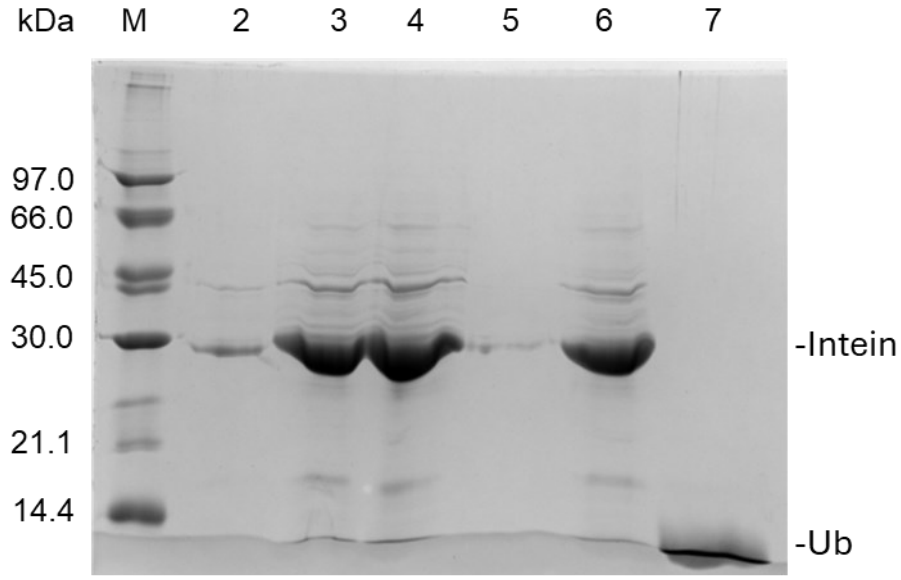

Figure 17 SDS PAGE of beads fraction after 6 M GndHCl treatment. Lane 1 Markjer, Lane 2 Supernatant after 5 min GndHCl treatment, Lane 3 Beads after 5 min GndHCl treatment, Lane 4 Beads before GndHCl treatment, Lane 5 Supernatant after 30 min GndHCl treatment, Lane 6 beads after 30 min GndHCl treatment, Lane 7 $Ub^{wt}AA$ as a reference.

As shown in Figure 17, even after 30 min of GndHCl treatment, the majority of the thioester was still in the beads fraction.

For the next expression of Ub^{K11C}, the MESNa cleavage was performed at 25 °C instead of 37 °C (conditions explored in experiments performed by Dr. Susanne Huhmann), whereby the thioester was found in the supernatant. However, our studies indicate that intein cleavage work more efficiently at higher temperatures.[64]

The protein solutions were purified by RP-HPLC as described in section 3.7.2, the pure fractions were identified by direct-infusion ESI-MS measurements, combined and lyophilized. The final products (10-15 mg per liter of expression medium for $Ub^{K11C}SR$ and 6-11 mg per liter of expression medium for $Ub^{K11C}NHNH_2$) were characterized by ESI-MS and RP-HPLC (Figure 18 and Figure 19).

$Ub^{K11C}NHNH_2$

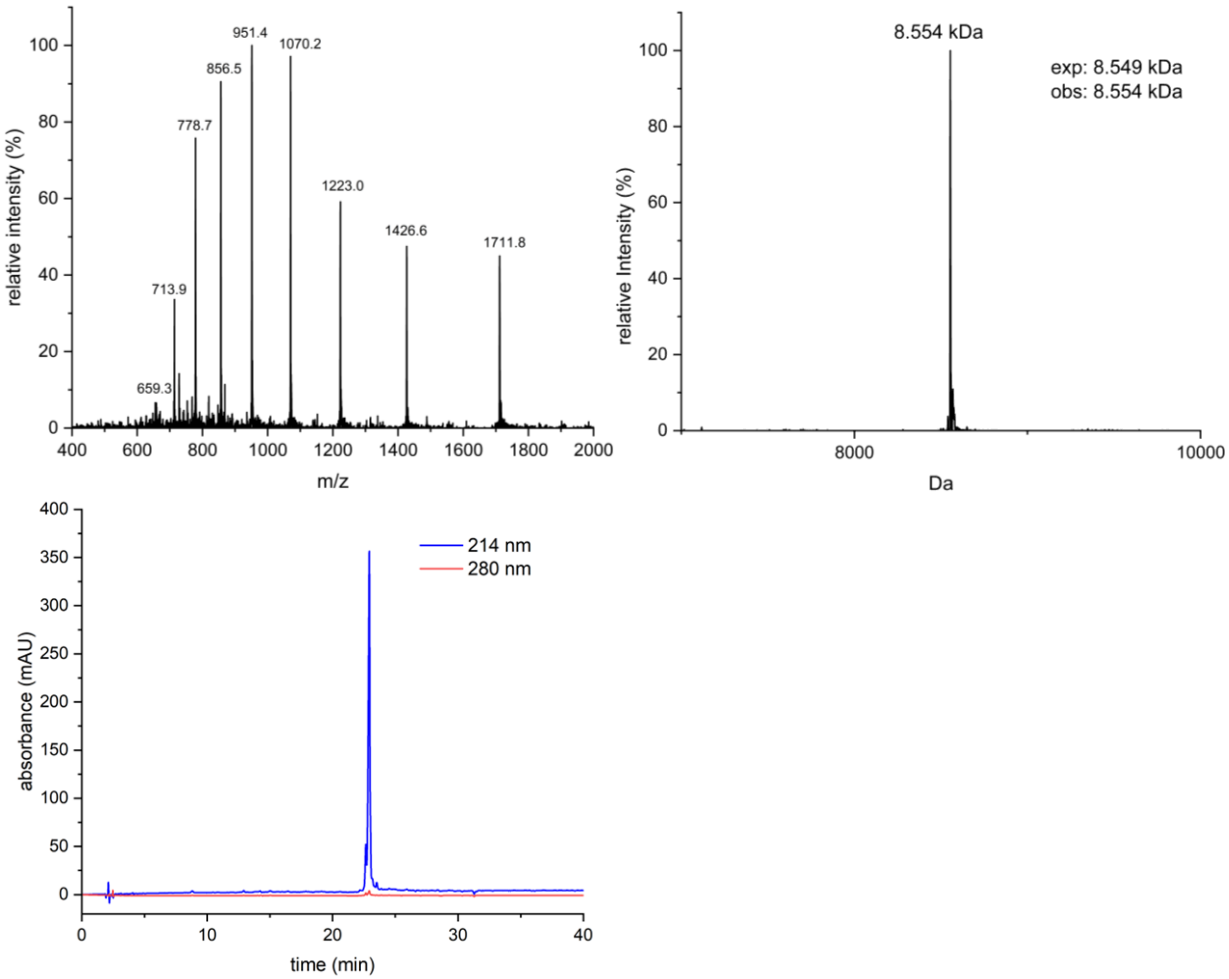

Figure 18 Characterization of isolated $Ub^{K11C}NHNH_2$. ESI-MS (left), deconvoluted mass spectrum (right), analytical RP-HPLC (bottom).

Figure 18 shows ESI-MS, deconvoluted mass spectrum and analytical RP-HPLC of isolated $Ub^{K11C}NHNH_2$.

Ub^{K11C}SR

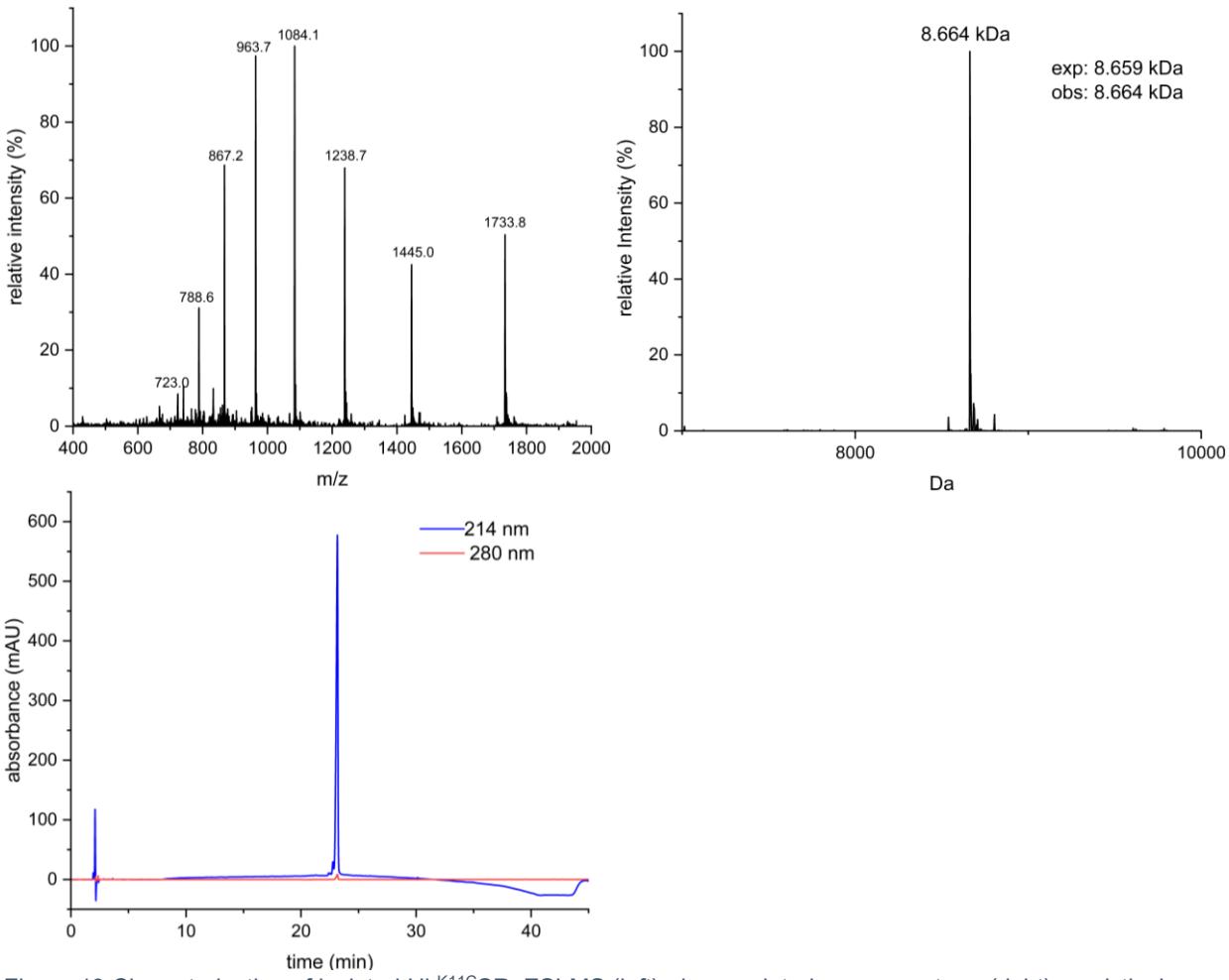

Figure 19 Characterization of isolated Ub^{K11C}SR. ESI-MS (left), deconvoluted mass spectrum (right), analytical RP-HPLC (bottom).

Figure 19 shows ESI-MS, deconvoluted mass spectrum and analytical RP-HPLC of isolated Ub^{K11C}SR.

4.1.6 Generation of Ub$^{K11C}_{pac}$AA:

Since the ubiquitins with cysteine mutation have a free thiol group, these were protected with a phenacyl group before conversion to allylamide to prevent the formation of by-products in the TEC. PAc protection of Ub^{K11C}SR was carried out on a small scale of in an Eppendorf tube. The protein was dissolved in 0.4 mM phosphate buffer (7.2 pH) and 2.5 eq. of PAcBr were added before incubation at 25 °C. The reaction was monitored via LC-MS (Figure 20).

All other reactions with PAcBr in this work were carried out as described in section 3.11.1.

$Ub^{K11C}_{pac}SR$

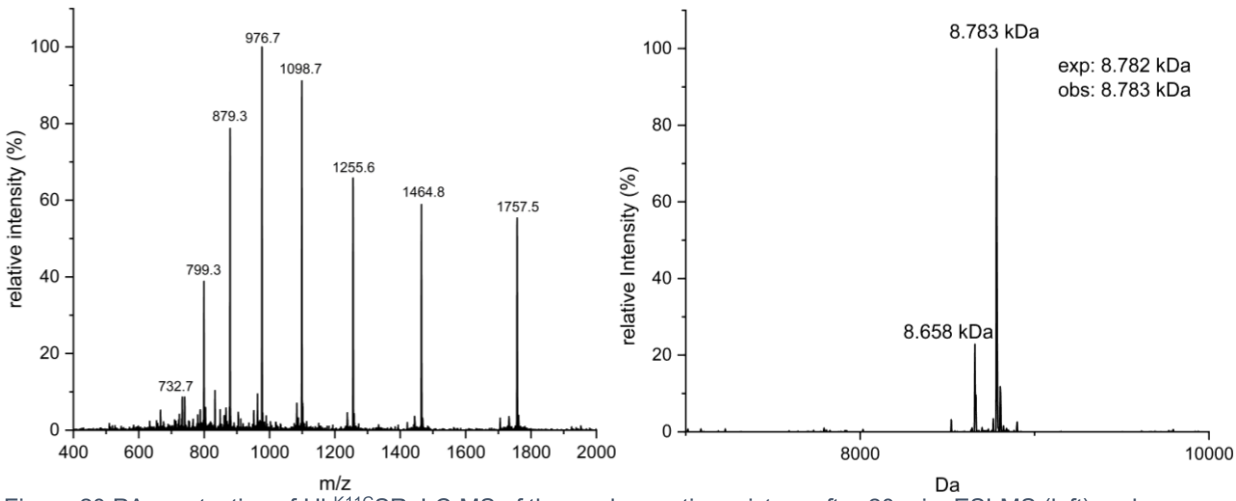

Figure 20 PAc-protection of Ub^{K11C}SR. LC-MS of the crude reaction mixture after 20 min. ESI-MS (left) and deconvoluted mass spectrum (right) of $Ub^{K11C}_{pac}SR$.

According to the masses in the deconvoluted mass spectrum of the crude reaction mixture in (Figure 20, right), the reaction worked, although small amounts of protected, hydrolysed thioester (8.658 kDa) is visible in the spectrum. Since this reaction was carried out on a small scale, the hydrolyzed thioester (8.658 kDa) in the spectrum was neglected.

The conversion of $Ub^{K11C}_{pac}SR$ into an allylamide was performed as described in section 3.9. In contrast to all subsequent reactions, incubation was carried out in a thermal shaker.

$Ub^{K11C}_{pac}AA$

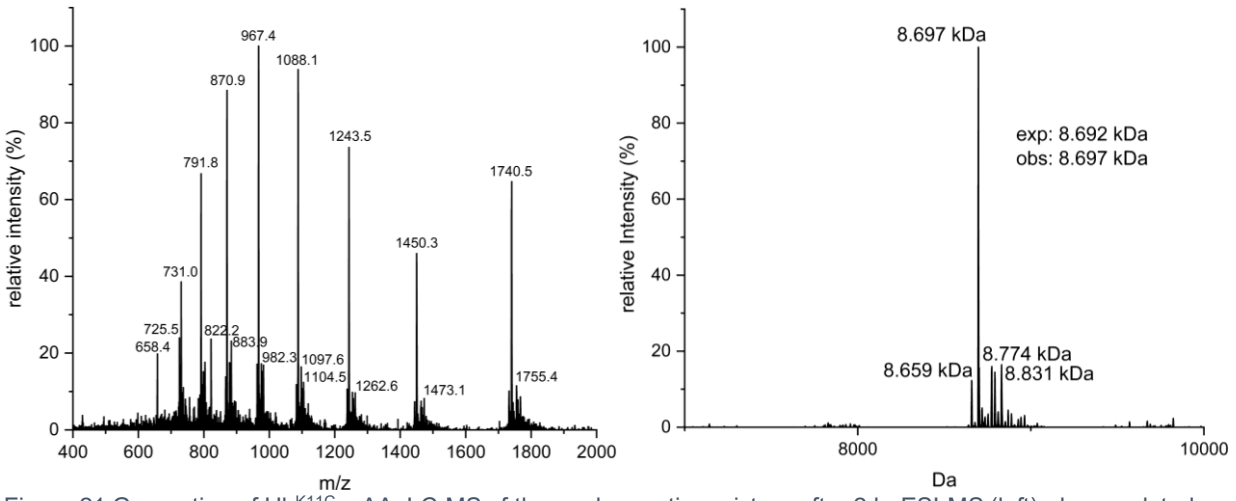

Figure 21 Generation of $Ub^{K11C}_{pac}AA$. LC-MS of the crude reaction mixture after 2 h. ESI-MS (left), deconvoluted mass spectrum (right) of $Ub^{K11C}_{pac}AA$.

Figure 21 shows LC-MS, deconvoluted mass spectrum and analytical RP-HPLC of isolated $Ub^{K11C}_{pac}AA$. Hydrolized, PAc-protected Ub^{K11C}_{pac} (8.659 kDa) is also found here.

4.3 Recombinant production of Ub^{K29C}

4.3.1 Expression and Cleavage of Ub^{K29C}

A 6 L expression of Ub^{K29C}-Mxe-H7-CBD fusion construct and Intein-mediated cleavage of Ub^{K29C}-Mxe-H7-CBD fusion construct was performed as described in section 3.6 and 3.7. The E. coli BL21 (DE3) Rosetta 2 stock which was already available, was used for this purpose.

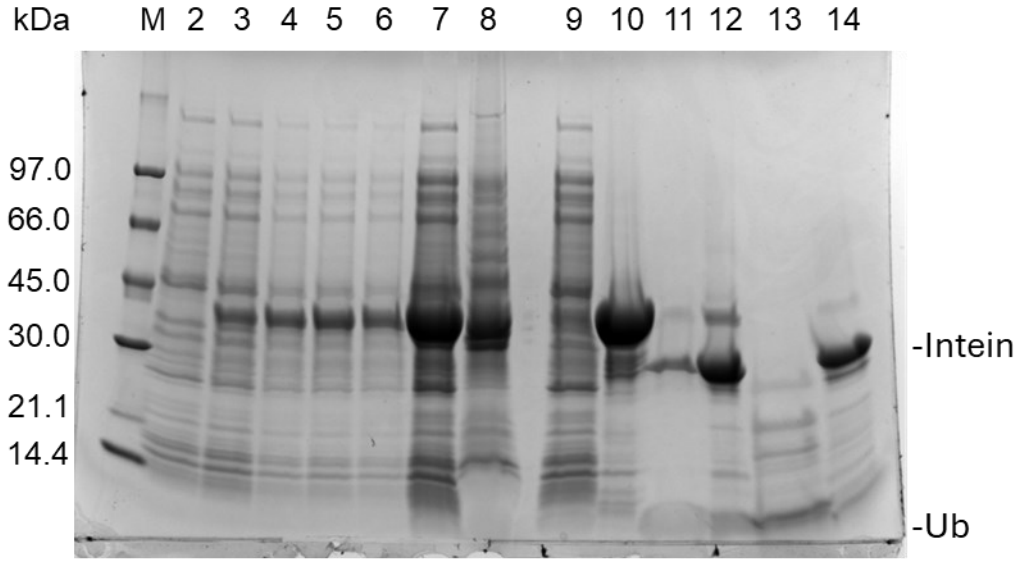

Figure 22 SDS PAGE of 6 L expression and lysis and cleavage of UbK29C. Lane 1 DNA ladder, Lane 2-6 before and every hour after induction, Lane 7 Supernatant after lysis, Lane 8 Pellet after lysis, Lane 9 Supernatant after loading, Lane 10 beads after loading, Lane 11 Supernatant after 72 h MESNa cleavage, Lane 12 beads after 72 h MESNa cleavage, Lane 13 Supernatant after 72 h Hydrazine cleavage, Lane 14 beads after 72 h Hydrazine cleavage.

As shown in the gel in Figure 22, for the mutant Ub^{K29C} expression and both cleavages worked. The mass of the Ub-intein fusion construct (Figure 22, lane 10, approx. 37 kDa) corresponds to the mass of ubiquitin (Ub) and intein (Intein), indicating cleavage. Since experiments by Dr. Susanne Huhmann showed that the optimal duration of protein expression for the wild type is 4 h, this was used for the variant.

The final products (5-9 mg per liter of expression medium for Ub^{K29C}SR and 5 mg per liter of expression medium for $Ub^{K29C}NHNH_2$) were characterized by ESI-MS and RP-HPLC (Figure 23 and Figure 24).

$Ub^{K29C}NHNH_2$

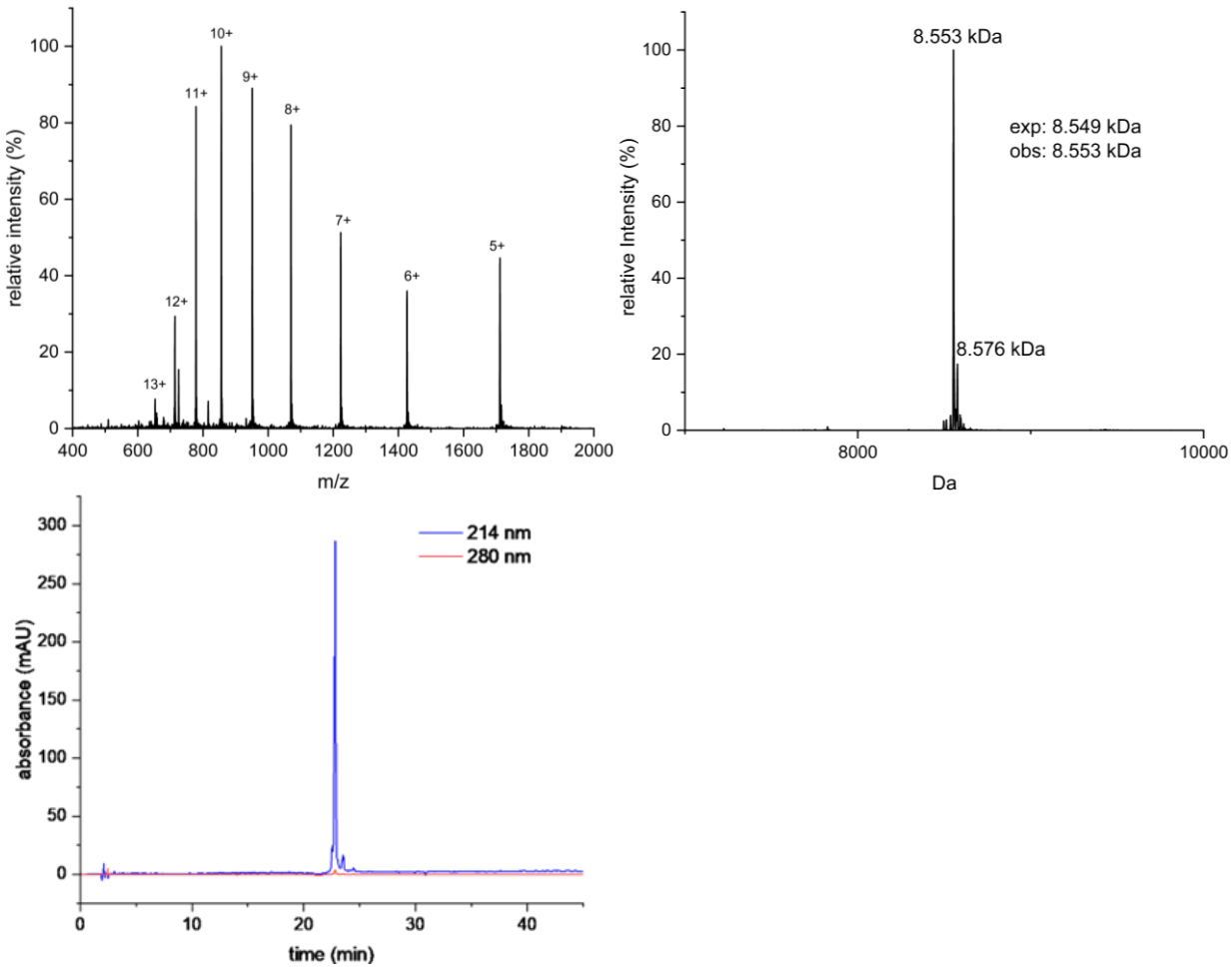

Figure 23 Characterization of isolated $Ub^{K29C}NHNH_2$. ESI-MS (left), deconvoluted mass spectrum (right), analytical RP-HPLC (bottom).

Figure 23 shows ESI-MS, deconvoluted mass spectrum and analytical RP-HPLC of isolated $Ub^{K29C}NHNH_2$.

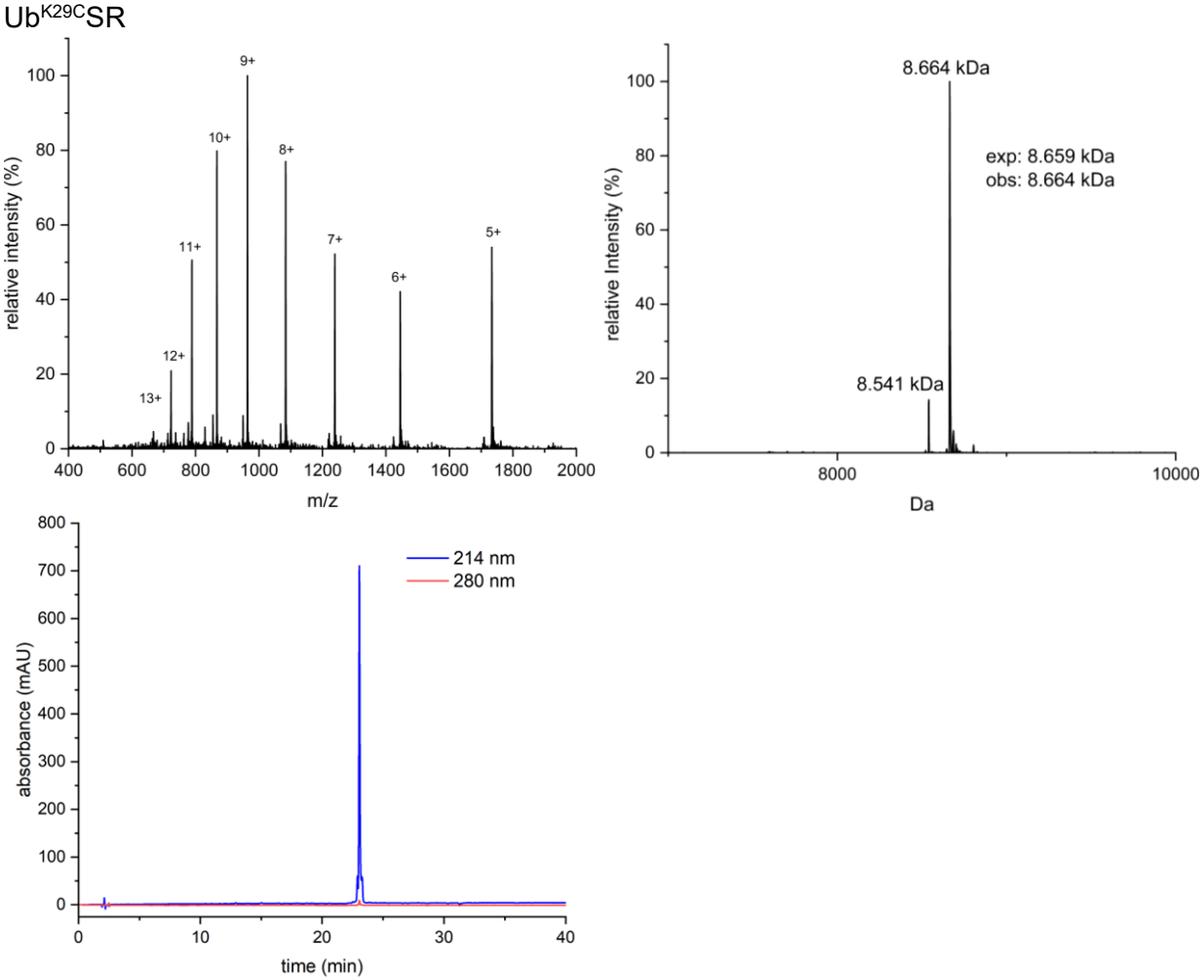

Figure 24 Characterization of isolated Ub^{K29C}SR. ESI-MS (left), deconvoluted mass spectrum (right), analytical RP-HPLC (bottom).

Figure 24 shows ESI-MS, deconvoluted mass spectrum and analytical RP-HPLC of isolated Ub^{K29C}SR Minor impurity of 8.541 kDa in this spectrum refers to the hydrolyzed thioester of Ub^{K29C}SR.

4.3.2 Generation of Ub$^{K29C}_{pac}$AA:

The chemoselective PAc-protection of the free thiol was performed at 25°C using 2.5 eq. PAcBr in 0.4 mM phoshate buffer (pH 7.2) (section 3.11.1). Reaction monitoring via LCMS (Figure 25) showed quantitative conversion (8.783 kDa) of the starting material after 20 min. The species with a mass of 8.658 kDa in the spectrum corresponds to the protected, but hydrolysed protein.

$Ub^{K29C}{}_{pac}SR$

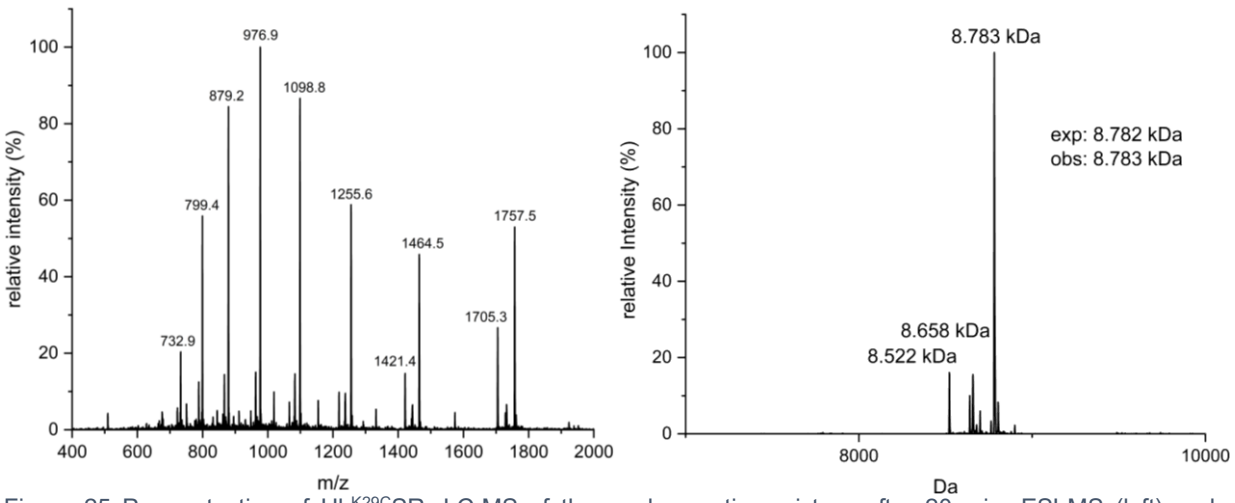

Figure 25 Pac-protection of $Ub^{K29C}SR$. LC-MS of the crude reaction mixture after 20 min. ESI-MS (left) and deconvoluted mass spectrum (right) of $Ub^{K29C}{}_{pac}SR$.

Conversion of the $Ub^{K29C}{}_{pac}SR$ to a C-terminal allylamide was carried out as described in section 3.9. Therefore, the crude reaction mixture from PAc-protection was diluted with water to a final protein concentration of 1.5 mg/mL. Next, allylamine was added to a final concentration of 500 mM and stirred on ice for 2 hours. Reaction monitoring via LCMS (Figure 26) showed quantitative conversion (8.783 kDa) of the starting material after 20 min with hydrolysed, protected thioester (8.658 kDa) being also visible in the spectrum. This mass is not visible in the spectrum after purification (Figure 21) which showed a successful separation of the desired protein.

$Ub^{K29C}{}_{pac}AA$

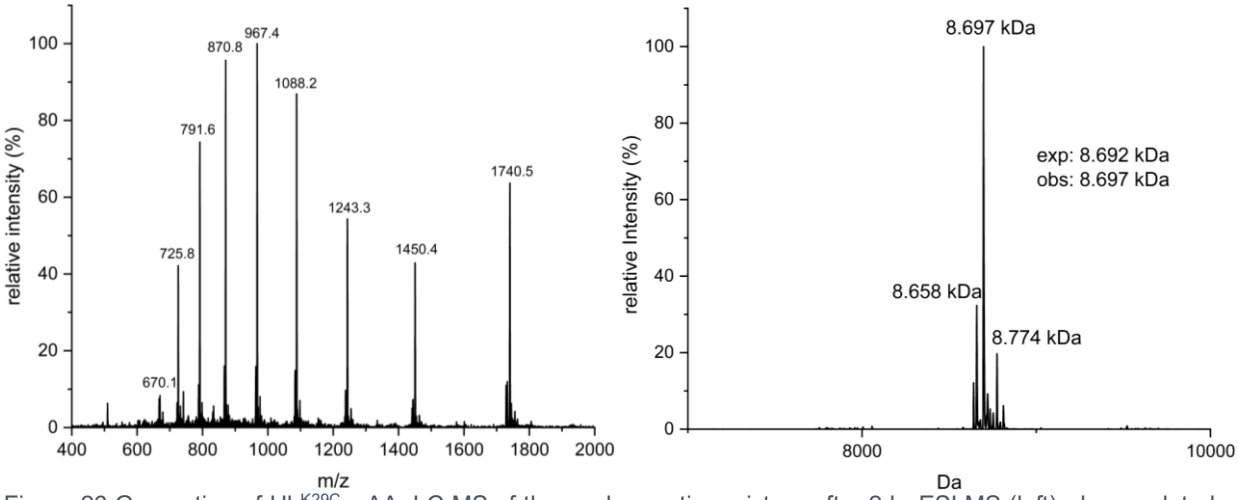

Figure 26 Generation of $Ub^{K29C}{}_{pac}AA$. LC-MS of the crude reaction mixture after 2 h. ESI-MS (left), deconvoluted mass spectrum (right) of $Ub^{K29C}{}_{pac}AA$.

The crude mixture was purified by RP-HPLC to yield 5.2 mg (42 %) of $Ub^{K29C}{}_{pac}AA$ from 3 L of E. coli culture for the first and 28.5 mg (61 %) from 3 L of E. coli culture for the second expression, which were characterized by ESI-MS and RP-HPLC (Figure 27).

Comparing the spectra (Figure 25 + Figure 26) of this species with those of Ub^{K11C} (Figure 20 + Figure 21), amount of hydrolysis seemed to be around the same level.

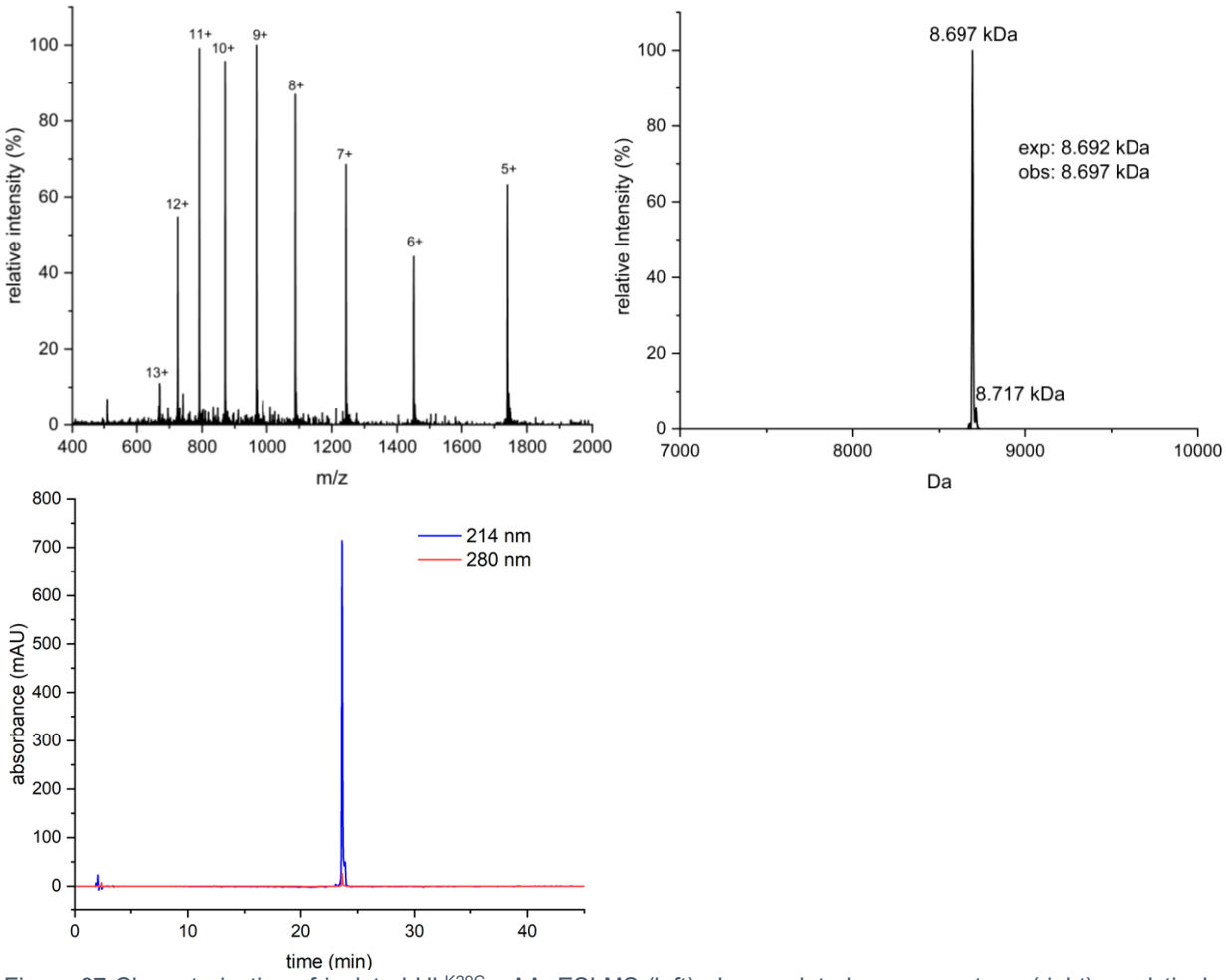

Figure 27 Characterization of isolated $Ub^{K29C}{}_{pac}AA$. ESI-MS (left), deconvoluted mass spectrum (right), analytical RP-HPLC (bottom).

Figure 27 shows ESI-MS, deconvoluted mass spectrum and analytical RP-HPLC of isolated $Ub^{K29C}{}_{pac}AA$

4.4 Recombinant production of Ub^{K48C}

4.4.1 Expression of Ub^{K48C}

A 6 L expression of Ub^{K48C}-Mxe-H7-CBD fusion construct was performed as described in section 3.6. The E. coli BL21 (DE3) Gold stock which was already available, was used for this purpose. Intein-mediated cleavage of Ub^{K48C}-Mxe-H7-CBD fusion construct was performed as described in section 3.7.

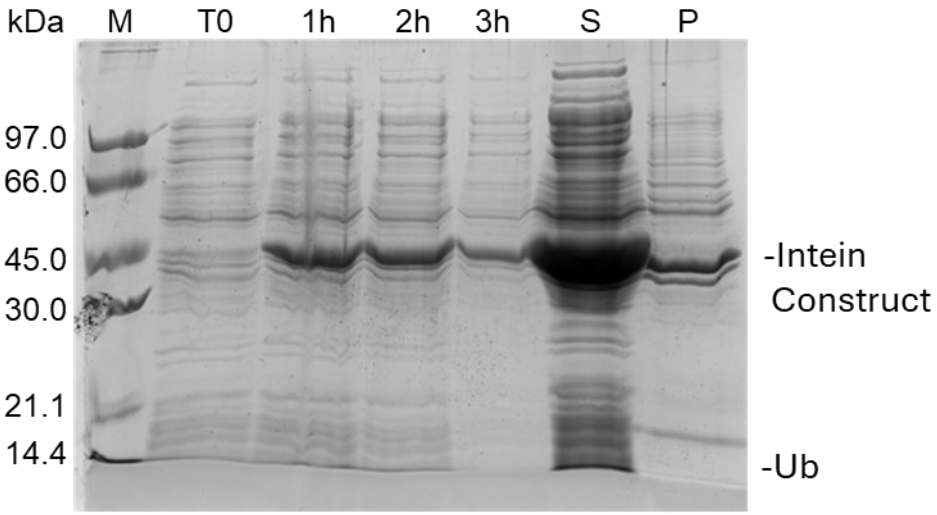

Figure 28 SDS PAGE of 6 L expression and lysis of Ub^{K48C}. Lane 1 DNA ladder, Lane 2-5 before and every hour after induction, Lane 6 Supernatant (S) after lysis, Lane 7 Pellet (P) after lysis.

Expression and lysis worked as usual (Figure *28*). Since experiments by Dr. Susanne Huhmann showed that the optimal duration of protein expression for the wild type is 3 h, this was used for the variant.

4.4.2 Cleavage of Ub^{K48C}-intein fusion construct

Cleavage of Ub^{K48C}-intein fusion construct was performed as described in section 3.7.

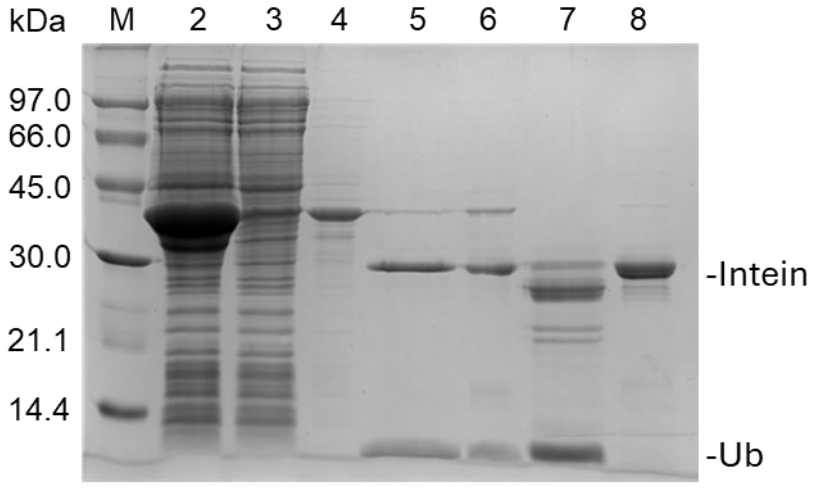

Figure 29 SDS PAGE of loading and cleavages for Ub^{K48C}. Lane 1 Marker, Lane 2 Supernatant before loading, Lane 3 Supernatant after loading, Lane 4 Beads after loading, Lane 5 Supernatant after 72 h MESNa cleavage, Lane 6 Beads 72 h after MESNa cleavage, Lane 7 Supernatant after 72 h Hydrazine cleavage, Lane 8 Beads after 72 h Hydrazine cleavage.

As shown in the SDS-PAGE in Figure 29, for the mutant Ub^{K48C} both cleavages worked as usual.

The final products (7.3-7.6 mg per liter of expression medium for $Ub^{K48C}SR$ and 6.7-8.7 mg per liter of expression medium for $Ub^{K48C}NHNH_2$) were characterized by ESI-MS and RP-HPLC (Figure 30 and Figure 31).

$Ub^{K48C}NHNH_2$

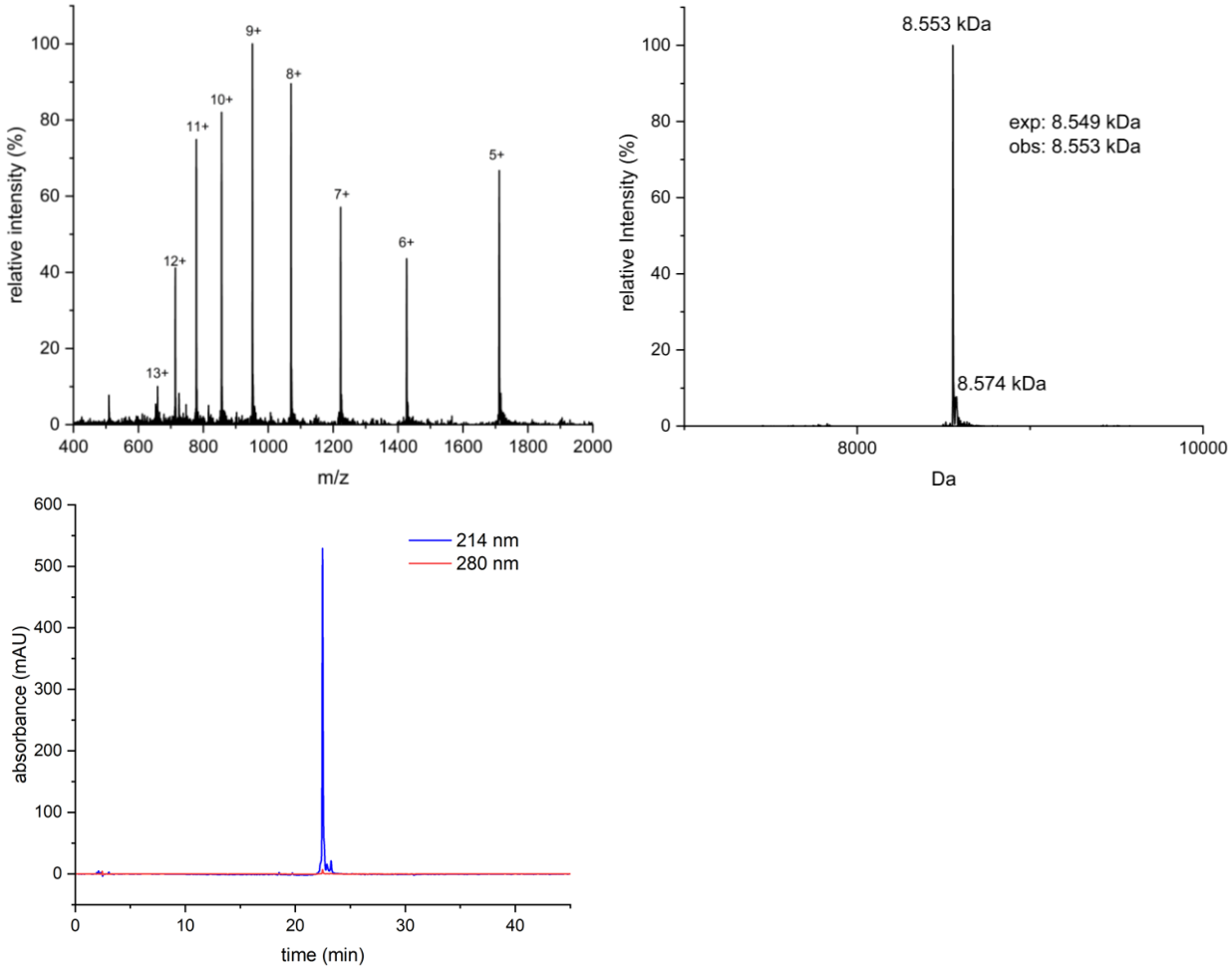

Figure 30 Characterization of isolated $Ub^{K48C}NHNH_2$. ESI-MS (left), deconvoluted mass spectrum (right), analytical RP-HPLC (bottom).

Figure 30 shows ESI-MS, deconvoluted mass spectrum and analytical RP-HPLC of isolated $Ub^{K48C}NHNH_2$.

Ub^{K48C}SR

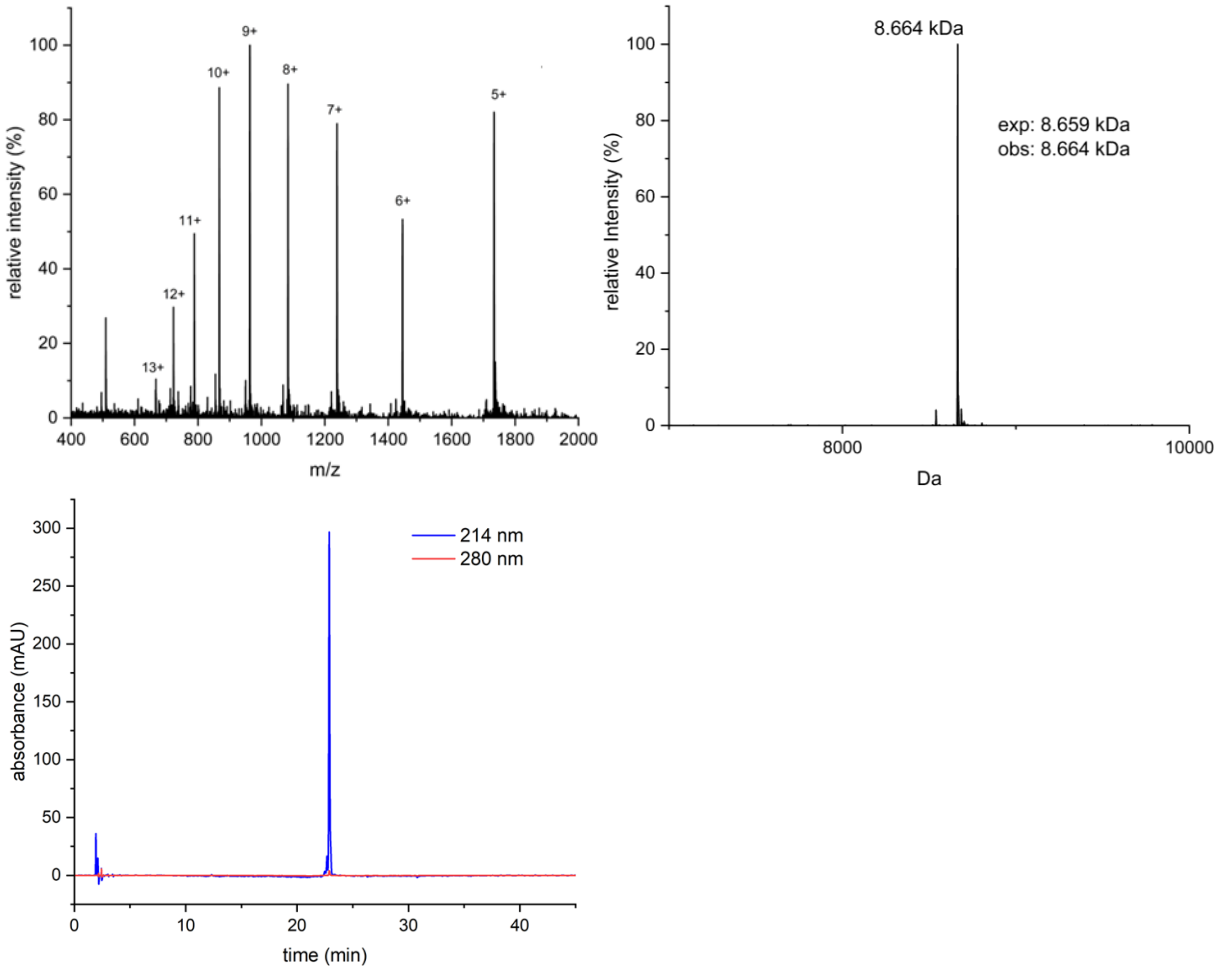

Figure 31 Characterization of isolated Ub^{K48C}SR. ESI-MS (left), deconvoluted mass spectrum (right), analytical RP-HPLC (bottom).

Figure 31 shows ESI-MS, deconvoluted mass spectrum and analytical RP-HPLC of isolated Ub^{K48C}SR.

.

4.4.3 Generation of $Ub^{K48C}{}_{pac}AA$:

PAc protection (Figure 32) was carried out as described in section 3.11.1.

$Ub^{K48C}{}_{pac}SR$

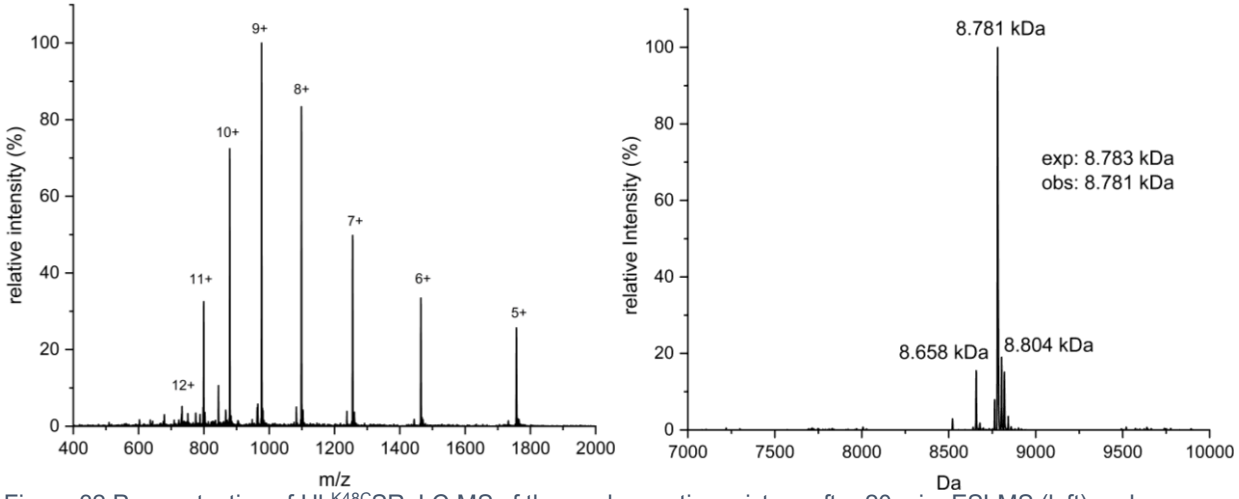

Figure 32 Pac-protection of $Ub^{K48C}SR$. LC-MS of the crude reaction mixture after 20 min. ESI-MS (left) and deconvoluted mass spectrum (right) of $UbK48C_{pac}SR$.

$Ub^{K48C}{}_{pac}AA$

The conversion of the $Ub^{K48C}{}_{pac}SR$ into a C-terminal allylamide (Figure 33) was carried out as described in section 3.9.

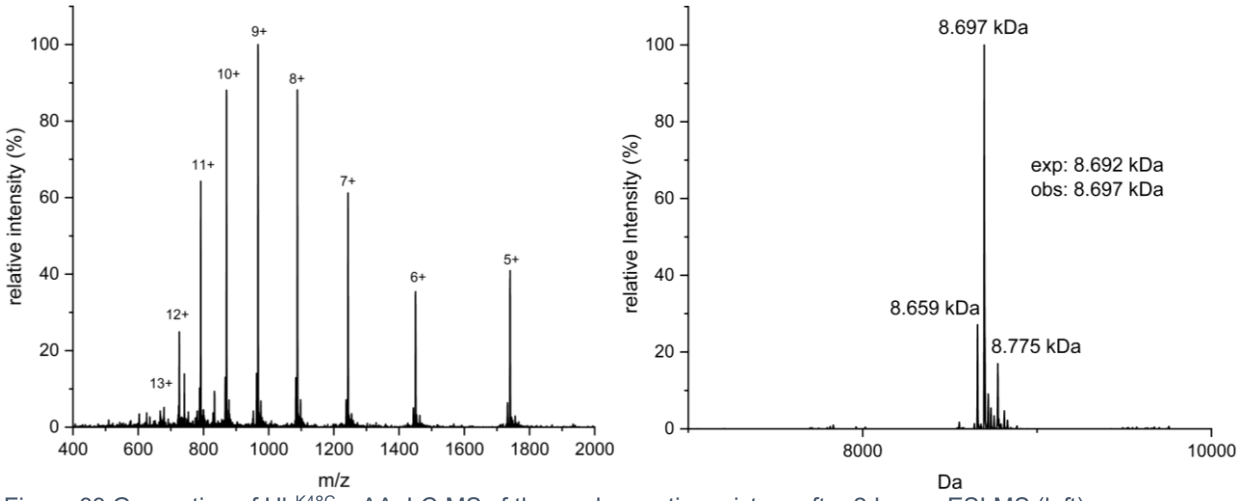

Figure 33 Generation of $Ub^{K48C}{}_{pac}AA$. LC-MS of the crude reaction mixture after 2 hours. ESI-MS (left), deconvoluted mass spectrum(right) of $Ub^{K48C}{}_{pac}AA$.

The crude mixture was purified by RP-HPLC to yield 13.3 mg (71%) of $Ub^{K48C}{}_{pac}AA$ from 3 L of E. coli culture for the first expression, 16.4 mg (80 %) from 3L of E. coli culture for the second expression and 19.5 mg (75 %) from 3 L of E. coli culture for the third expression, which were characterized by ESI-MS and RP-HPLC (Figure 34).

Comparing the spectra (Figure 32 + Figure 33) of this species with those of Ub^{K29C} and Ub^{K11C}, the level of hydrolysis is at the same level.

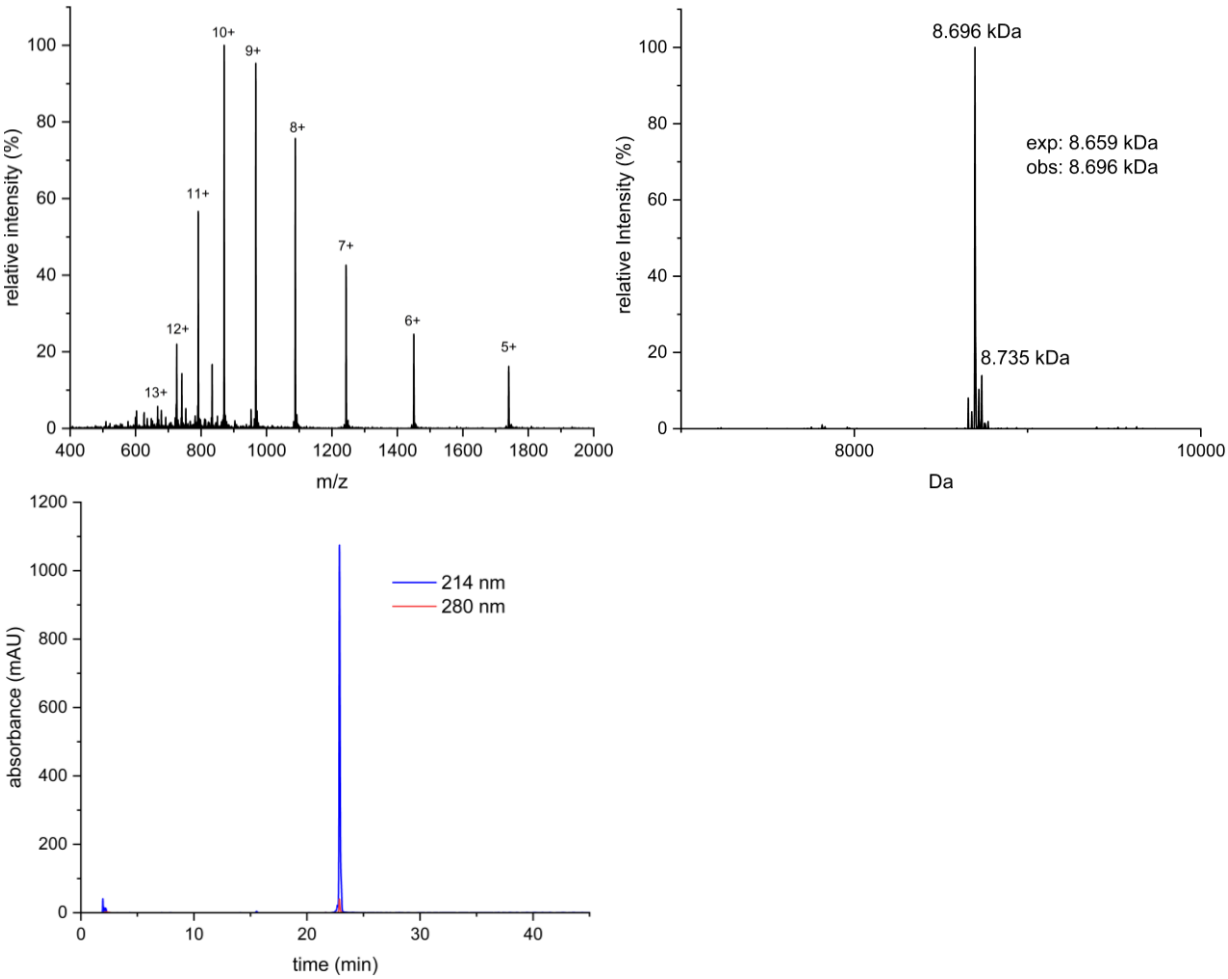

Figure 34 Characterization of isolated $Ub^{K48C}{}_{pac}AA$. ESI-MS (left), deconvoluted mass spectrum (right), analytical RP-HPLC (bottom).

Figure 34 shows ESI-MS, deconvoluted mass spectrum and analytical RP-HPLC of isolated $Ub^{K48C}{}_{pac}AA$

4.5 Recombinant production of Ub^{K63C}

4.5.1 Expression of Ub^{K63C} fusion construct

A 6 L expression of Ub^{K63C}-Mxe-H7-CBD fusion construct was performed as described in section 3.6. The E. coli BL21 (DE3) Gold stock which was already available, was used for this purpose. Intein-mediated cleavage of Ub^{K63C}-Mxe-H7-CBD fusion construct was performed as described in section 3.7.

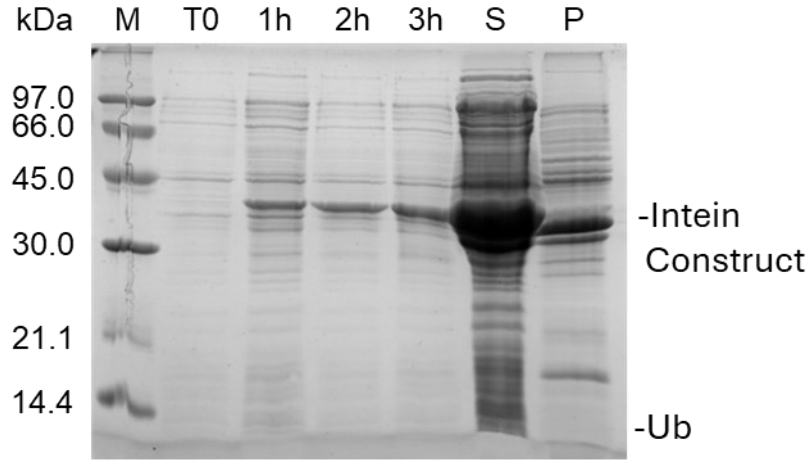

Figure 35 SDS PAGE of 6 L expression and lysis of Ub^{K63C}. Lane 1 DNA ladder, Lane 2-5 before and every hour after induction, Lane 6 Supernatant after lysis, Lane 7 Pellet after lysis.

Expression and lysis worked as usual (Figure *35*). Since experiments by Dr. Susanne Huhmann showed that the optimal duration of protein expression for the wild type is 3 h, this was used for the variant.

4.5.2 Cleavage of Ub^{K63C}-intein fusion construct

Cleavage of Ub^{K63C}-intein fusion construct was performed as described in section 3.7.

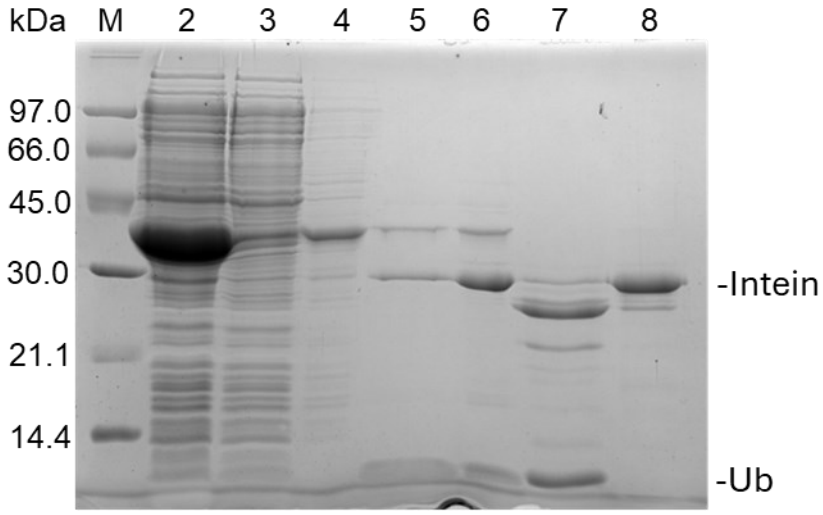

Figure 36 SDS PAGE of loading and cleavages for Ub^{K63C}. Lane 1 Marker, Lane 2 Supernatant before loading, Lane 3 Supernatant after loading, Lane 4 Beads after loading, Lane 5 Supernatant after 72 h MESNa cleavage, Lane 6 Beads after 72 h MESNa cleavage, Lane 7 Supernatant after 72 h Hydrazine cleavage, Lane 8 Beads after 72 h Hydrazine cleavage.

As shown on the SDS-PAGE in Figure 36, for the mutant Ub^{K63C} expression and both cleavages worked.

The final product (3-10 mg per liter of expression medium for $Ub^{K63C}SR$ and 6-7 mg per liter of expression medium for $Ub^{K63C}NHNH_2$) was characterized by ESI-MS and RP-HPLC (Figure 37 and Figure 38).

$Ub^{K63C}NHNH_2$

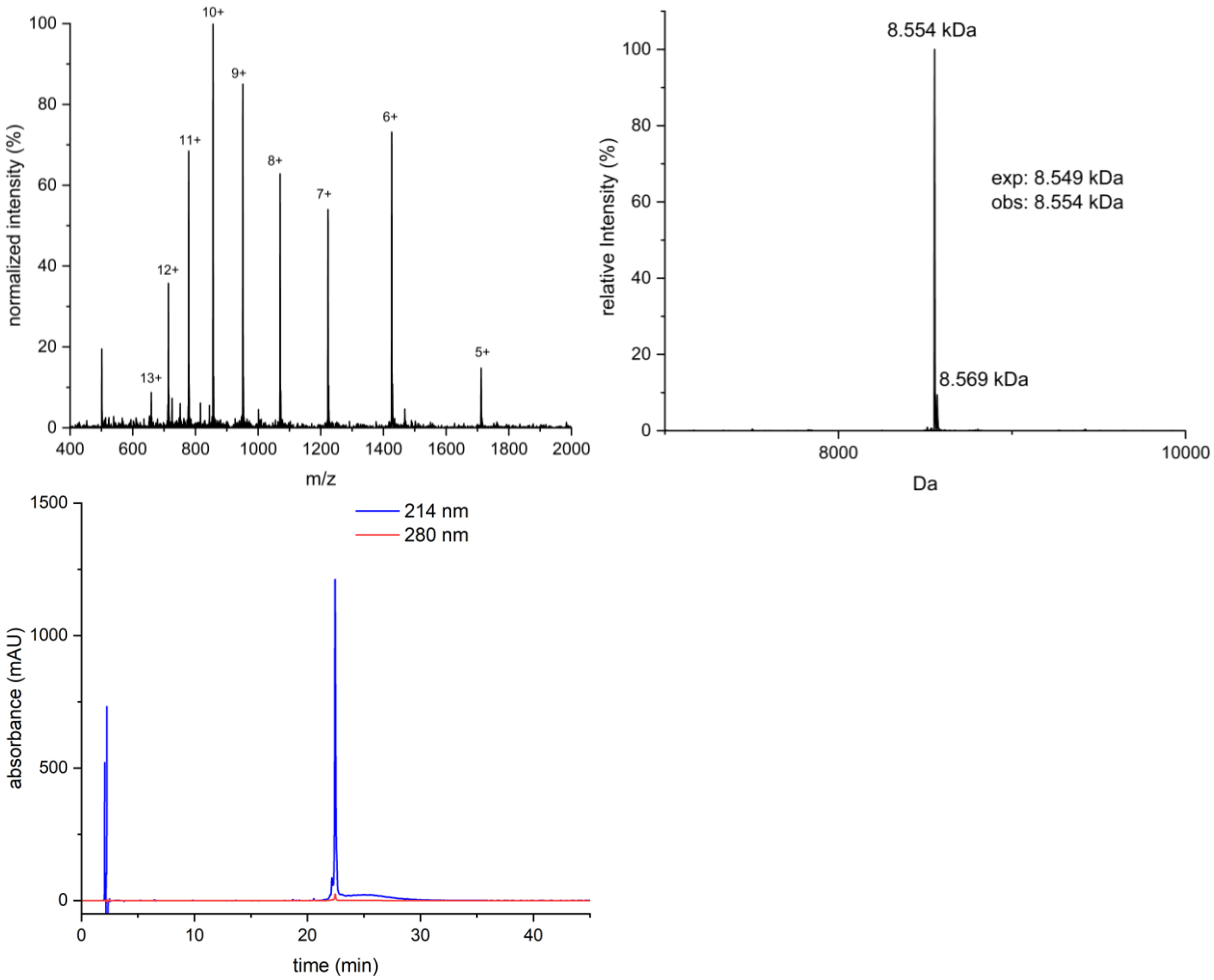

Figure 37 Characterization of isolated $Ub^{K63C}NHNH_2$. ESI-MS (left), deconvoluted mass spectrum (right), analytical RP-HPLC (bottom).

Figure 37 shows ESI-MS, deconvoluted mass spectrum and analytical RP-HPLC of isolated $Ub^{K63C}NHNH_2$. The species with a mass of 8.569 kDa may correspond to $Ub^{K63C}NHNH_2$ which is also modificated on the N-terminus with a hydrazide group.

$Ub^{K63C}SR$

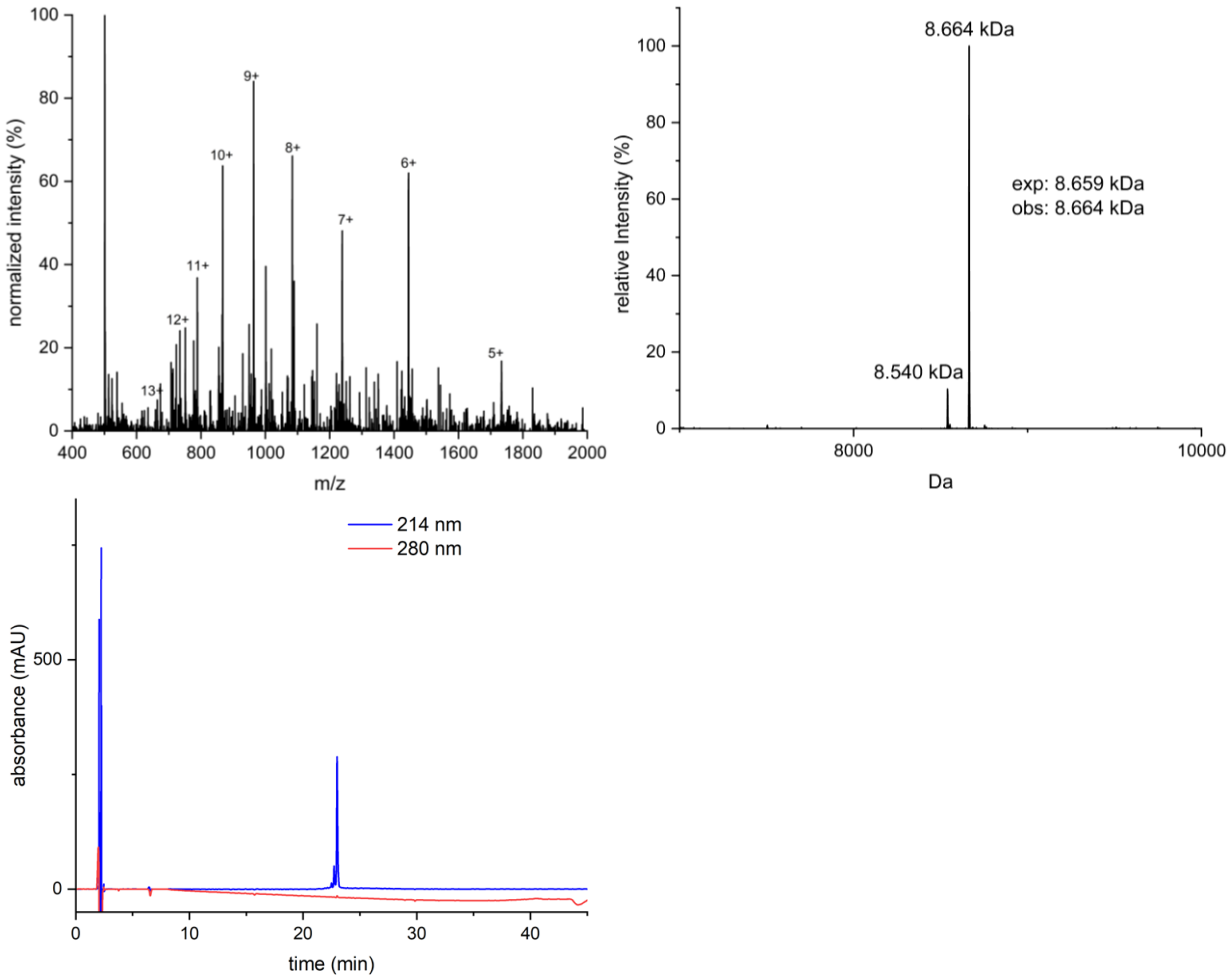

Figure 38 Characterization of isolated $Ub^{K63C}SR$. ESI-MS (left), deconvoluted mass spectrum (right), analytical RP-HPLC (bottom).

Figure 38 shows ESI-MS, deconvoluted mass spectrum and analytical RP-HPLC of isolated $Ub^{K63C}SR$. Hydrolyzed thioester (8.540 kDa) is also visible in the spectrum. When comparing the two spectra in Figure 38, it is noticeable that the spectrum (left) looks significantly less clean than the deconvoluted spectrum calculated from it (right). It is possible that the dissolved concentration of protein was too low and the remaining signals in the spectrum represent background signals that could not be assigned to a mass by the program. This also is in accordance with the absorbance shown in the RP- HPLC chromatogram (bottom) which is significantly lower than for other spectra.

4.5.3 Generation of $Ub^{K63C}{}_{pac}AA$

The PAc protection was carried out as described in section 3.11.1.

$Ub^{K63C}{}_{pac}SR$

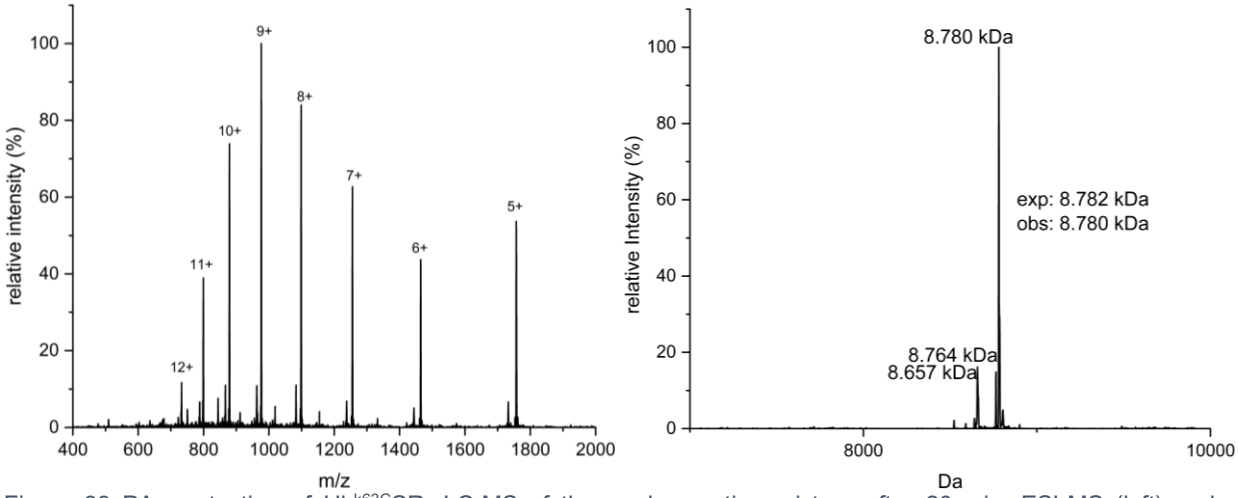

Figure 39 PAc-protection of $Ub^{k63C}SR$. LC-MS of the crude reaction mixture after 20 min. ESI-MS (left) and deconvoluted mass spectrum (right) of $Ub^{K63C}{}_{pac}SR$.

The conversion of the $Ub^{K63C}{}_{pac}SR$ into a C-terminal allylamide was carried out as described in section 3.9.

$Ub^{K63C}{}_{pac}AA$

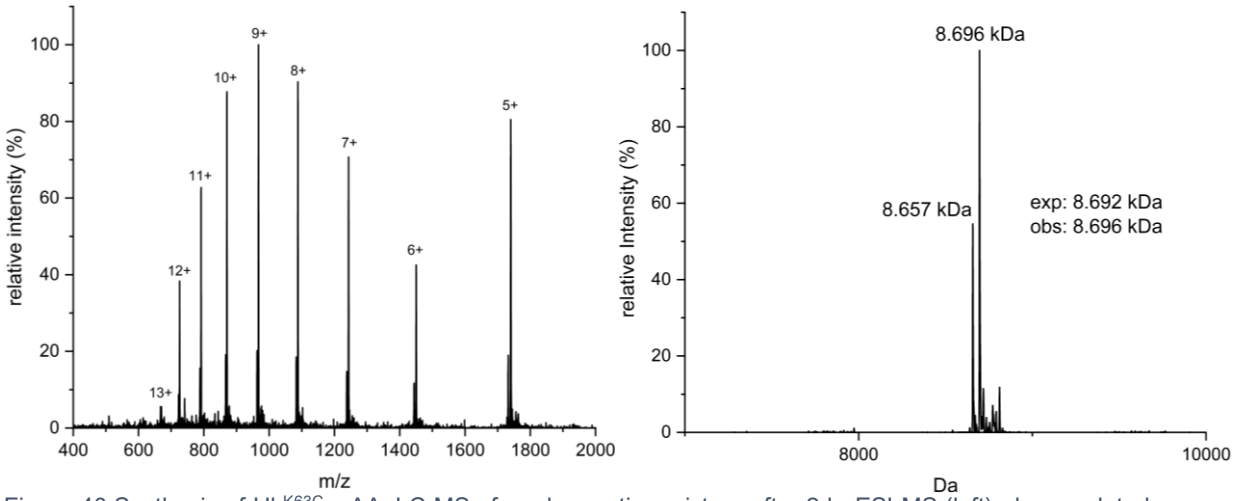

Figure 40 Synthesis of $Ub^{K63C}{}_{pac}AA$. LC-MS of crude reaction mixture after 2 h. ESI-MS (left), deconvoluted mass spectrum (right) of $Ub^{K63C}{}_{pac}AA$.

The crude mixture was purified by RP-HPLC to yield 6.7 mg (25 %) of $Ub^{K63C}{}_{pac}AA$ from 3 L of E. coli culture and characterized by ESI-MS and RP-HPLC (Figure 41).

Comparing the spectra (Figure 39 + Figure 40) of this mutant with those of Ub^{K11C}, Ub^{K29C} and Ub^{K48C}, hydrolysis (8.657 kDa) is the same level.

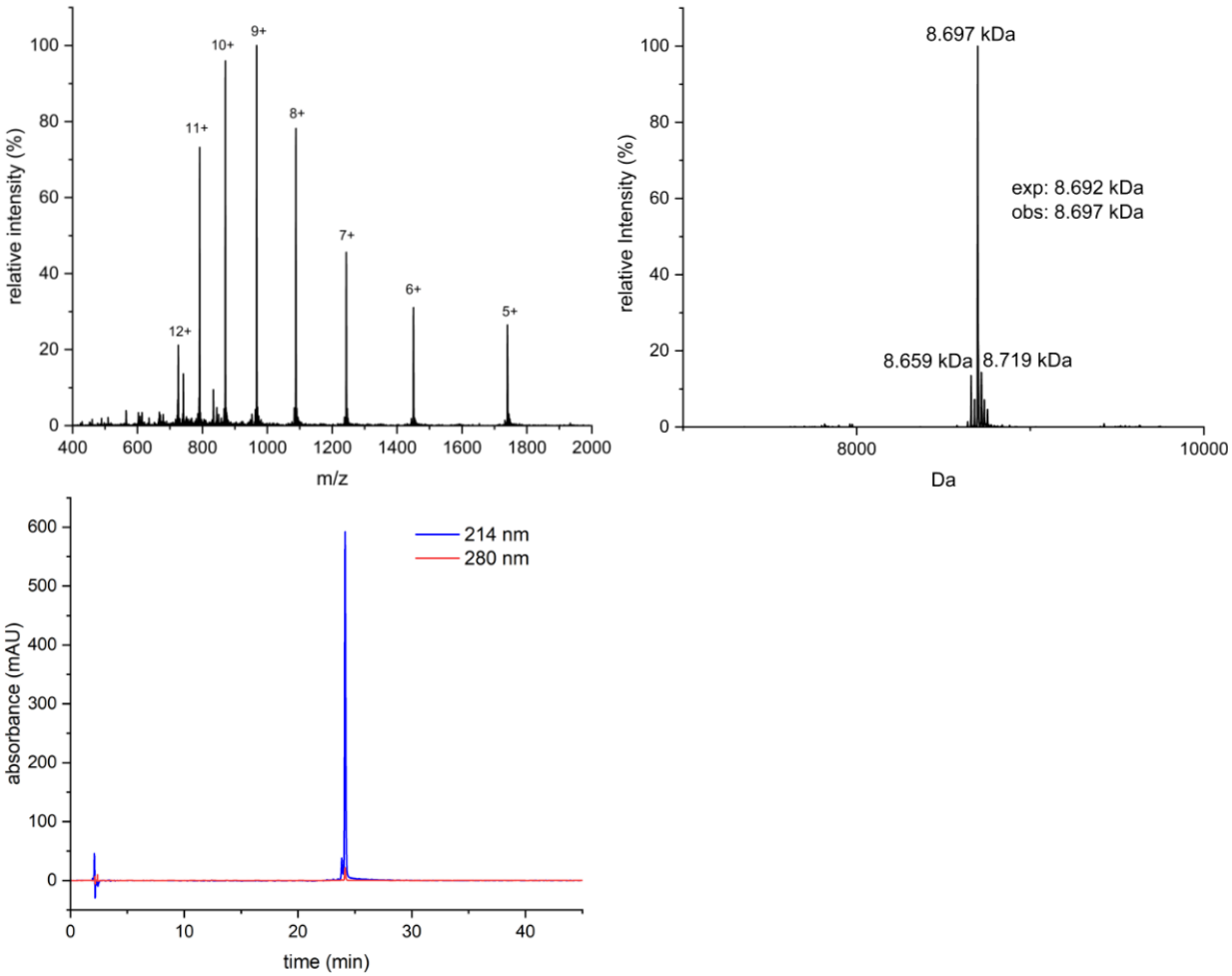

Figure 41 Characterization of isolated of $Ub^{K63C}{}_{pac}AA$. ESI-MS (left), deconvoluted mass spectrum (right), analytical RP-HPLC (bottom).

Figure 41 shows ESI-MS, deconvoluted mass spectrum and analytical RP-HPLC of isolated $Ub^{K63C}{}_{pac}AA$.

4.5 Discussion of the Expression of Ub building blocks

When expressing the C-terminal thioester of Ub^{wt}, the yield was 16.7 mg per liter of expression volume.

In comparison to the wildtype, the yields of the cysteine mutants of ubiquitin building blocks were significantly lower and differed greatly from one another. In the case of the thioester, the yields of the pure protein for the variants Ub^{K11C} and Ub^{K29C} were 10-15 mg per liter and 5-9 mg per liter. Ub^{K48C} and Ub^{K63C} yielded significantly less pure protein with 0-2.6 mg per liter with most of the protein ending up in a less pure pool. For the thioester also impure pools were used to get the corresponding allylamide, since another purification step happened afterwards. The different amounts and distributions among the pools are strongly dependent on the expressed amount (visible in SDS-PAGE of the respective expression), cleavage (turnover visible in SDS-PAGE of the respective cleavage) and the purification.

For the hydrazide, the yields were also lower than for the wildtype with 6.6-8.6 mg per liter but similar for the different mutant expressions.

In literature, the yield of recombinantly expressed ubiquitin is described higher than in this thesis. Here[36], the yield was stated to be 50-100 mg of purified ubiquitin per liter of cell culture. However, it should be mentioned here that this is only the wild type with an additional amino acid (D77 at the C-terminus) or the mutant UbK48C. Also, in this study another plasmid (pET3a) and possibly another vector was used and no intein, CBD or His-tag at the C-terminus of the ubiquitin were additionally expressed in E. coli. Comparing the yield with this work would not be fair as of different constructs used and since the Intein fusion construct is much larger. Furthermore, the ubiquitin monomers in this study were purified by acid precipitation using perchloric acid (>90 % purity) instead of RP-HPLC.

When $Ub^{wt}SR$ was converted into allylamide, the yield was 71.6 % with around 90 % purity in the deconvoluted mass spectrum (Figure 11).

For the cysteine mutants, the conversion yield was lower being around 40-70%. Also, there was significantly more hydrolysed thioester found after PAc-protection and generation of the allylamide visible than for the wildtype (Figure 10). The additional step of protection at room temperature may enhance hydrolysis here.

In a study[61], synthesis of C-terminal allylamide was carried out by a C-terminal hydrolase (UCH) with a yield of 30% rather than starting from a thioester. Purification was carried out using cation exchange chromatography. This is significantly lower compared to the yields in this work and highlights that inteins are suitable tools to generate sufficient amounts of C-terminally modified Ub building blocks.

4.6 TEC without PAc protection

Initially, all four $Ub^{KxC}NHNH_2$ mutants were coupled to $Ub^{wt}AA$ using standard conditions as described in section 3.10. Therefore, the building blocks were dissolved in buffer (250 mM NaOAc, 6 M GndHCl, pH 5.4), TCEP and LAP added for a final concentration of 1.5 mM and 5 mM. After radiation the crude reaction mixture was frozen at -80°C until purification.

4.6.1 $DiUb^{wt\text{-}K11C}NHNH_2$

For this reaction $Ub^{wt}AA$ and $Ub^{K11C}NHNH_2$ were used as building blocks to generate the respective diubiquitin (reaction scheme shown in Figure 42).

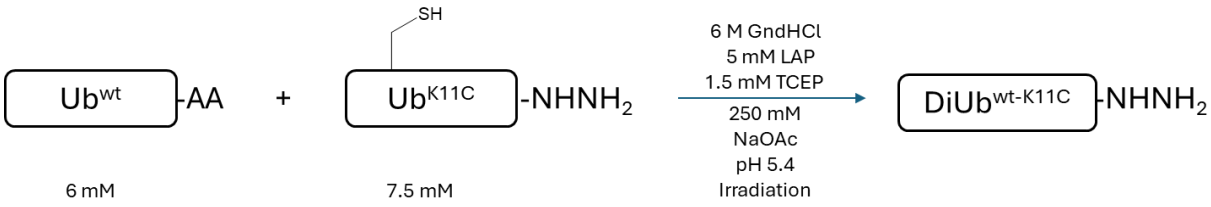

Figure 42 Reaction scheme for the TEC reaction between $Ub^{wt}AA$ and $Ub^{K11C}NHNH_2$.

RP-HPLC, ESI-MS and deconvoluted mass spectrum of this reaction is shown in Figure 43.

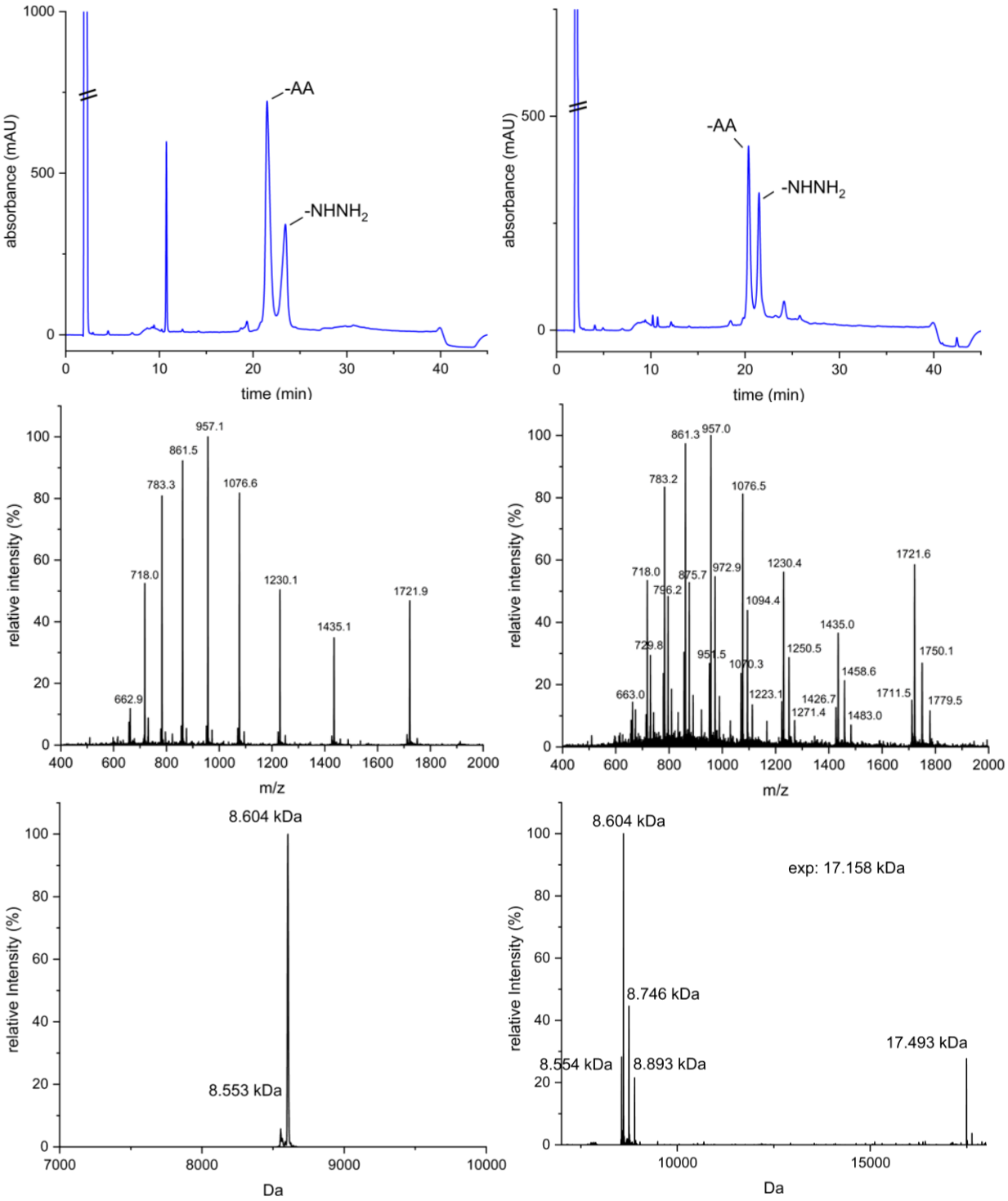

Figure 43 Photoinitiated TEC between $Ub^{wt}AA$ and $Ub^{K11C}NHNH_2$. Characterization of the crude reaction mixture before (left) and after (right) irradiation. Analytical RP-HPLC (top), ESI-MS (middle) and deconvoluted mass spectrum (bottom).

Despite multiple freeze-thaw cycles, the $Ub^{K11C}NHNH_2$ could not be brought into solution in the required concentration. This is consistent with the peak height of the RP-HPLC chromatogram in Figure 43 (bottom, left), as the associated mass (8.553 kDa) is barely visible in the deconvoluted spectrum before the actual reaction.

Under these conditions, no product could be detected via LC-MS. As shown in the deconvoluted mass spectrum of the crude after the reaction in Figure 43 (bottom, right), there is no corresponding mass (17.158 kDa) of the desired protein chain. Furthermore, the starting

materials are the dominating species in the mass spectrum after TEC, even though LAP adduct (phosphinate adduct from LAP to the C-terminal allylamide) is visible. Another mass (17.493 kDa) appears in this spectrum which could belong to a modificated diubiquitin species. This mass is approx. 335 Da higher than that of the desired diubiquitin, which suggests that one or more reactions have taken place, but that by-product is being formed instead. However, a closer look at the RP-HPLC chromatogram (Figure 43, top, right) reveals that this species represents only a minimal proportion of the actual reaction mixture, since the corresponding peak (23 min) is barely visible. High intensity in the mass spectra may occur because of relatively high ionisation efficiency of this species.

In the next reaction, an attempt was made to dissolve $Ub^{wt}AA$ in a higher concentration and $Ub^{K11C}NHNH_2$ at a lower concentration.

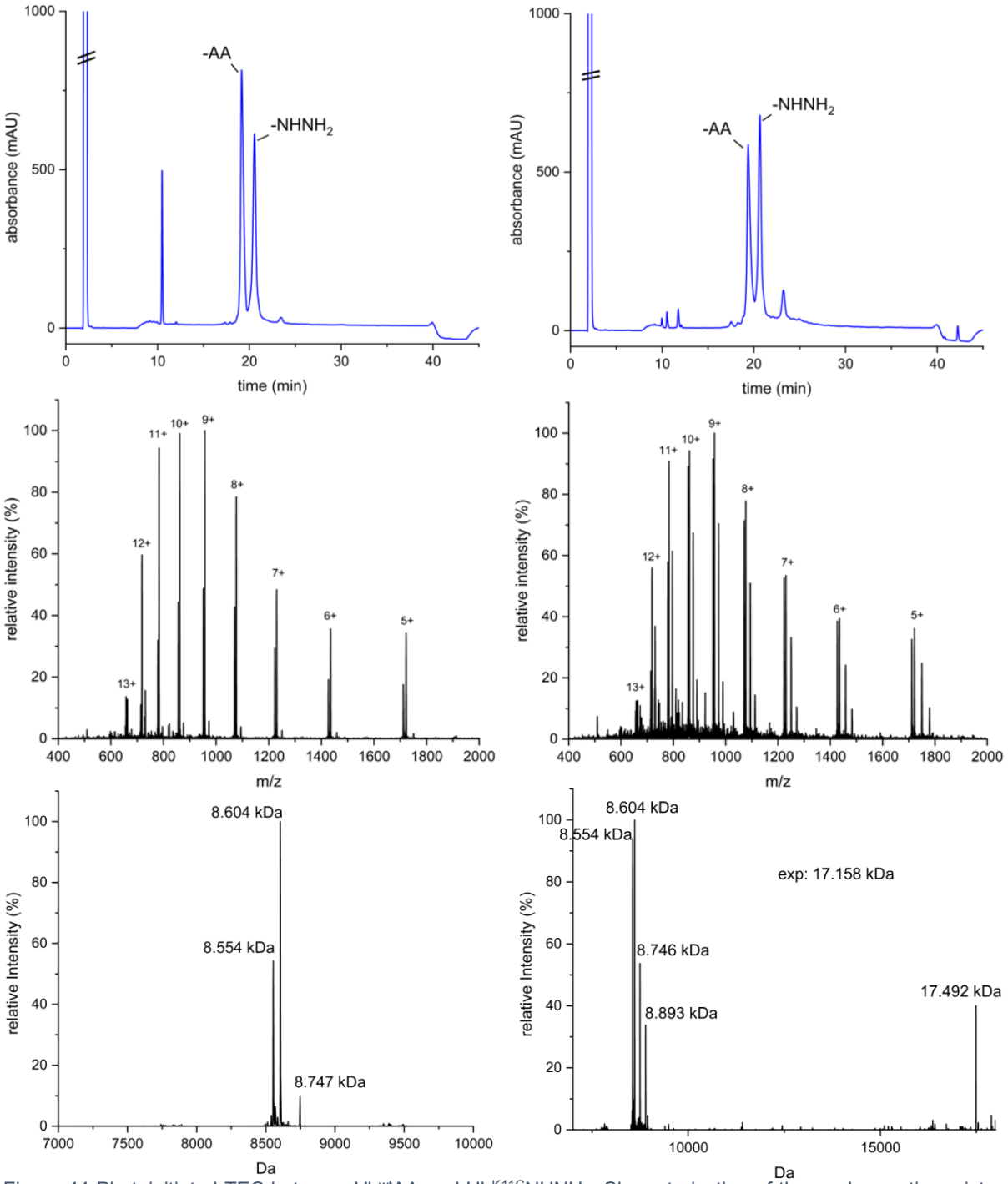

Figure 44 Photoinitiated TEC between $Ub^{wt}AA$ and $Ub^{K11C}NHNH_2$. Characterization of the crude reaction mixture before (left) and after (right) irradiation. Analytical RP-HPLC (top), ESI-MS (middle) and deconvoluted mass spectrum (bottom).

As shown in Figure 44 (left), due to the lower concentration while dissolving the hydrazide, the amount of hydrazide (8.554 kDa) in the ESI spectrum and HPLC chromatogram before the reaction increased, but the desired product could not be found in the deconvoluted spectrum after this reaction either (Figure 44, right). Instead the unknown diubiquitin species (17.492 kDa) is visible here.

For the next reaction, the concentration of the proteins and the radical initiator LAP was reduced to one third of the original conditions to get all the proteins into solution and try to enable coupling.

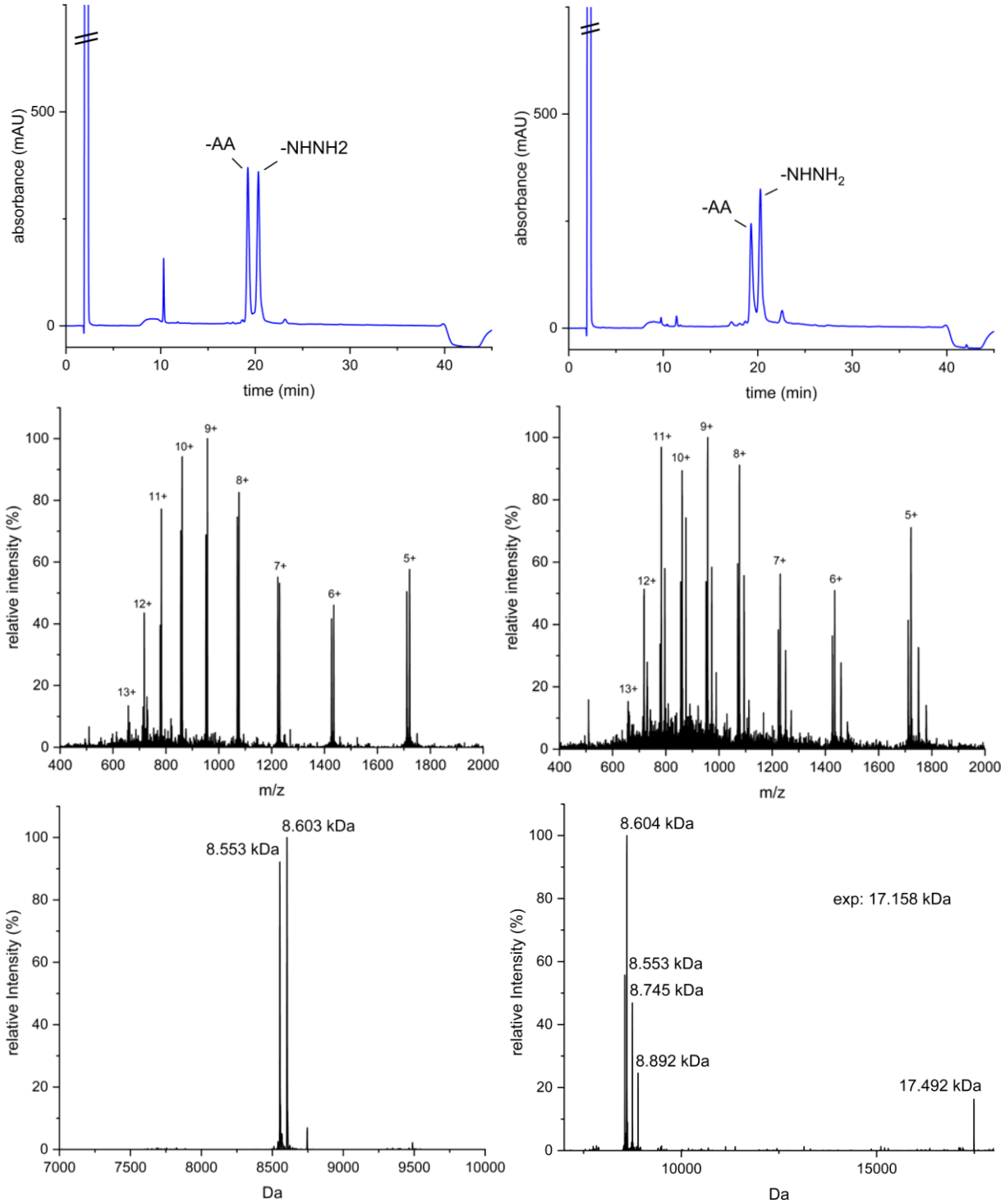

Figure 45 Photoinitiated TEC between $Ub^{wt}AA$ and $Ub^{K11C}NHNH_2$. Characterization of the crude reaction mixture before (left) and after (right) irradiation. Analytical RP-HPLC (top), ESI-MS (middle) and deconvoluted mass spectrum (bottom).

In this approach, it was possible to bring both building blocks into solution. This can also be seen in Figure 45 (top, left), as the relative intensity of the hydrazide (8.553 k Da) in the RP-HPLC chromatogram is comparable to the allylamide.

The desired product could not be found after irritation either but the same species (17.493 kDa) as in the last reactions. Furthermore, the building blocks also represent the majority of the intensity in this spectrum, which suggests that no actual reaction took place.

For the next reaction, the buffer was changed to phosphate buffer (10 mM Na_2HPO_4, 1.8 mM KH_2PO_4, pH 7.16) in order to enable the thiol-ene reaction and obtain the desired diubiquitin. Also, the concentration of the proteins as well as LAP and TCEP was reduced to one third like in the previous reaction.

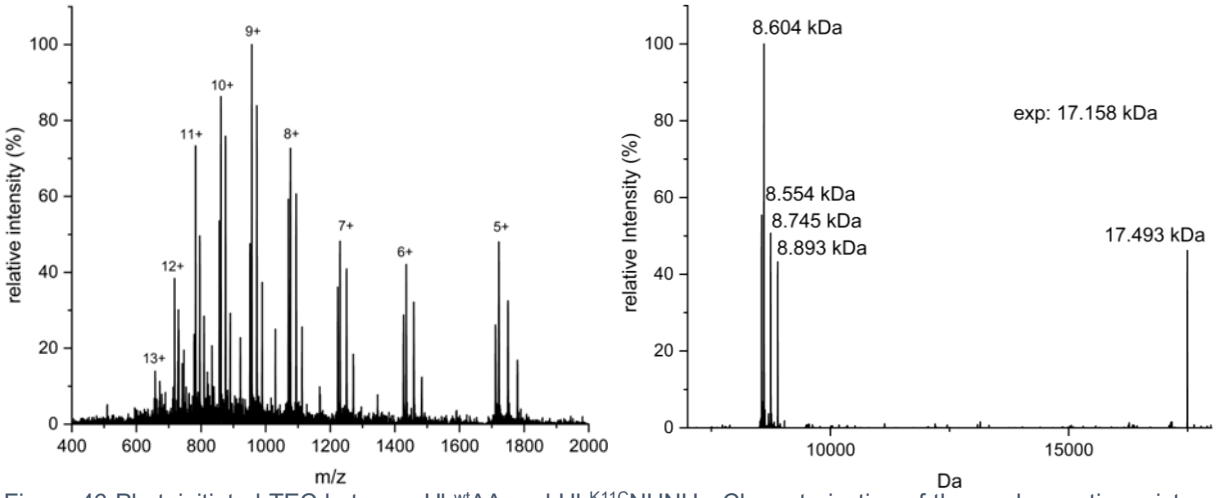

Figure 46 Photoinitiated TEC between $Ub^{wt}AA$ and $Ub^{K11C}NHNH_2$. Characterization of the crude reaction mixture after irradiation. ESI-MS (left) and deconvoluted mass spectrum (right).

As in the previous experiments, the desired diubiquitin could not be detected by ESI-MS. (Figure 46).

As a last attempt, the reaction was performed under conditions given in the literature[61]. The proteins were dissolved in 250 mM NaOAc pH 5.1 without GndHCl, at a concentration of 2 mM for $Ub^{wt}AA$ and 2.5 mM for $Ub^{K11C}NHNH_2$, and LAP was added to a concentration of 25 mM. The reaction was performed without TCEP.

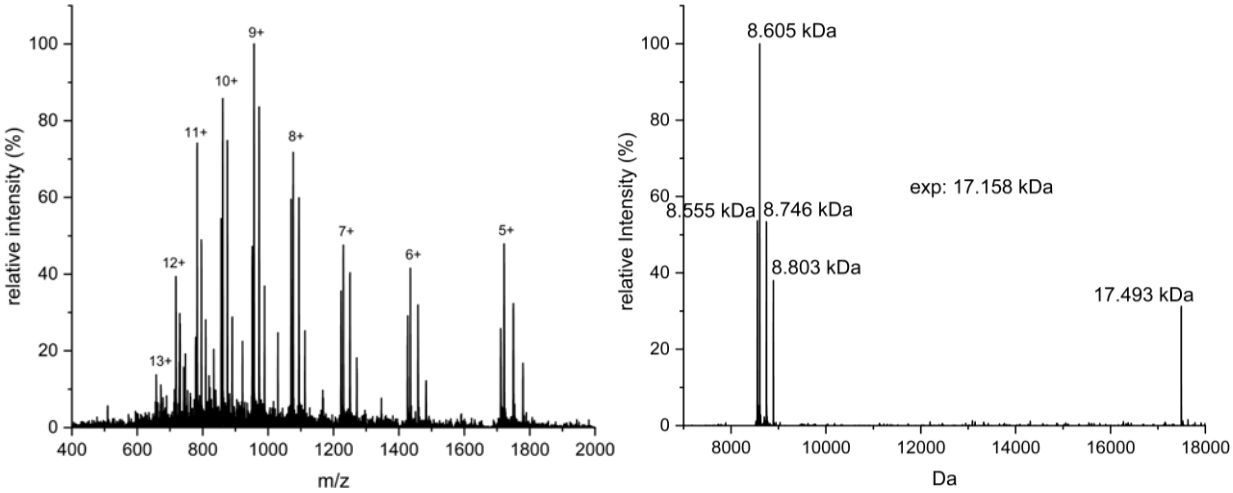

Figure 47 Photoinitiated TEC between $Ub^{wt}AA$ and $Ub^{K11C}NHNH_2$. Characterization of the crude reaction mixture after irradiation. ESI-MS (left) and deconvoluted mass spectrum (right).

Similar to the previous reactions, the desired diubiquitin could not be found in the ESI-MS (Figure 47).

Since none of the reaction conditions was suitable to generate $DiUb^{wt\text{-}K11C}NHNH_2$, it was examined, if the thiol group of Ub^{K11C} was accessible towards a small molecule electrophile. To this end, an attempt to react the cysteine with PAcBr (conditions see 3.11.1) was made and

yielded PAc-protected $Ub^{K11C}SR$ (see section 4.1.5), confirming that the thiol in Ub^{K11C} is accessible for small molecules. In the future, it could be tested whether a small peptide with a mass between PAc and ubiquitin could be coupled with $Ub^{K11C}NHNH_2$ using TEC. HR mass spectrometry could be used to identify the minor side-product (17.492 kDa), which wasn't done during this work due to lack of time.

For this reason, no further attempt was made to produce $DiUb^{wt\text{-}K11C}NHNH_2$ and to focus on other diubiquitin isomers

4.6.2 $Ub^{wt}AA+Ub^{K29C}NHNH_2$

For this reaction $Ub^{wt}AA$ and $Ub^{K29C}NHNH_2$ were used as building blocks to generate the respective diubiquitin (reaction scheme shown in Figure 48).

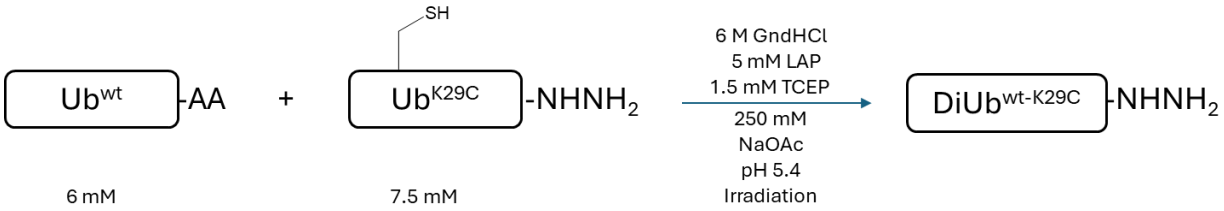

Figure 48 Reaction scheme for the TEC reaction between $Ub^{wt}AA$ and $Ub^{K29C}NHNH_2$.

RP-HPLC, ESI-MS and deconvoluted mass spectrum of this reaction is shown in Figure 49.

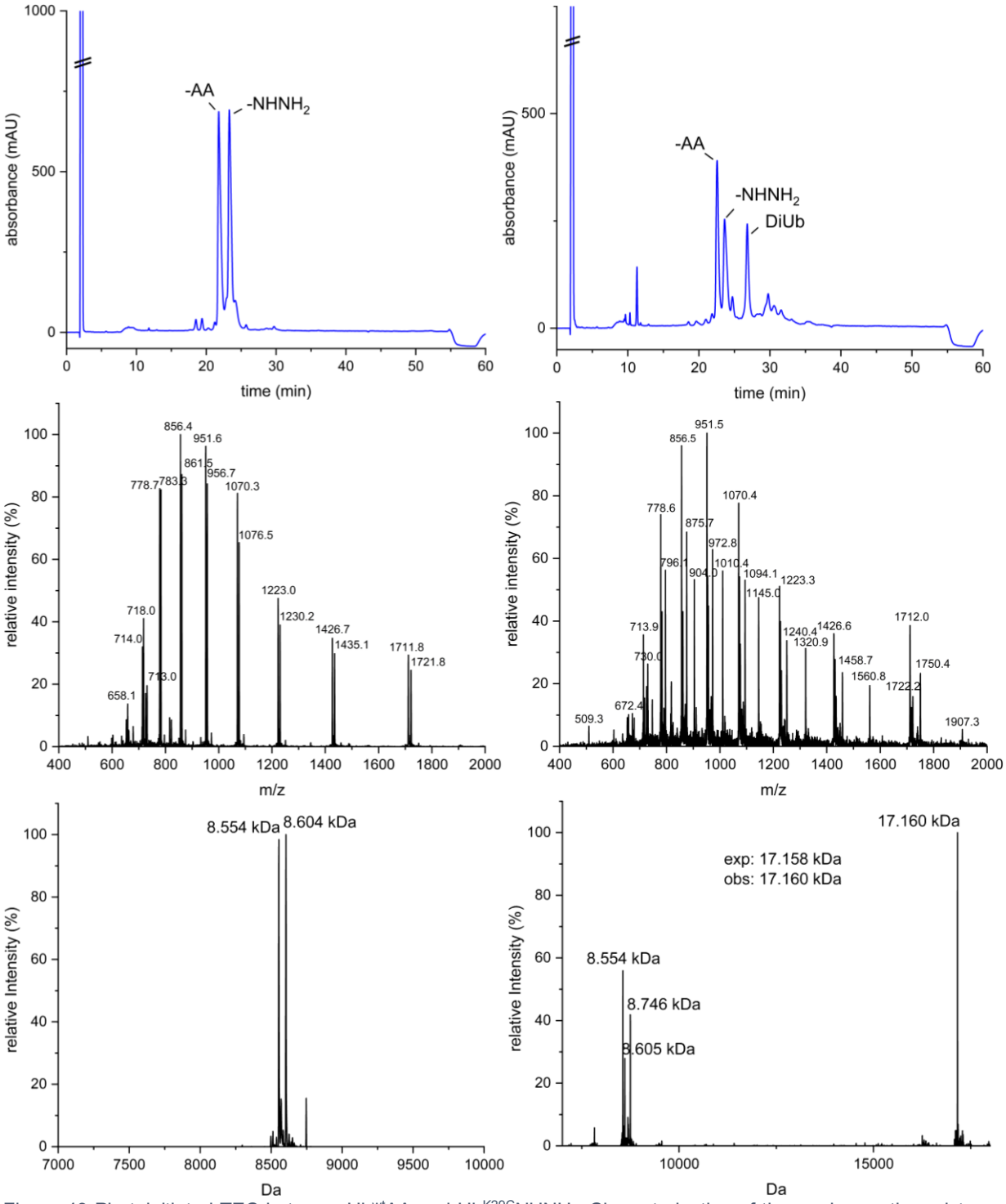

Figure 49 Photoinitiated TEC between $Ub^{wt}AA$ and $Ub^{K29C}NHNH_2$. Characterization of the crude reaction mixture before (left) and after (right) irradiation. Analytical RP-HPLC (top), ESI-MS (middle) and deconvoluted mass spectrum (bottom).

Coupling of $Ub^{wt}AA$ and $Ub^{K29C}NHNH_2$ using standard conditions (6 mM UbAA, 7.5 mM $Ub^{KxC}NHNH_2$, 5 mM LAP, 1.5 mM TCEP) worked. In the HPLC chromatogram measured after irradiation in Figure 49 (top, right), the peak of the desired diubiquitin nearly as high as the remaining hydrazide. The product peak (top, right) is also clearly visible in the RP-HPLC chromatogram and is well separated from the reactants. Since the conversion under these conditions was not as good as with other ubiquitin mutants, it was decided to assemble longer chains with diubiquitins with linked via K48 and K36.

The crude mixture of each reaction was purified by RP-HPLC to yield 0.3 (5.8 %) - 1.4 mg (27.2 %) of DiUb$^{wt\text{-}K29C}$NHNH$_2$ and characterized in Figure 50.

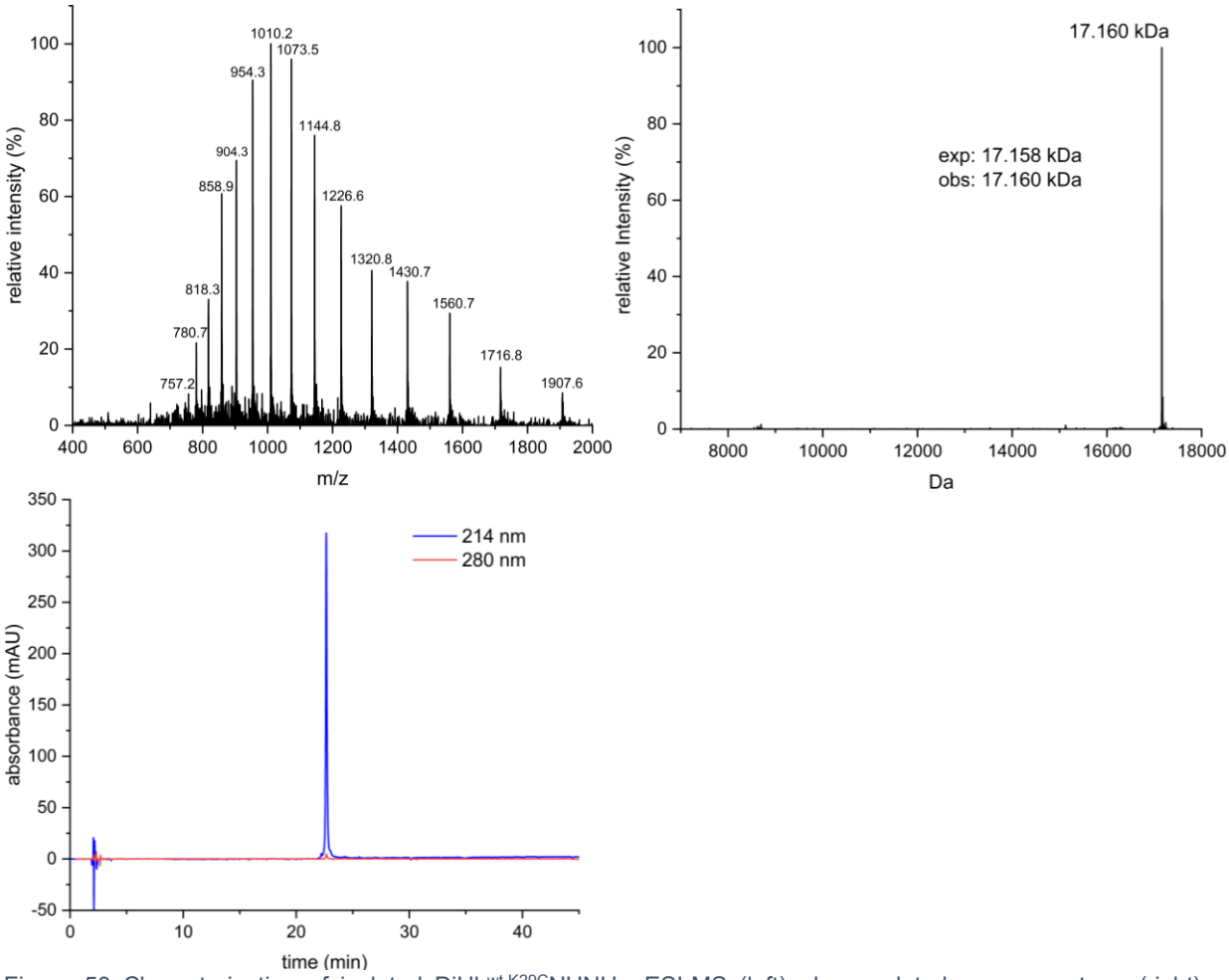

Figure 50 Characterization of isolated DiUb$^{wt\text{-}K29C}$NHNH$_2$. ESI-MS (left), deconvoluted mass spectrum (right), analytical RP-HPLC (bottom).

Figure 50 shows ESI-MS, deconvoluted mass spectrum and analytical RP-HPLC of isolated DiUb$^{wt\text{-}K29C}$NHNH$_2$.

4.6.3 Ub^{wt}_AA+Ub^{K48C}NHNH$_2$

For this reaction Ub^{wt}AA and Ub^{K48C}NHNH$_2$ were used as building blocks to generate the respective diubiquitin (reaction scheme shown in Figure 51).

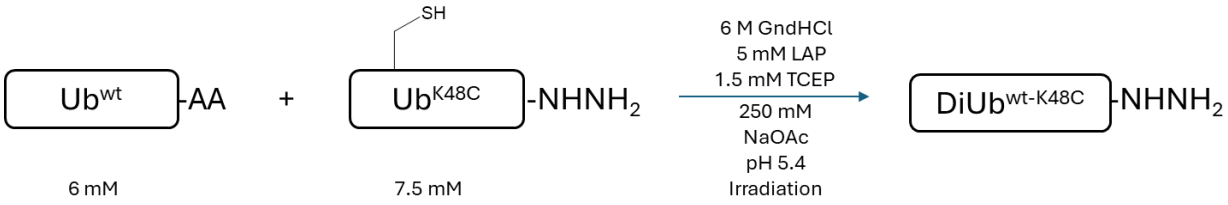

Figure 51 Reaction scheme for the TEC reaction between Ub^{wt}AA and Ub^{K48C}NHNH$_2$.

RP-HPLC, ESI-MS and deconvoluted mass spectrum of this reaction is shown in Figure 52.

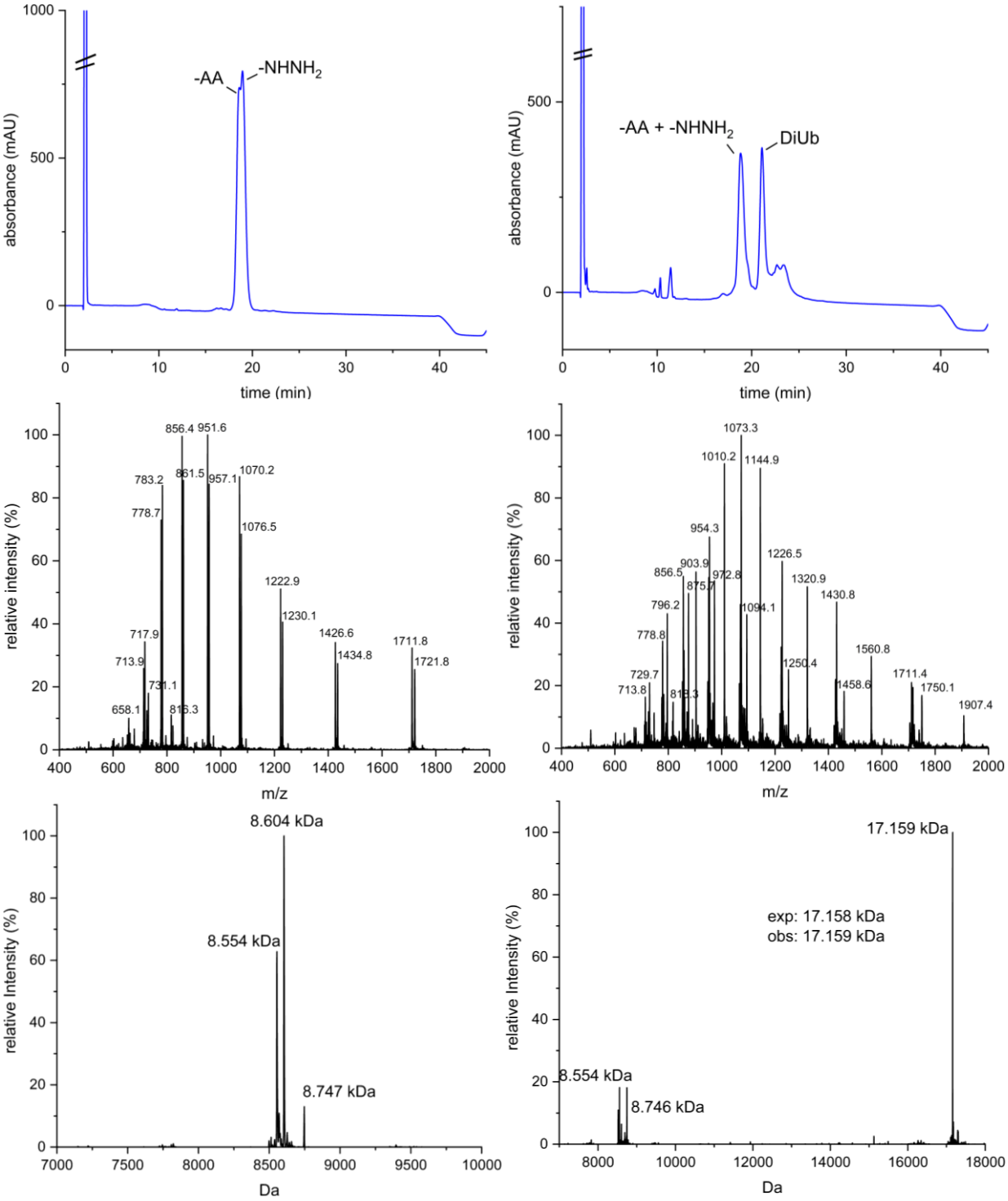

Figure 52 Photoinitiated TEC between $Ub^{wt}AA$ and $Ub^{K48C}NHNH_2$. Characterization of the crude reaction mixture before (left) and after (right) irradiation. Analytical RP-HPLC (top), ESI-MS (middle) and deconvoluted mass spectrum (bottom).

Coupling of $Ub^{wt}AA$ and $Ub^{K48C}NHNH_2$ using standard conditions worked well. In the RP-HPLC chromatogram after irradiation, the peak of the desired diubiquitin is even higher than both allylamide and hydrazide (Figure 52, top, right). It is also well separated from the reactants, which merge into one peak. For this reason, the conditions were maintained for the following reactions.

The crude mixtures were purified by RP-HPLC to yield 0.7 mg (13.6 %) – 1.7 mg (33 %) of DiUb$^{wt\text{-}K48C}$NHNH$_2$.

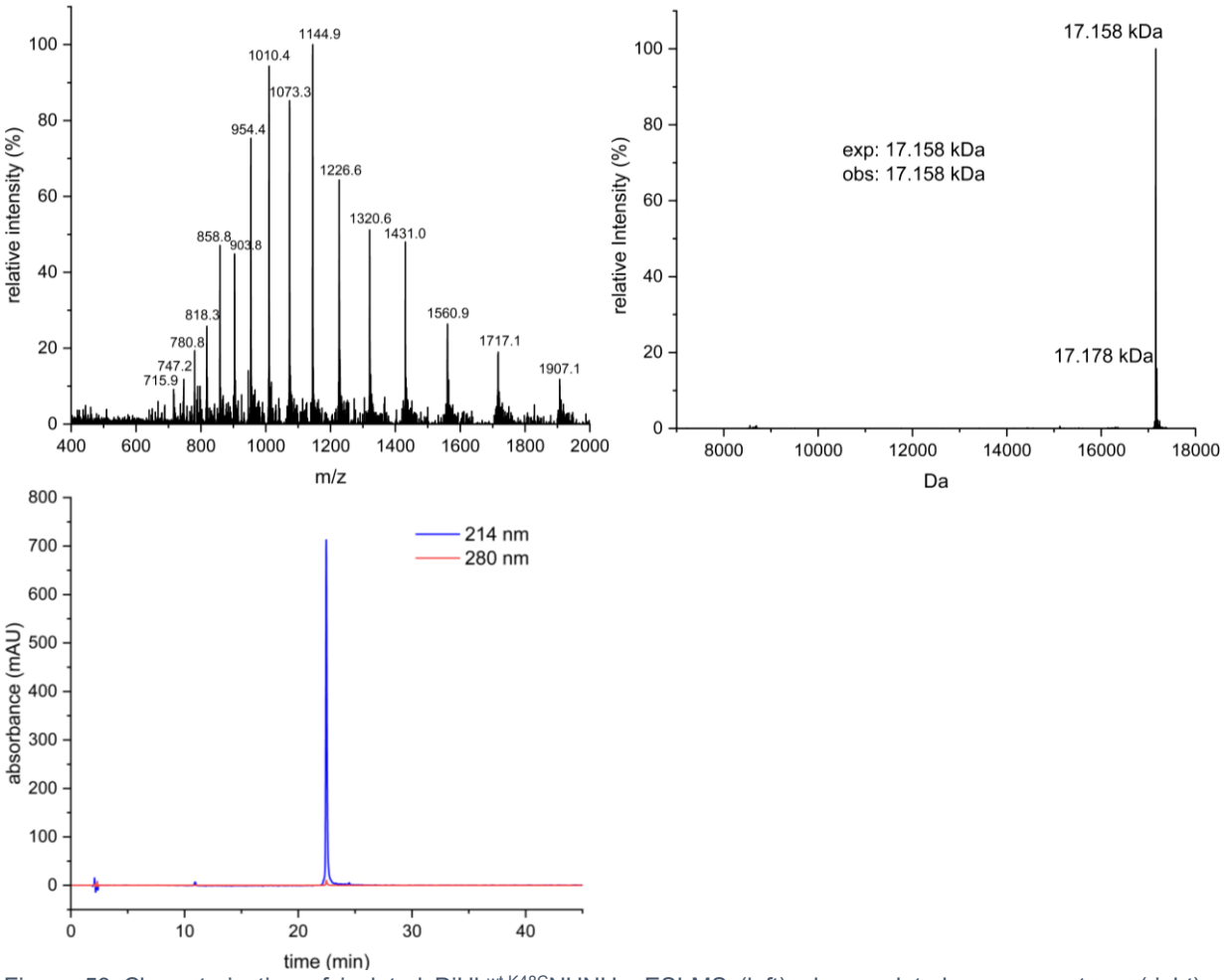

Figure 53 Characterization of isolated DiUb$^{wt\text{-}K48C}$NHNH$_2$. ESI-MS (left), deconvoluted mass spectrum (right), analytical RP-HPLC (bottom).

Figure 53 shows ESI-MS, deconvoluted mass spectrum and analytical RP-HPLC of isolated DiUb$^{wt\text{-}K48C}$NHNH$_2$

After combining all reactions and purifying all pools with considerable amount of diubiquitin, it was possible to optain 17.4 mg (38 %) of isolated product.

4.6.4 Ub^{wt}AA+Ub^{K63C}NHNH$_2$

For this reaction Ub^{wt}AA and Ub^{K63C}NHNH$_2$ were used as building blocks to generate the respective diubiquitin (reaction scheme shown in Figure 54).

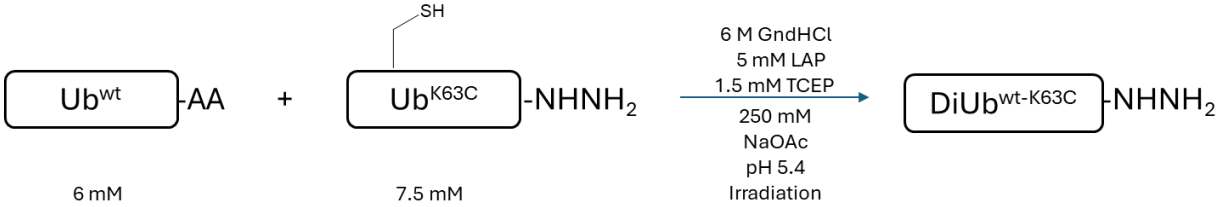

Figure 54 Reaction scheme for the TEC reaction between Ub^{wt}AA and Ub^{K63C}NHNH$_2$.

RP-HPLC, ESI-MS and deconvoluted mass spectrum of this reaction is shown in Figure *55*.

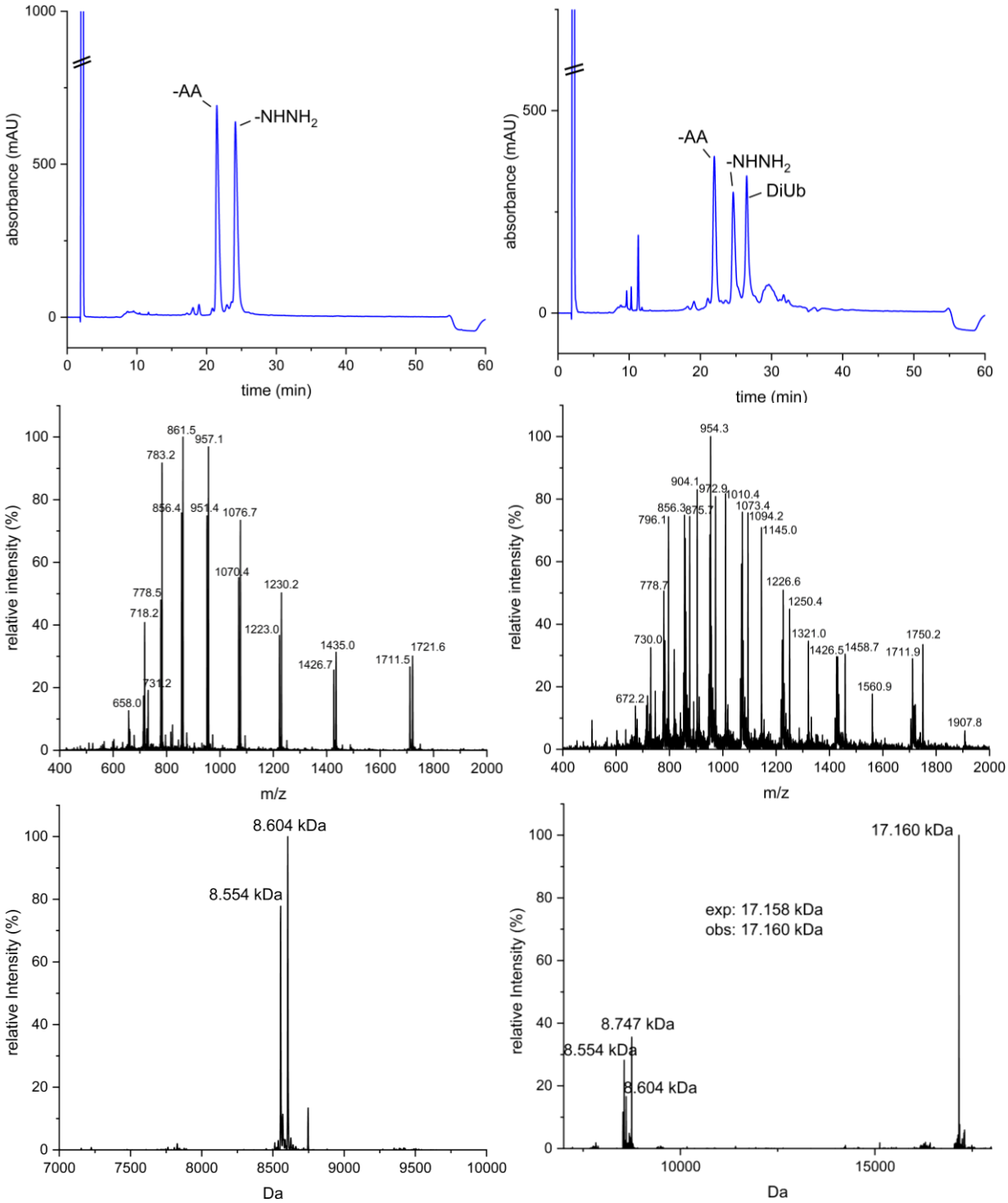

Figure 55 Photoinitiated TEC between $Ub^{wt}AA$ and $Ub^{K63C}NHNH_2$. Characterization of the crude reaction mixture before (left) and after (right) irradiation. Analytical RP-HPLC (top), ESI-MS (middle) and deconvoluted mass spectrum (bottom).

Coupling of $Ub^{wt}AA$ and $Ub^{K63C}NHNH_2$ using standard conditions worked. In the RP-HPLC chromatogram after irradiation, the peak of the desired diubiquitin even higher than the remaining hydrazide (Figure 55, top, right and is well separated from the reactants. Since the turnover under these conditions was not as good as with other ubiquitin mutants, it was decided to build up the final chains with other diubiquitins.

The crude mixture of each reaction was purified by RP-HPLC to yield on average 0.3 mg (5.8 %) of $DiUb^{wt\text{-}K63C}NHNH_2$ (Figure 56).

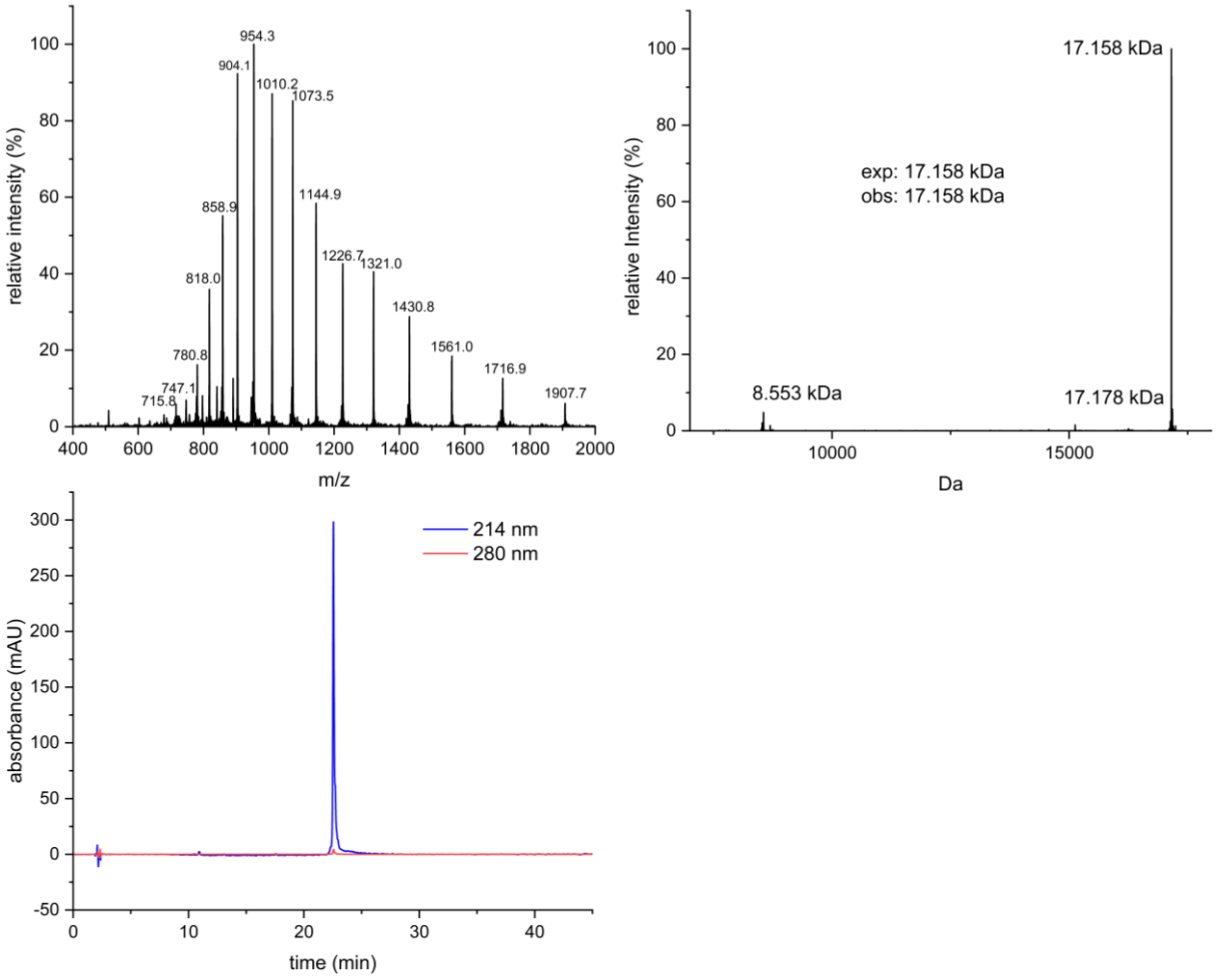

Figure 56 Characterization of isolated DiUb$^{wt\text{-}K63C}$NHNH$_2$. ESI-MS (left), deconvoluted spectrum (right), analytical RP-HPLC (bottom).

Figure 56 shows ESI-MS, deconvoluted mass spectrum and analytical RP-HPLC of isolated DiUb$^{wt\text{-}K63C}$NHNH$_2$. Ubiquitin monomers (Ub^{K63C}NHNH$_2$, 8.553 kDa) in this spectrum are still visible in the deconvoluted mass spectrum (right).

4.7 TEC with PAc-protected Mutants

It was also tested to couple two cysteine-containing mutants - a strategy that provides the opportunity for flexible chain assembly as the direction of chain elongation can be changed. In order to prohibit the formation of by-products, PAc-protected building blocks were used as allylamide components. The reactions were initially carried out under standard conditions and individual parameters were gradually adjusted to improve conversion of the respective diubiquitins.

4.7.1 $Ub^{K29C}{}_{pac}AA+Ub^{K63C}NHNH_2$

For this reaction $Ub^{K29C}AA$ and $Ub^{K63C}NHNH_2$ were used as building blocks to generate the respective diubiquitin (reaction scheme shown in Figure 57).

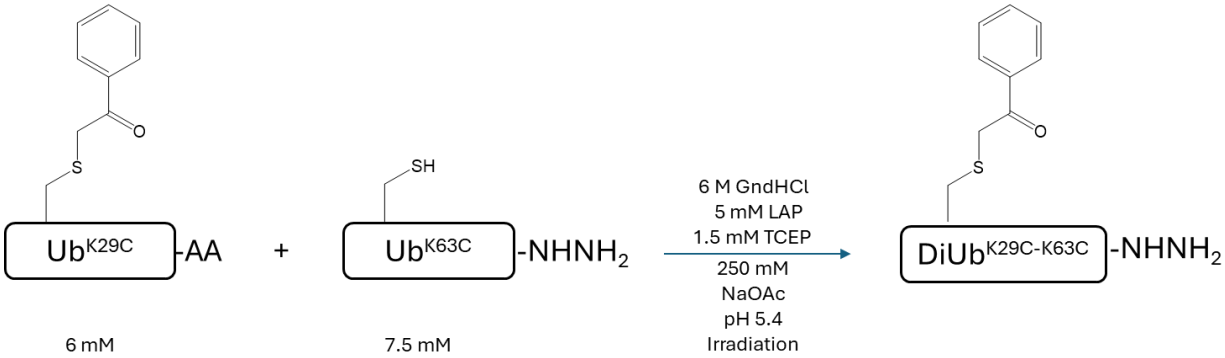

Figure 57 Reaction scheme for the TEC reaction between $Ub^{K29C}{}_{pac}AA$ and $Ub^{K63C}NHNH_2$.

RP-HPLC, ESI-MS and deconvoluted mass spectrum of this reaction is shown in Figure 58.

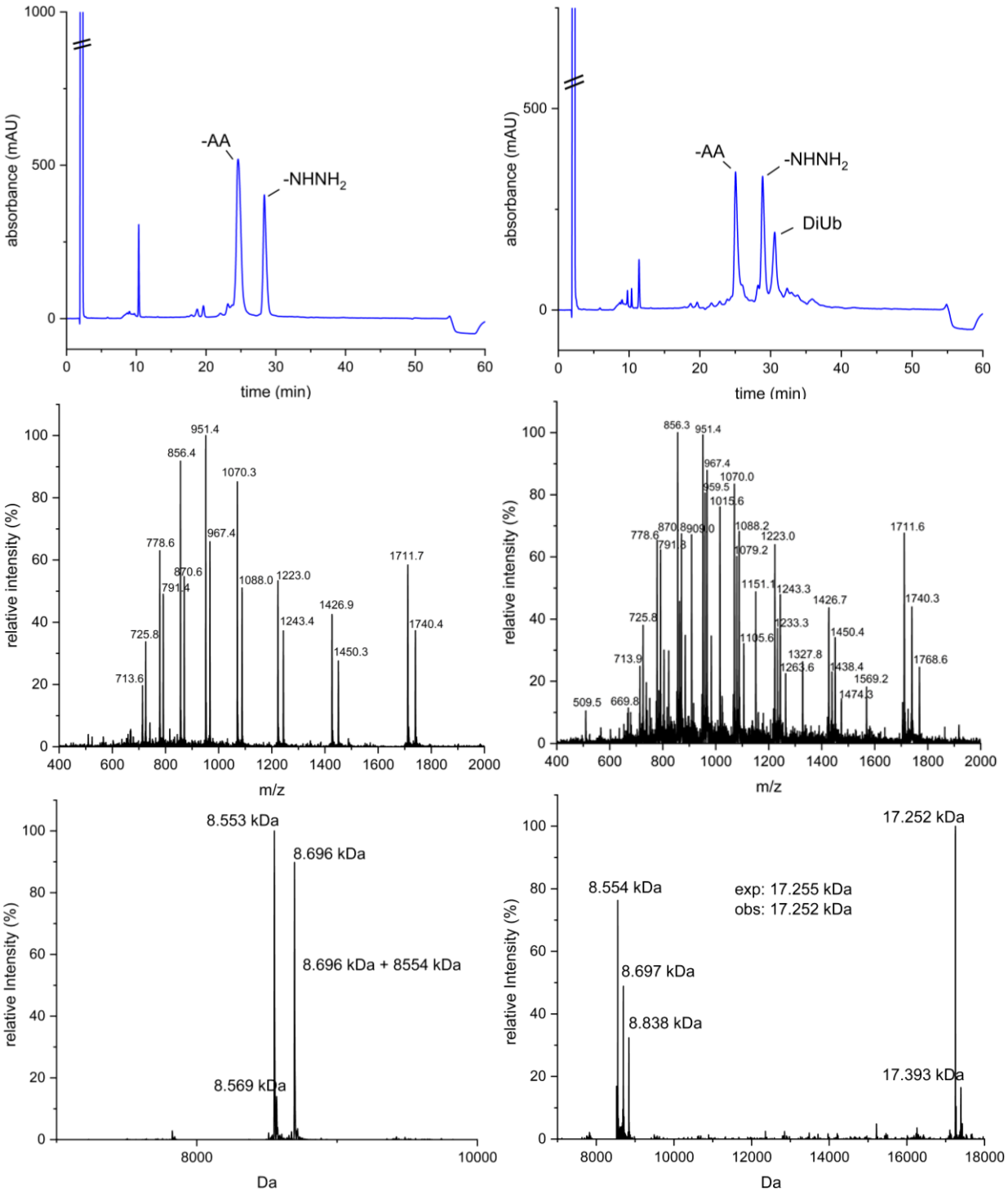

Figure 58 Photoinitiated TEC between $Ub^{K29C}{}_{pac}AA$ and $Ub^{K63C}NHNH_2$. Characterization of the crude reaction mixture before (left) and after (right) irradiation. Analytical RP-HPLC (top), ESI-MS (middle) and deconvoluted mass spectrum (bottom).

Coupling of $Ub^{K29C}{}_{pac}AA$ with the $Ub^{K63C}NHNH_2$ worked as shown in Figure 58. As clearly recognizable in the RP-HPLC chromatogram, a product peak forms, which elutes after the reactants. However, the turnover at standard conditions is still relatively low.

For the next reactions, the concentration of the radical initiator LAP was increased to 5.25 mM since the intensity of allylamide is still higher than that of the LAP adduct (bottom, right).

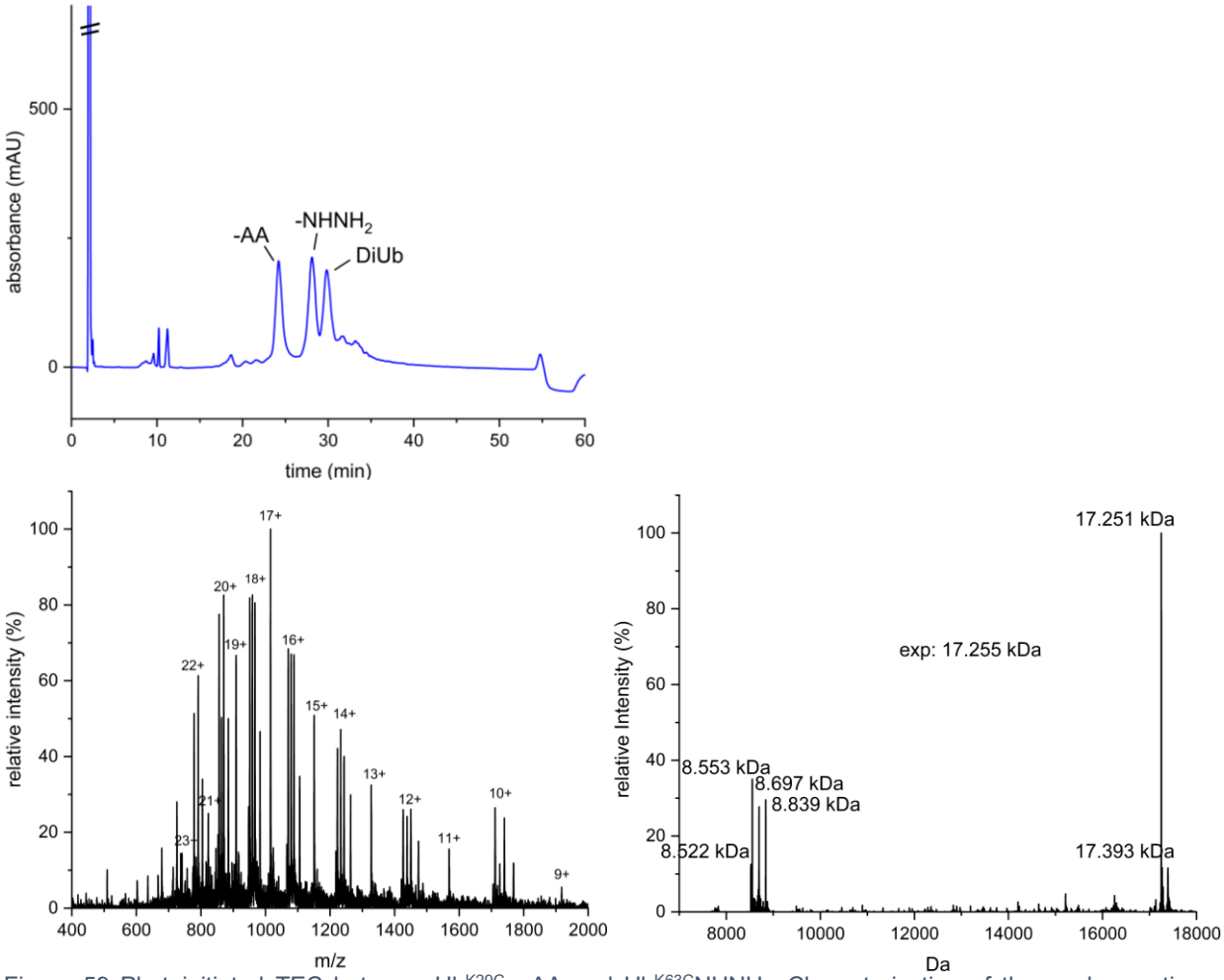

Figure 59 Photoinitiated TEC between $Ub^{K29C}{}_{pac}AA$ and $Ub^{K63C}NHNH_2$. Characterization of the crude reaction mixture after irradiation. Analytical RP-HPLC (top), ESI-MS (bottom, left) and deconvoluted mass spectrum (bottom, right).

In the spectra (Figure *59*), the desired diubiquitin (17.251 kDa) now already represents a higher intensity. This fits to the corresponding peak in the RP-HPLC chromatogram (top), which is nearly as high as the building blocks.

Since the intensity of the LAP adduct (8.839 kDa) of the allylamide (8.697 kDa) was not noticeably higher than that of the allylamide, the concentration of LAP was increased to 5.5 mM in the next reaction. Since desulfurized hydrazide (8.522 kDa) is also visible in the spectrum, the concentration of TCEP was also increased to 2 mM. In addition, the reaction was carried out simultaneously with 5.5 mM LAP and 1.5 mM TCEP to be able to estimate the respective influence of the concentrations.

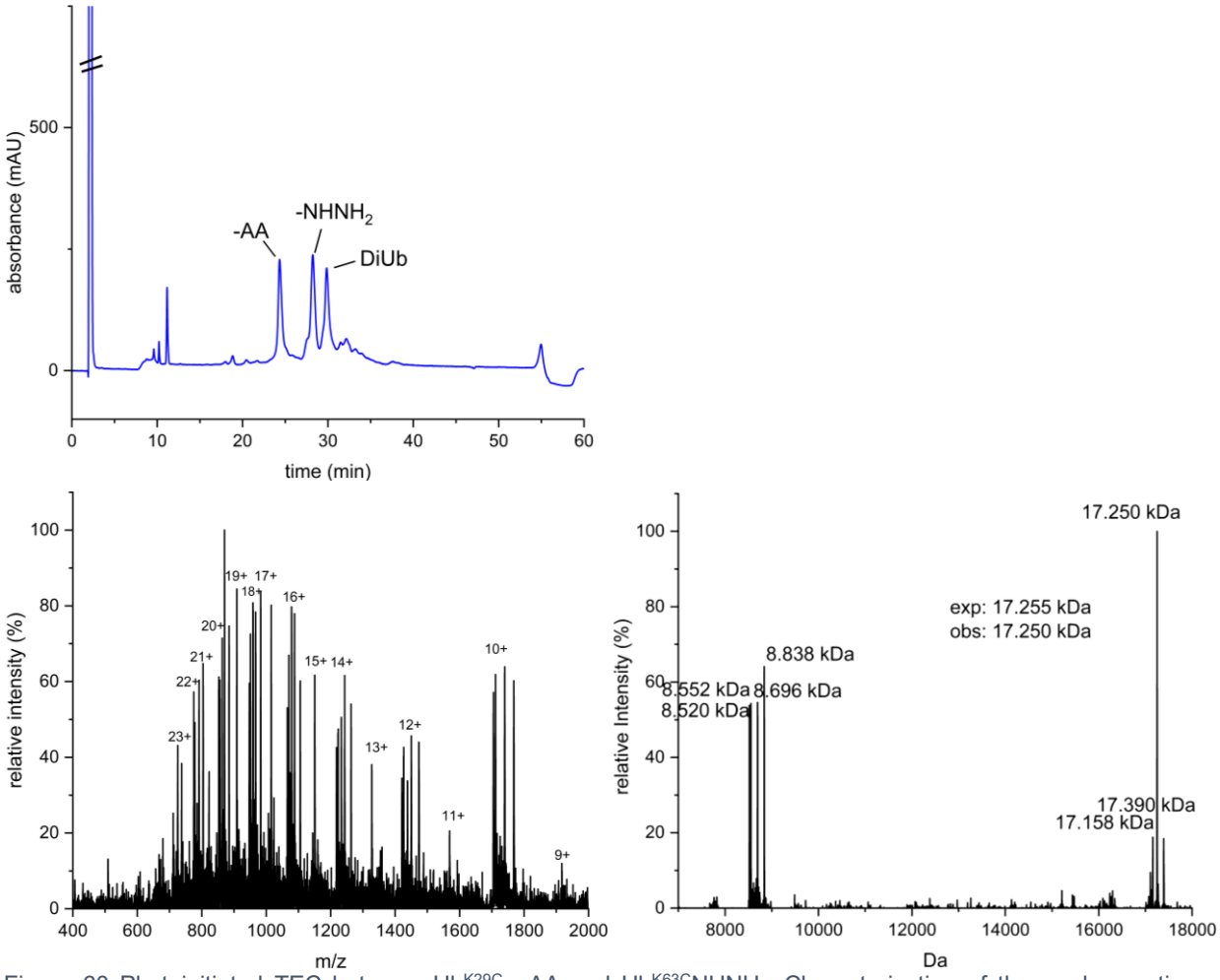

Figure 60 Photoinitiated TEC between $Ub^{K29C}{}_{pac}AA$ and $Ub^{K63C}NHNH_2$. Characterization of the crude reaction mixture after irradiation. Analytical RP-HPLC (top), ESI-MS (bottom, left) and deconvoluted mass spectrum (bottom, right).

As shown in Figure 60, the desired diubiquitin (17.250 kDa) represents the highest intensity at 5.5 mM LAP and 2 mM TCEP. However, since the remaining building blocks all show a higher intensity than in Figure 59, it appears that the reaction turnover is lower. The intensity of the LAP adduct is slightly higher than that of the allylamide. However, the intensity of the desulfurized hydrazide is almost as high as that of the hydrazide, which is worse than with 1.5 mM TCEP.

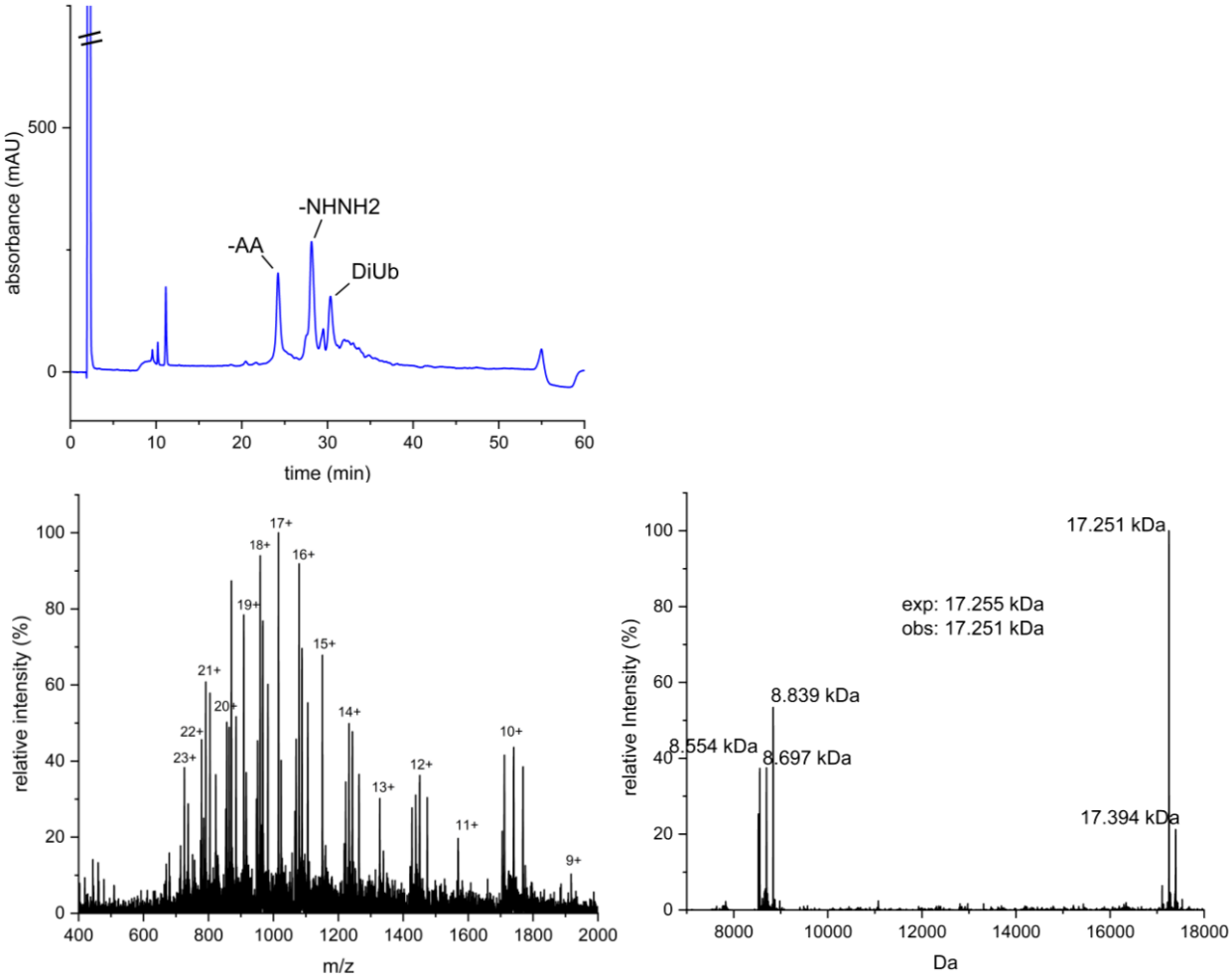

Figure 61 Photoinitiated TEC between $Ub^{K29C}{}_{pac}AA$ and $Ub^{K63C}NHNH_2$. Characterization of the crude reaction mixture after irradiation. Analytical RP-HPLC (top), ESI-MS (bottom, left) and deconvoluted mass spectrum (bottom, right).

As shown in Figure 61, the intensities with 5.5 mM LAP and 1.5 mM TCEP behave more similarly to the reaction with 5.25 mM LAP and 1.5 mM TCEP (Figure 59) than with an additional 2 mM TCEP (Figure 60). Since the other proteins show a lower intensity compared to the spectrum in Figure 54, the turnover of the desired diubiquitin seems to be better here, but slightly lower than with 5.25 mM LAP and 1.5 mM TCEP. Furthermore, the intensity of the LAP adduct is significantly higher than that of the allylamide and that of the desulfurized hydrazide is significantly lower compared to 2 mM TCEP.

For diubiquitins made from coupling two cysteine mutants, as described in more detail in section 4.8, the PAc protecting group was first removed (180 mg/mL Zn, 45 % (v/v) acetic acid) prior to purification of each reaction mixture via semipreparative RP-HPLC. Characterization here already represent the deprotected diubiquitin.

The crude mixtures were purified by RP-HPLC To yield 0.3 mg (5.8 %) – 0.9 (17.5 %) of $DiUb^{K29C\text{-}K63C}NHNH_2$. The yield of every reaction was pooled and characterized in Figure 62.

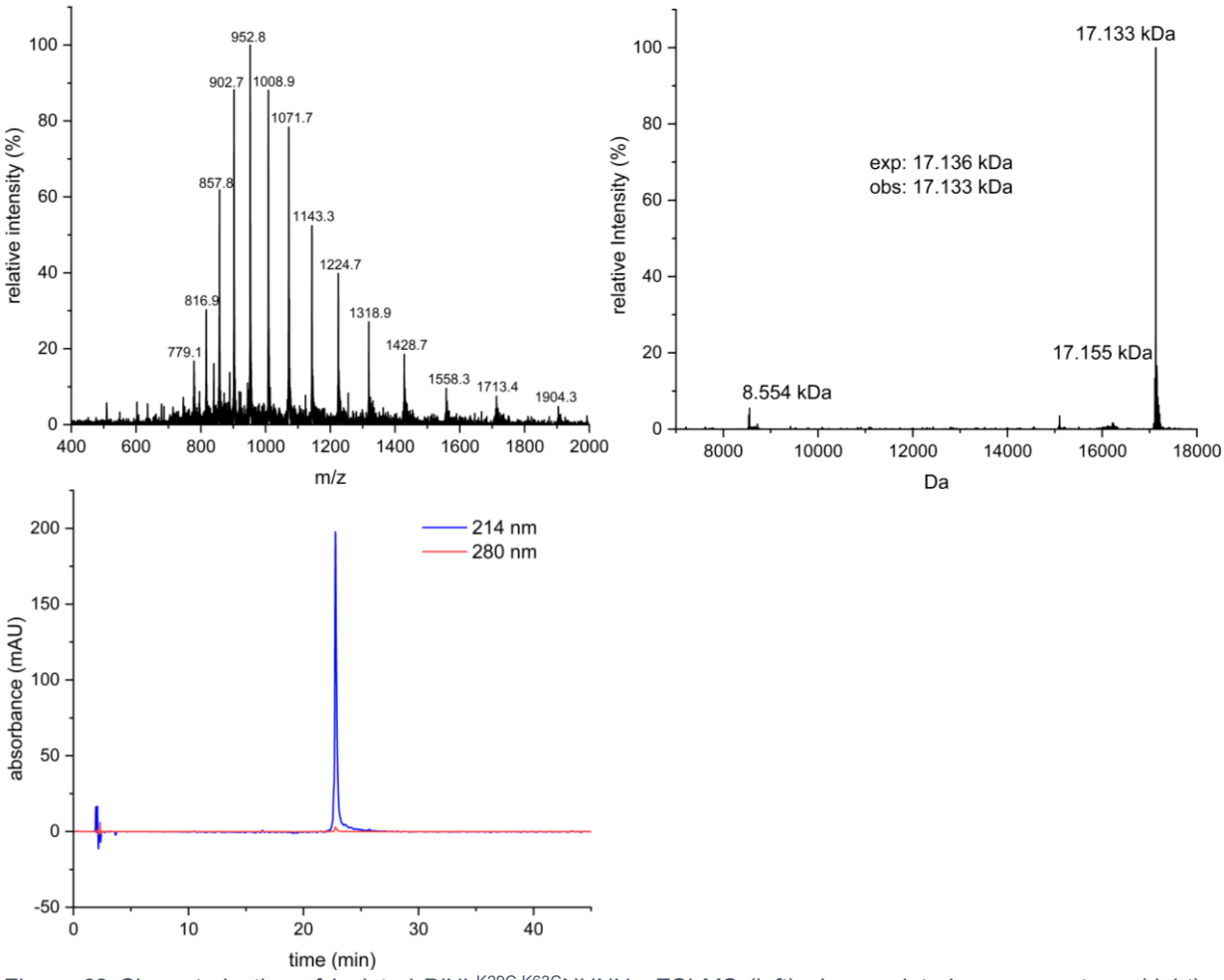

Figure 62 Characterization of isolated DiUb$^{K29C-K63C}$NHNH$_2$. ESI-MS (left), deconvoluted mass spectrum (right), analytical RP-HPLC (bottom).

Figure 62 shows ESI-MS, deconvoluted mass spectrum and analytical RP-HPLC of isolated DiUb$^{K29C-K63C}$NHNH$_2$.

After combining all reactions and purifying all pools with considerable amount of diubiquitin, it was possible to get 6.5 (14 %) mg of isolated product.

4.7.2 Ub$^{K48C}{}_{pac}$AA+Ub^{K48C}NHNH$_2$

For this reaction Ub^{K48C}AA and Ub^{K48C}NHNH$_2$ were used as building blocks to generate the respective diubiquitin (reaction scheme shown in Figure 63).

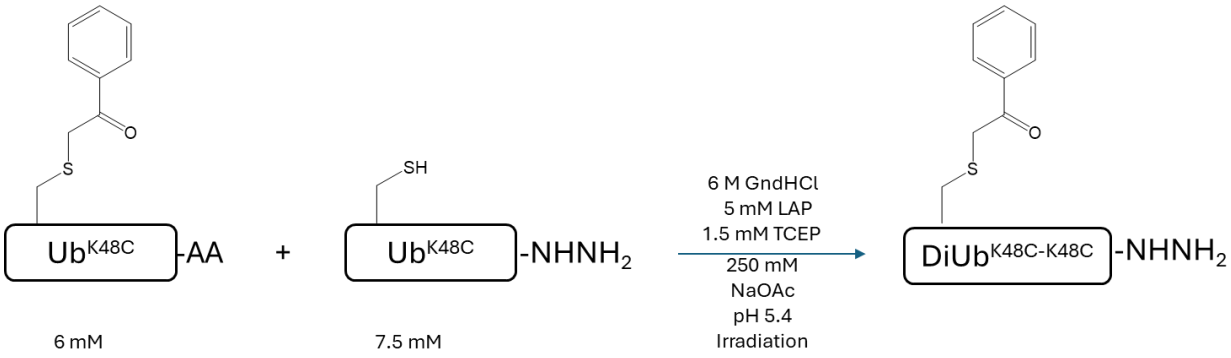

Figure 63 Reaction scheme for the TEC reaction between Ub$^{K48C}{}_{pac}$AA and Ub^{K48C}NHNH$_2$.

RP-HPLC, ESI-MS and deconvoluted mass spectrum of this reaction is shown in Figure 64.

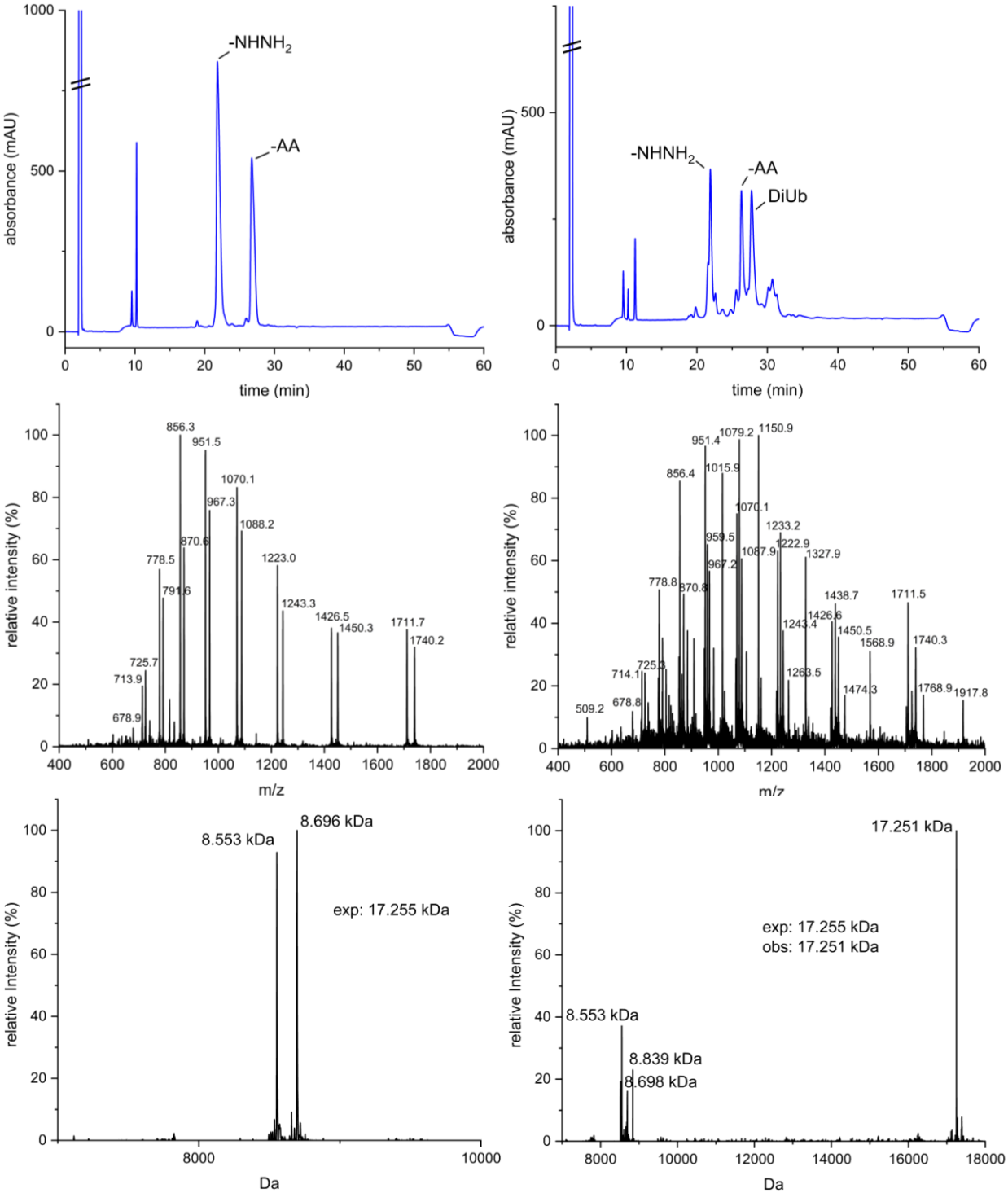

Figure 64 Photoinitiated TEC between $Ub^{K48C}{}_{pac}AA$ and $Ub^{K48C}NHNH_2$. Characterization of the crude reaction mixture before (left) and after (right) irradiation. Analytical RP-HPLC (top), ESI-MS (middle) and deconvoluted mass spectrum (bottom).

Similar to the coupling reaction of the Ub^{K48C} variant to the wild type, the coupling of two Ub^{K48C}s worked well under standard conditions. The corresponding peak in the RP-HPLC chromatogram after irradiation (Figure 64, top, right) to $DiUb^{K48C\text{-}K48C}NHNH_2$ (17.251 kDa).

Since desulfurized hydrazide and LAP-adduct of the allylamide were still in the spectrum in this reaction, an attempt was made to improve the conversion in the subsequent reactions by changing the concentration of LAP and TCEP.

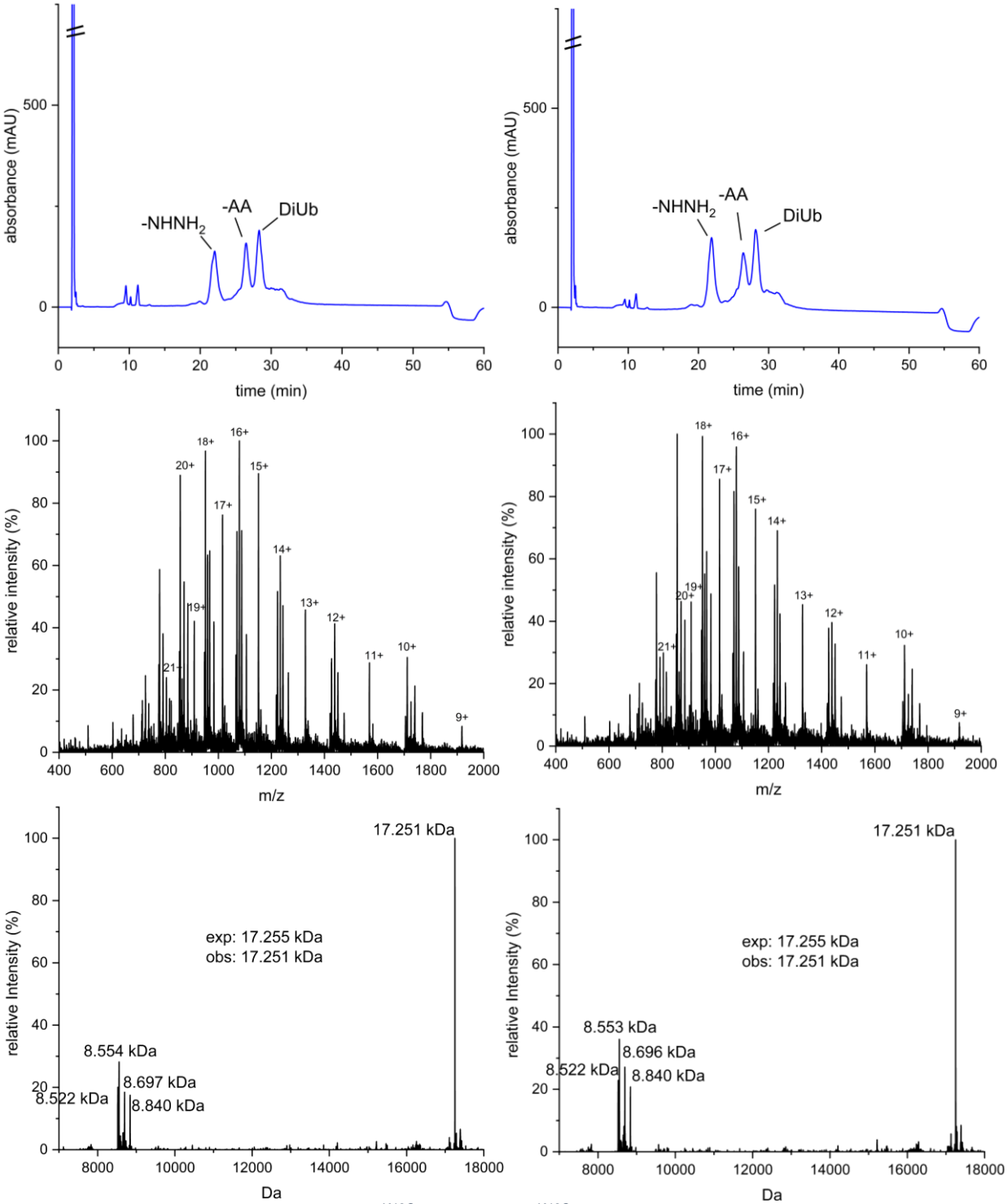

Figure 65 Photoinitiated TEC between $Ub^{K48C}{}_{pac}AA$ and $Ub^{K48C}NHNH_2$. Characterization of the crude reaction mixture after irradiation. Analytical RP-HPLC (top), ESI-MS (middle) and deconvoluted mass spectrum (bottom).

The next two reactions were carried out with the same stock solutions of reactants on the same day to be able to compare the results as closely as possible. One reaction was carried out with 5.25 mM LAP (Figure 65, left), the other as before with 5 mM (right). As shown in Figure 65, this shows nearly no change in the intensity ratio of the desired diubiquitin to the other proteins.

The intensity of the LAP adduct appears slightly higher at 5.25 mM LAP (left) than at 5 mM (right).

Since the proportion of desulfurized hydrazide in this spectrum was relatively high compared to the hydrazide and that of the LAP adduct relatively low compared to the allylamide. Therefore, the concentration of both LAP and TCEP was increased in the next reactions.

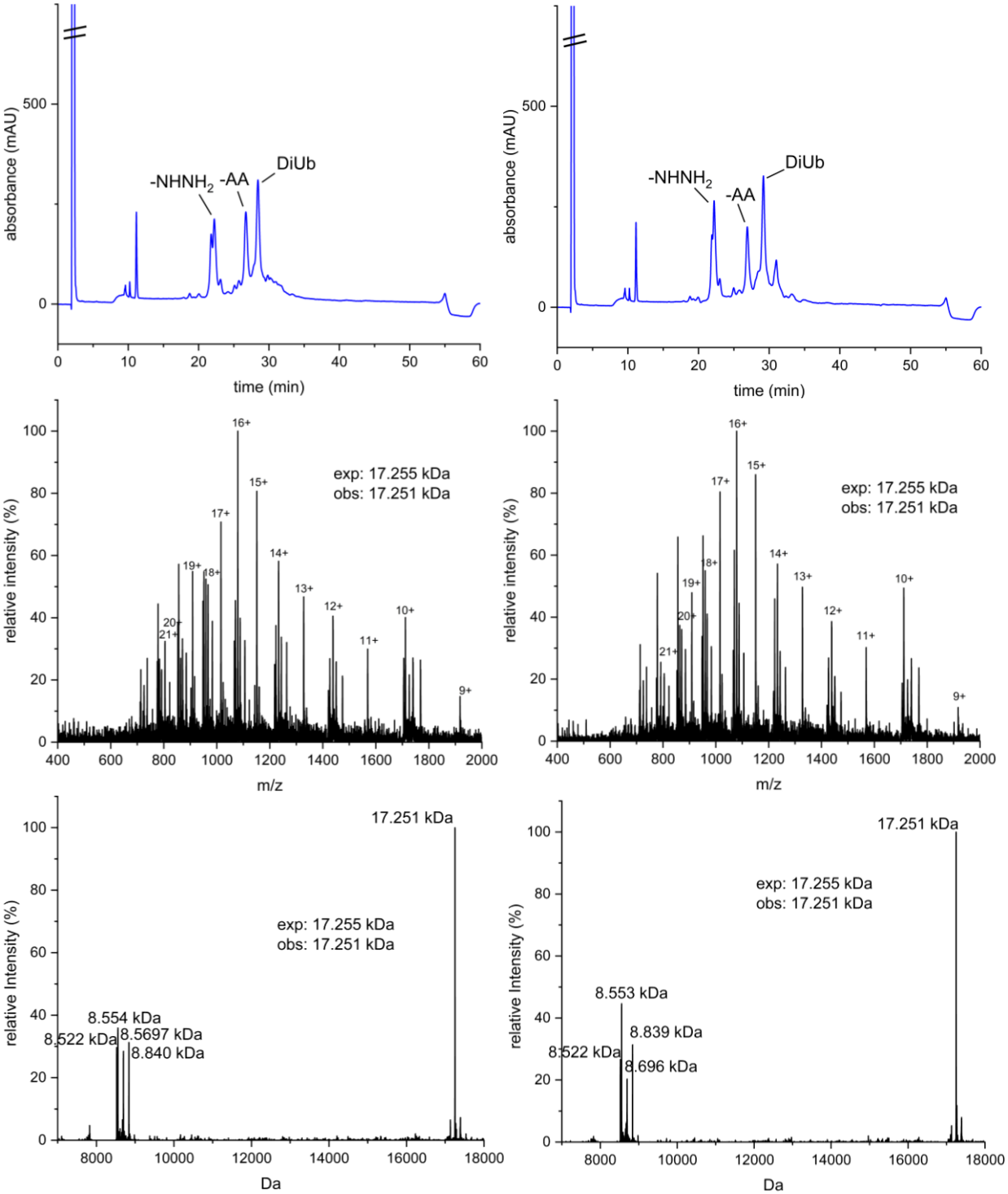

Figure 66 Photoinitiated TEC between $Ub^{K48C}{}_{pac}AA$ and $Ub^{K48C}NHNH_2$. Characterization of the crude reaction mixture after irradiation. Analytical RP-HPLC (top), ESI-MS (middle) and deconvoluted mass spectrum (bottom).

For the next two reactions, the concentration of LAP was increased to 5.5 mM (Figure 66, left) and for the second reaction the concentration of TCEP was also increased to 2 mM (Figure 66, right).

The conversion of the reaction with 5.5 mM LAP was slightly lower than that with 5.25 mM LAP. This can be seen from the fact that the intensities of the remaining proteins are generally higher (Figure 66) in comparison to 5.25 mM LAP (Figure 65). However, significantly more allylamide is present than LAP adduct.

When comparing the spectra of (Figure 66), it appears that increasing the concentration of TCEP from 1.5 mM (left) to 2 mM (right) has no positive effect on the reaction. On the contrary, the proportion of desulfurized hydrazide (8.522 kDa) is even higher.

The crude mixtures were purified by RP-HPLC To yield 0.3 mg (5.8 %) – 0.75 mg (15 %) of $DiUb^{K48C\text{-}K48C}NHNH_2$. The yield of every reaction was pooled and characterized in Figure 67.

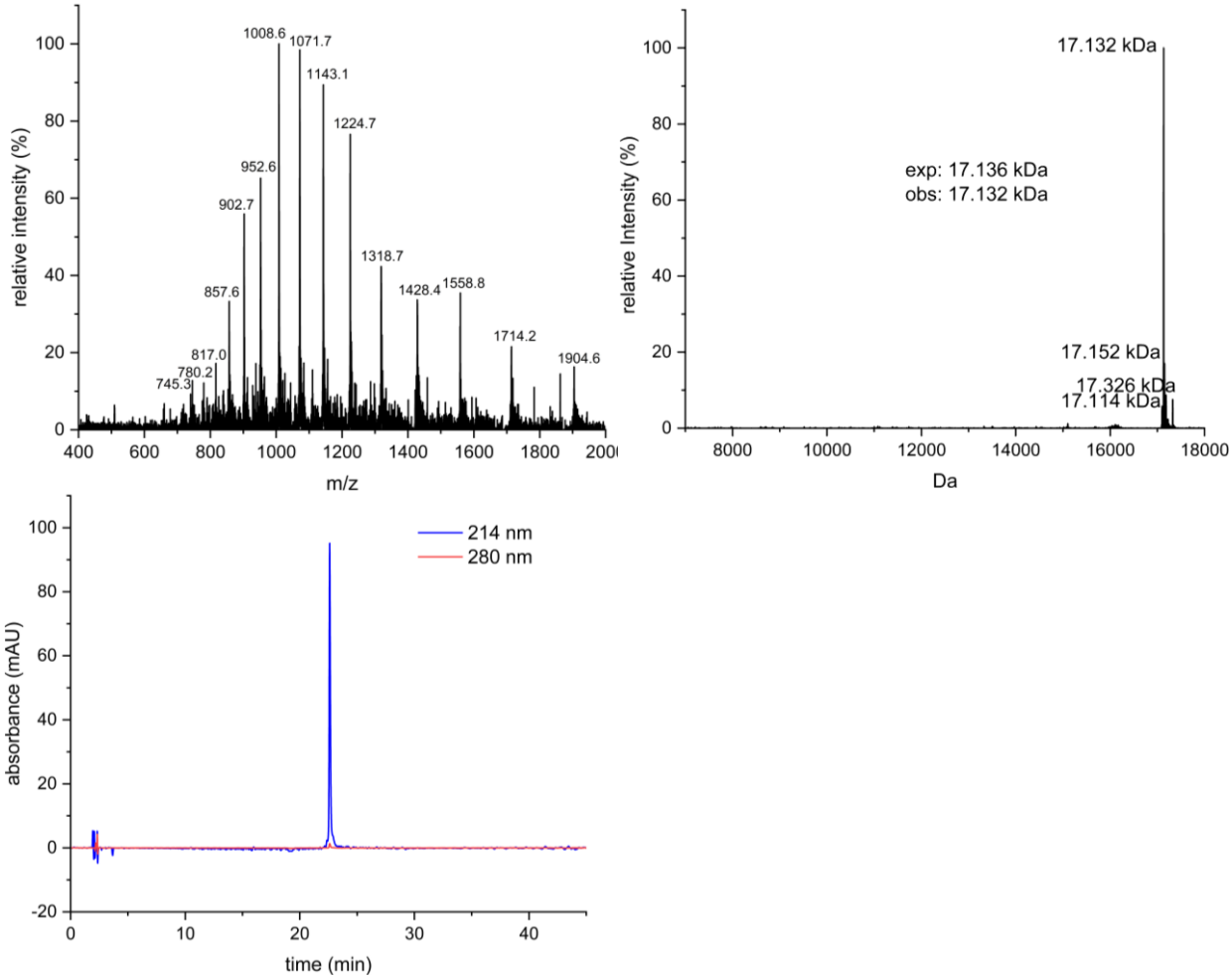

Figure 67 Characterization of isolated $DiUb^{K48C\text{-}K48C}NHNH_2$. ESI-MS (left), deconvoluted mass spectrum (right), analytical RP-HPLC (bottom).

Figure 67 shows ESI-MS, deconvoluted mass spectrum and analytical RP-HPLC of isolated $Ub^{K48C\text{-}K48C}NHNH_2$.

After combining all reactions and purifying all pools with considerable amount of diubiquitin, it was possible to get 4.99 mg (12 %) isolated product.

4.7.3 $Ub^{K63C}{}_{pac}AA+Ub^{K29C}NHNH_2$

For this reaction $Ub^{K63C}AA$ and $Ub^{K29C}NHNH_2$ were used as building blocks to generate the respective diubiquitin (reaction scheme shown in Figure 68).

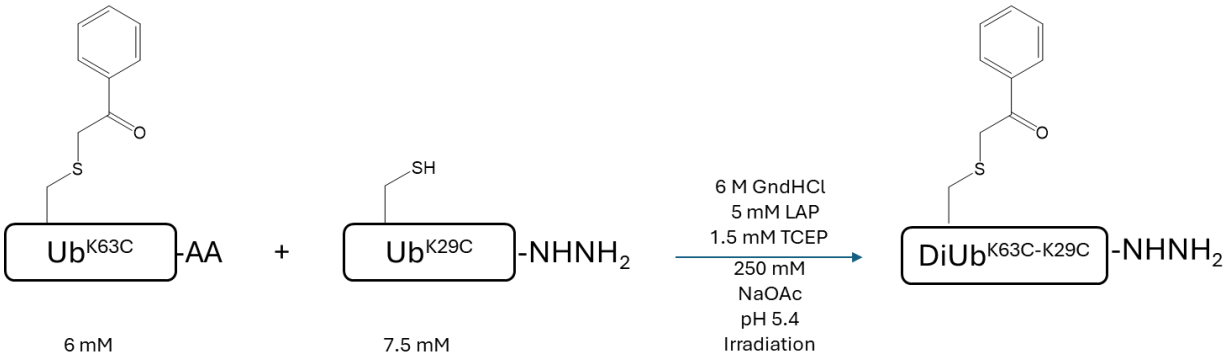

Figure 68 Reaction scheme for the TEC reaction between $Ub^{K63C}{}_{pac}AA$ and $Ub^{K29C}NHNH_2$.

RP-HPLC, ESI-MS and deconvoluted mass spectrum of this reaction is shown in Figure 69.

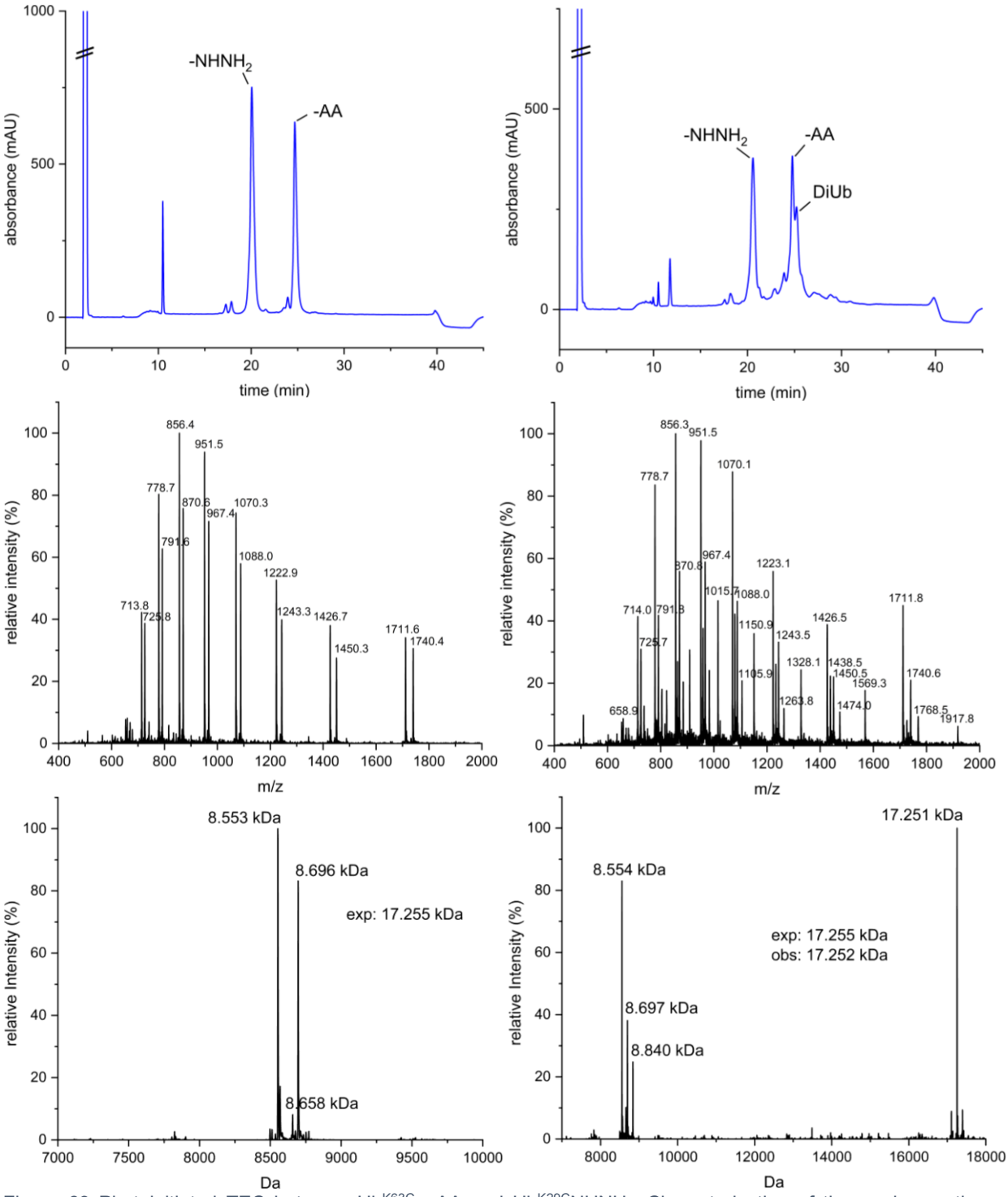

Figure 69 Photoinitiated TEC between $Ub^{K63C}{}_{pac}AA$ and $Ub^{K29C}NHNH_2$. Characterization of the crude reaction mixture before (left) and after (right) irradiation. Analytical RP-HPLC (top), ESI-MS (middle) and deconvoluted mass spectrum (bottom).

Coupling of these ubiquitin mutants worked, as shown in Figure 69. However, the diubiquitin reaction product coelutes with the ubiquitin allylamide rendering purification difficult. The conversion of this reaction is very low. Since the intensity of the LAP adduct signal in the mass spectrum is low, it was decided to increase the concentration of LAP in the next reaction.

Since this reaction was the first TEC reaction with two cysteine mutants in this work, an attempt was first made to purify the PAc-protected diubiquitin and deprotect it afterwards. After optimizing gradient elution profiles towards baseline-separation of the compounds in analytical

RP-HPLC, an attempt was made to isolate the product from the reaction mixture using a semipreparative RP-HPLC column. However, the separation was unsuccesful as the product was obtained as a mixture with other ubiquitin species. Therefore, it was decided to first deprotect and then purify in all subsequent reactions.

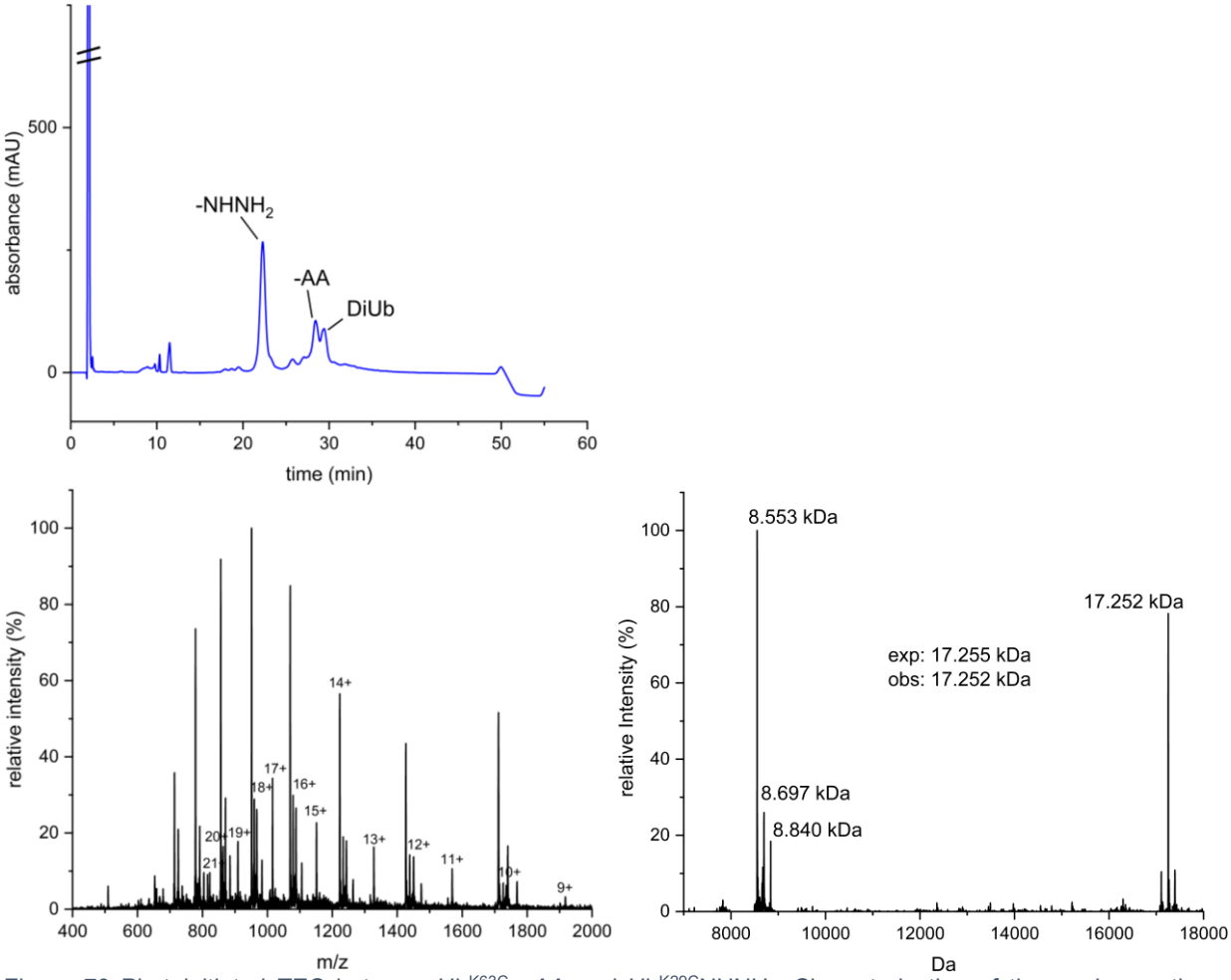

Figure 70 Photoinitiated TEC between $Ub^{K63C}{}_{pac}AA$ and $Ub^{K29C}NHNH_2$. Characterization of the crude reaction mixture after irradiation. RP-HPLC (top), ESI-MS (bottom, left) and deconvoluted mass spectrum (bottom, right).

In the next reaction, a concentration of 5.5 mM LAP was used. Since the turnover of the reaction (Figure 70) was even lower than with 5 mM LAP and at that time the low amount of $Ub^{K63C}{}_{pac}AA$ available from expression was almost completely consumed the focus was shifted towards on other diubiquitin chains for the final reactions.

The crude mixture of was purified by RP-HPLC to yield 0.28 mg (5.4 %) of $DiUb^{K63C\text{-}K29C}NHNH_2$ and characterized in Figure 50.

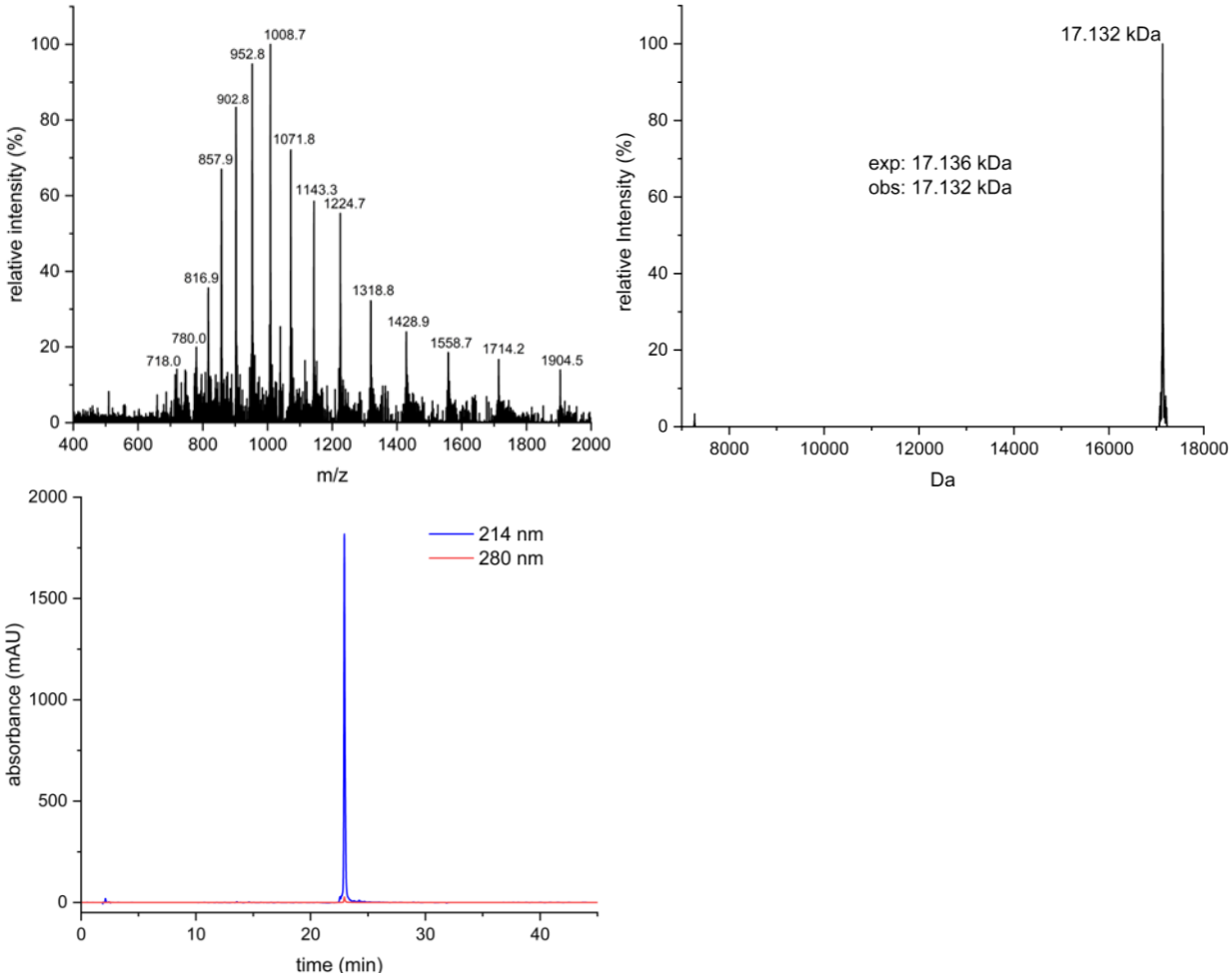

Figure 71 Characterization of isolated DiUb$^{K63C\text{-}K29C}$NHNH$_2$. ESI-MS (left), deconvoluted mass spectrum (right), analytical RP-HPLC (bottom).

Figure 71 shows ESI-MS, deconvoluted mass spectrum and analytical RP-HPLC of isolated DiUb$^{K63C\text{-}K29C}$NHNH$_2$.

The following table summarizes all reactions toward diubiquitin species, which were used for the final reactions. For some of the following reactions in the table, for both pure isolated product and an impure pool with considerable amount of the desired protein, yield is identical. This is due to the fact that these reactions were performed on the same day and all crude reaction mixtures were purified in a single preparative RP-HPLC run. As a result, the value corresponds to the average of both reactions.

Table 1 Summary yields TEC.

$DiUb^{29+63}$	MP [mg]	SP [mg]	$DiUb^{wt+48}$	pure [mg]	impure [mg]	$DiUb^{48+48}$	pure [mg]	impure [mg]
	0.3	0.4		1.7	0.9		0.3	2.9
	0.55	1.15		1.7	0.9		0.3	2.9
	0.55	1.15		1.7	0.9		0.55	1.35
	0.9	2.5		0.7	0.9		0.55	1.35
	0.9	2.5		1.6	2.2		0.75	1.9
	0.55	1.65		1.4	1.7		0.75	1.9
	0.55	1.65		1.4	1.7		0.35	1.8
	0.3	1.65		1.3	1.2		0.35	1.8
	0.3	1.65		1.3	1.2			

Here you can see the reaction turnover improves slightly over time (top to bottoms). In the example of $DiUb^{K29C-K63C}NHNH_2$, the yield of pure protein from the first TEC reaction was only 0.3 mg and that of the impure pool only 0.4 mg. In the following reactions, up to 0.9 mg pure protein and 2.5 mg impure pool could be purified per reaction. The last two reactions had a slightly lower turnover, although proportionally more protein ended up in the impure pool. A concentration of 5.25 mM LAP and 1.5 mM TCEP worked best for this diubiquitin, in terms of the yield.

Creating $DiUb^{wt-K48C}NHNH_2$ generated more pure protein with up to 1.7 mg per reaction and additionally up to 2 mg of impure pool. The lack of deprotection definitely plays a role here, which leads to the undesired by-product in section 4.8 and is difficult to separate from the desired product. The best condition for this diubiquitin was the standard concentration of 5 mM LAP and 1.5 mM TCEP, in terms of the yield.

The yield of $DiUb^{K48C-K48C}NHNH_2$ was rather low, like that of $DiUb^{K29C-K63C}NHNH_2$. The challenging purification after deprotection makes this further challenging. The best condition for this diubiquitin was the standard concentration of 5 mM LAP and 1.5 mM TCEP.

SDS-PAGEs of all TEC reactions to generate diubiquitins are found in the appendix.

4.8 Deprotection

Crude reaction mixtures after TEC with cysteine mutants (section 4.7) were initially deprotected before purification via preparative RP-HPLC.

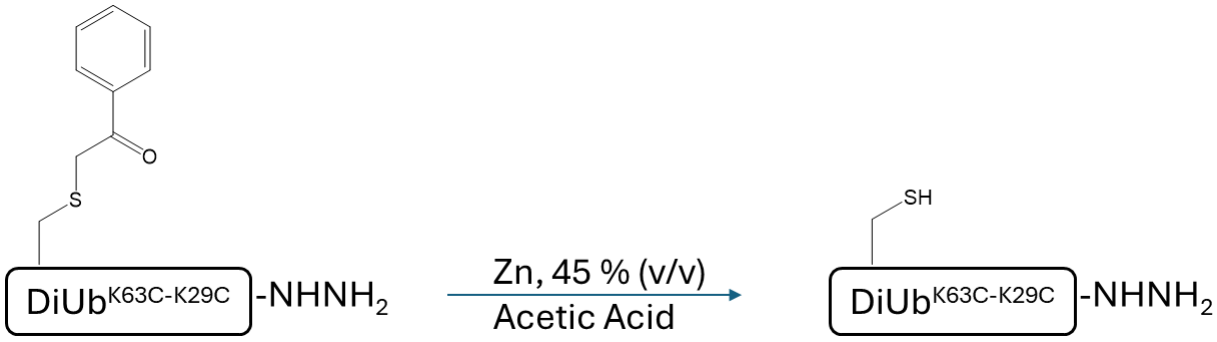

Figure 72 Reaction scheme for the deprotection reaction of $DiUb^{K63C-K29C}NHNH_2$.

For first deprotection reaction, the TEC reaction mixture was diluted with acetic acid (45% v/v final concentration) and Zn powder (180 mg/mL) was added. The reaction was then incubated on a thermal shaker at 25°C and 400 rpm and monitored by LC-MS until completion.

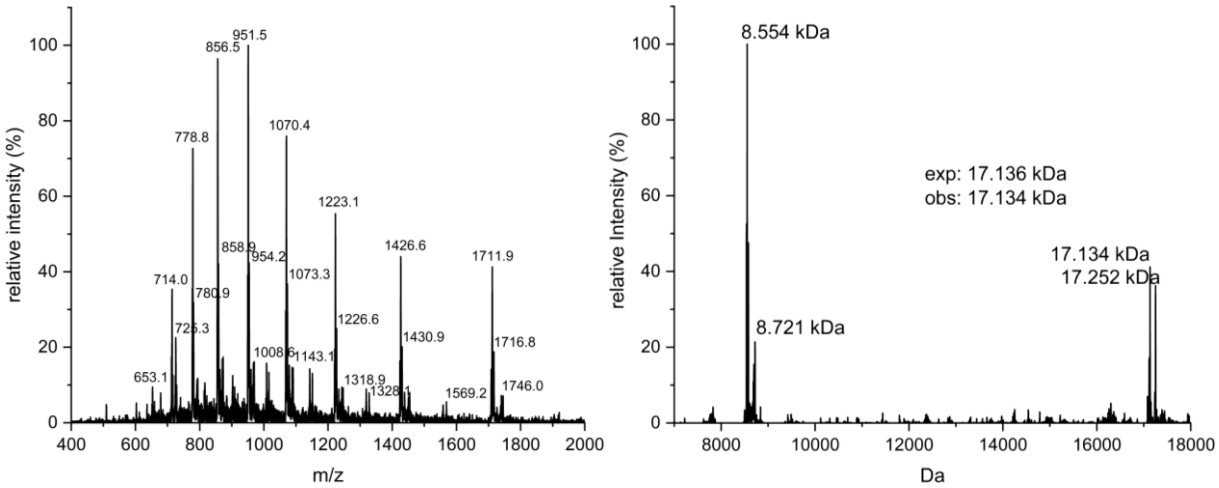

Figure 73 Deprotection reaction of the crude reaction mixture after TEC. ESI-MS (left) and deconvoluted mass spectrum (right).

As shown in Figure 73, the reaction was not yet complete after 1 hour. The signal with the mass 17.134 kDa corresponds to the deprotected $DiUb^{K63C\text{-}K29C}NHNH_2$, whereby unprotected diubiquitin (17.252 kDa) still has almost the same intensity.

Since the reaction was not yet complete after 1 h, a second sample was analyzed by LC-MS after 3 h.

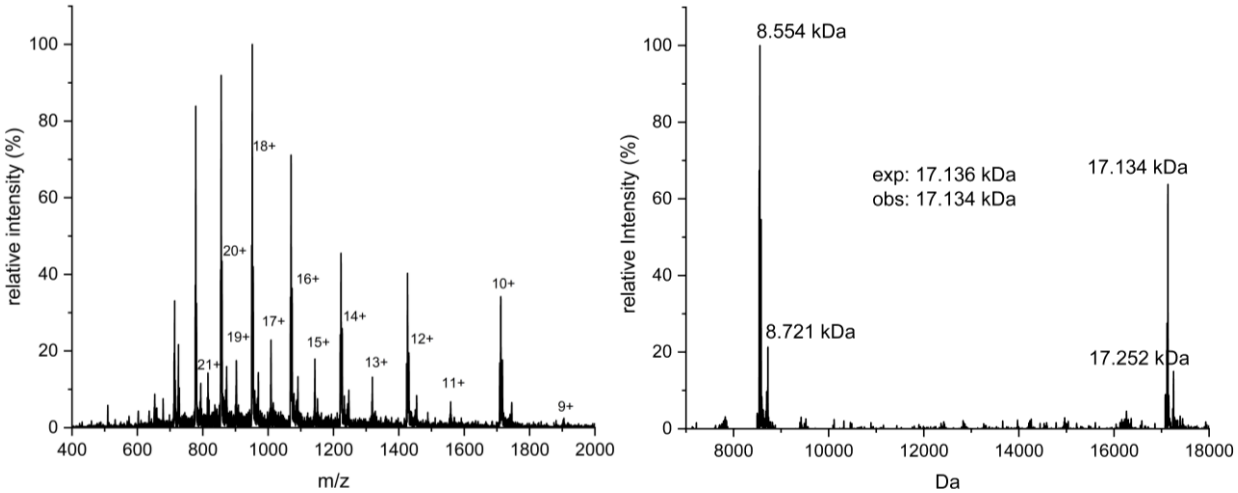

Figure 74 Deprotection reaction of the crude reaction mixture after TEC. ESI-MS (left) and deconvoluted mass spectrum (right).

Even after 3 h, protected diubiquitin is still recognizable in the spectrum (Figure 74).

For this reason, an attempt was made to shorten the duration of the following reactions. For the next reaction (Figure 75), instead of a thermal shaker, the Eppendorf tube was equipped with a small stirring bar to enable better mixture and deprotected on a magnetic stirring table.

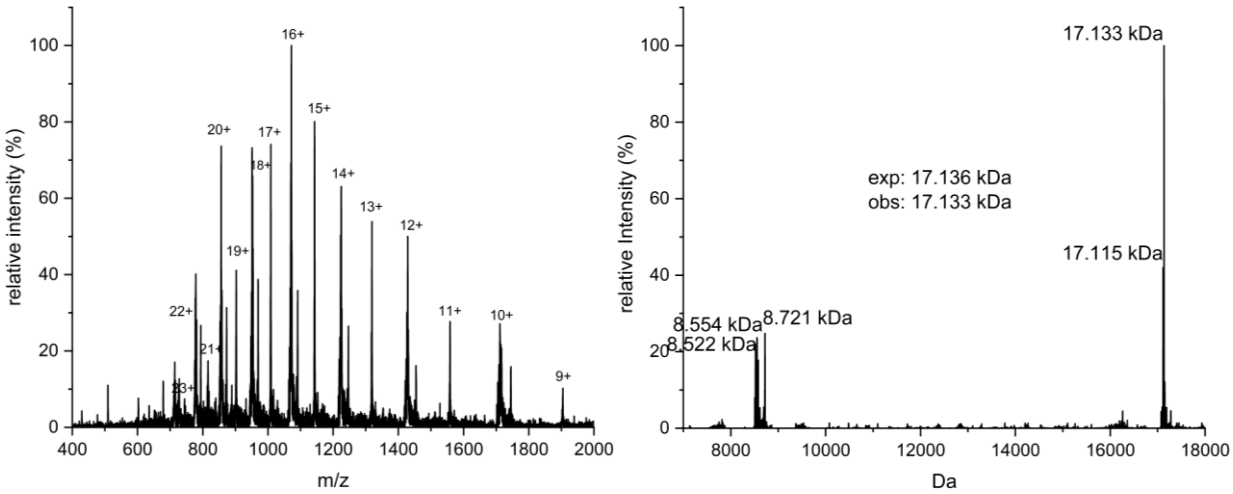

Figure 75 Deprotection reaction of the crude reaction mixture after TEC. ESI-MS (left) and deconvoluted mass spectrum (right).

Due to more efficient mixing, the reaction proceeded faster and no protected diubiquitin was recognizable in the spectrum after 2.5 h (Figure 75). However, a previously unknown mass (17.115-17.120 kDa which shows measured by high resolution mass spectrometry 17.117,2 kDa Figure A 7 and Figure A 8) is visible now. This mass appears to have a higher intensity compared to earlier spectra due to the better turnover of the reactions and this by-product further complicates the purification of the desired diubiquitin, as these two elute from the column almost simultaneously (Figure 76).

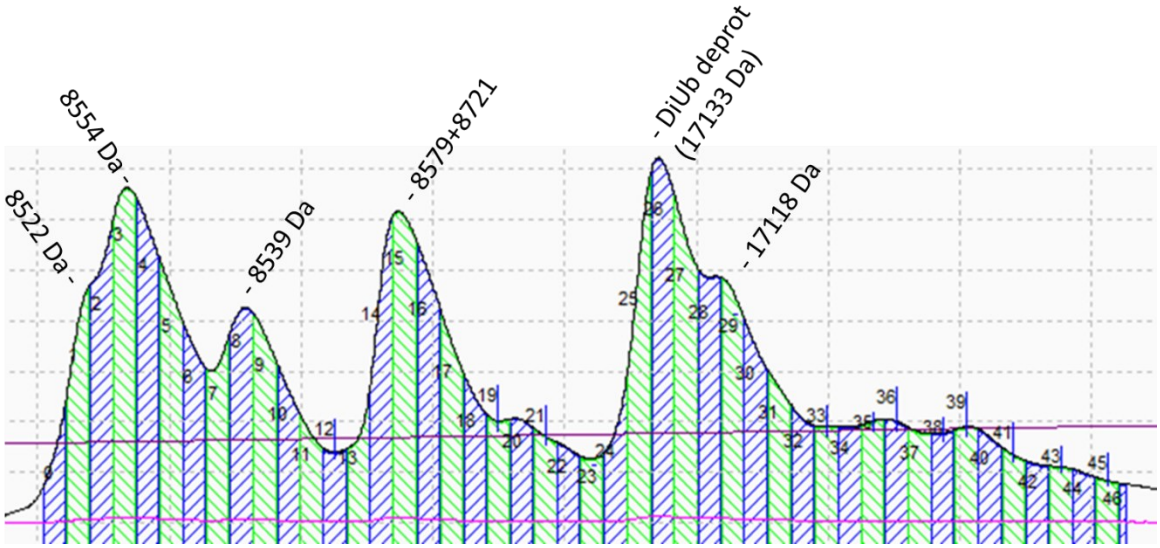

Figure 76 Purification of $DiUb^{K48C\text{-}K48C}NHNH_2$ after deprotection reaction.

Figure 76 shows a zoomed section of the semipreparative RP-HPLC chromatogram recorded during purification. The numbered vertical areas, alternating between green and blue, represent the individual fractions collected by the fraction collector. Despite the use of a long gradient, none of the peaks shown are baseline-separated. Since the peaks all merge, it is relatively difficult to obtain clean fractions of the individual peaks. From left to right, the following components elute from the column: desulfurized hydrazine (8.522 kDa), hydrazine (8.554 kDa), hydrolyzed $Ub^{KxC}COOH$ (8.539 kDa), PAc-deprotected allylamide (8.579 kDa),

allylamide (8.721 kDa), deprotected diubiquitin (17.133 kDa) and the unknown mass (17.117 kDa), which seems to coelute with the desired diubiquitin.

As the unknown side-product is formed during deprotection, further attempts were made to shorten the duration of the reaction in order to minimize the formation of the by-product. Since the overall protein concentration of the crude reaction mixture is quite high (13.5 mM) compared to this study[65] where protein concentration is under 1 mM, in the following reactions the solution was split into two Eppendorf tubes, each diluted 1:1 with 6 M GndHCl and mixed with acetic acid and Zn to achieve the respective 45% (v/v) and 180 mg/mL. This allowed the duration of the reaction to be reduced to 1h (Figure 77).

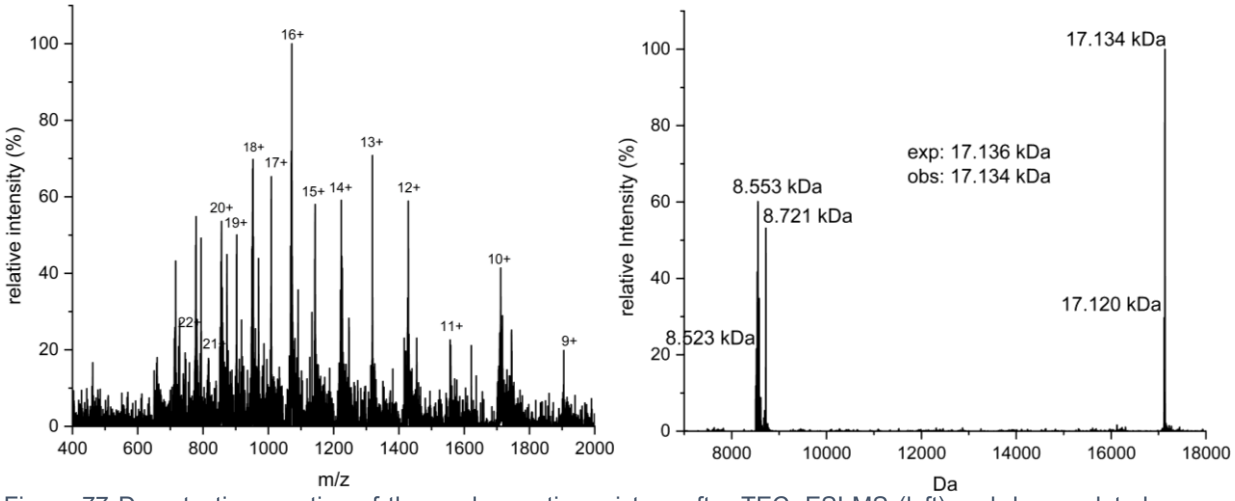

Figure 77 Deprotection reaction of the crude reaction mixture after TEC. ESI-MS (left) and deconvoluted mass spectrum (right).

The shortened reaction time made it possible to keep the intensity of the mass 17.117 kDa lower compared to the intensity of the desired ubiquitin (Figure 77). Since it was not possible to completely separate the desired diubiquitin from the side-product, a sample containing both was measured with high-resolution mass spectrometry in order to identify the unknown species. The spectrum and the corresponding deconvoluted spectrum are shown in the appendix in section 7 (Figure A 7 and Figure A 8).

As shown in the deconvoluted spectrum in the appendix, the mass difference between the unknown mass and the desired diubiquitin is exactly 14.0 Da. This would indicate an exchange of the C-terminal hydrazide to a carboxylic acid.

4.9 Generation of DiUb$^{wt\text{-}K48C}$AA

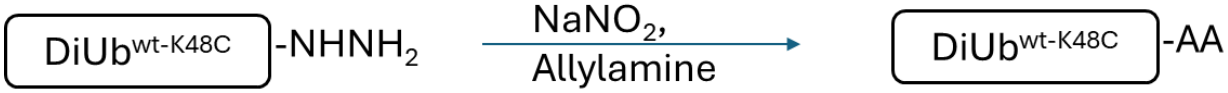

Figure 78 Reaction scheme for the synthesis of DiUb$^{wt\text{-}K48C}$AA.

The purified DiUb$^{wt\text{-}K48C}$NHNH$_2$ from section 4.7.3 with a C-terminal hydrazine was converted to a C-terminal allylamide in order to enable further chain elongation. For this purpose, it was activated as acyl azide using sodium nitrite and then converted into an allylamide using allylamine as described in section 3.12.

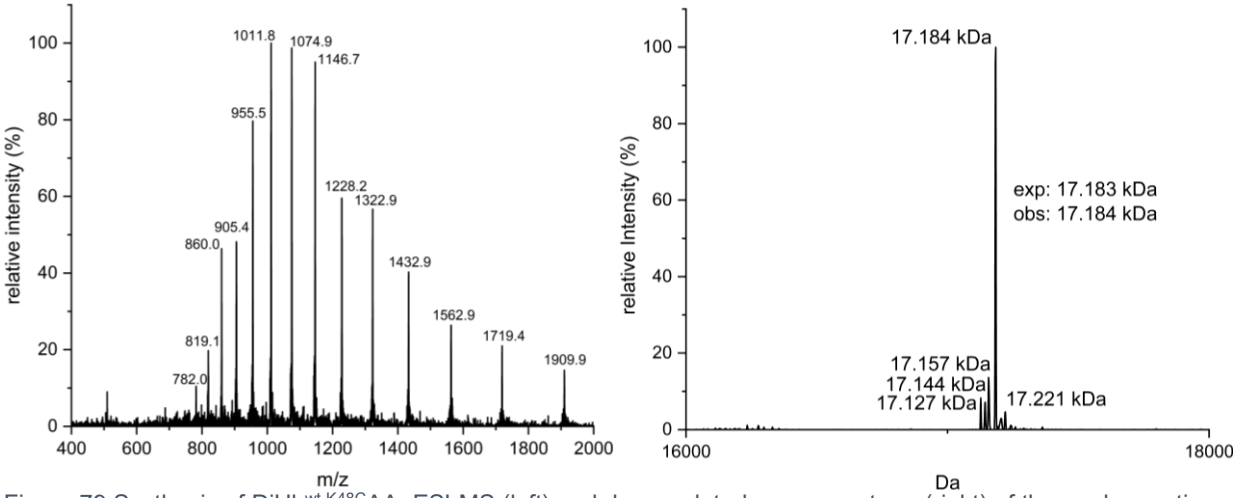

Figure 79 Synthesis of DiUb$^{wt\text{-}K48C}$AA. ESI-MS (left) and deconvoluted mass spectrum (right) of the crude reaction mixture after 2h.

The reaction progress was monitored by LC-MS and showed complete conversion to the allylamide after 2 h (Figure 79).

Purification semipreparative by RP-HPLC, starting with 17.4 mg of diubiquitin from section 4.6.3, yielded 10.4 mg (59.8 %) of isolated product (Figure 80).

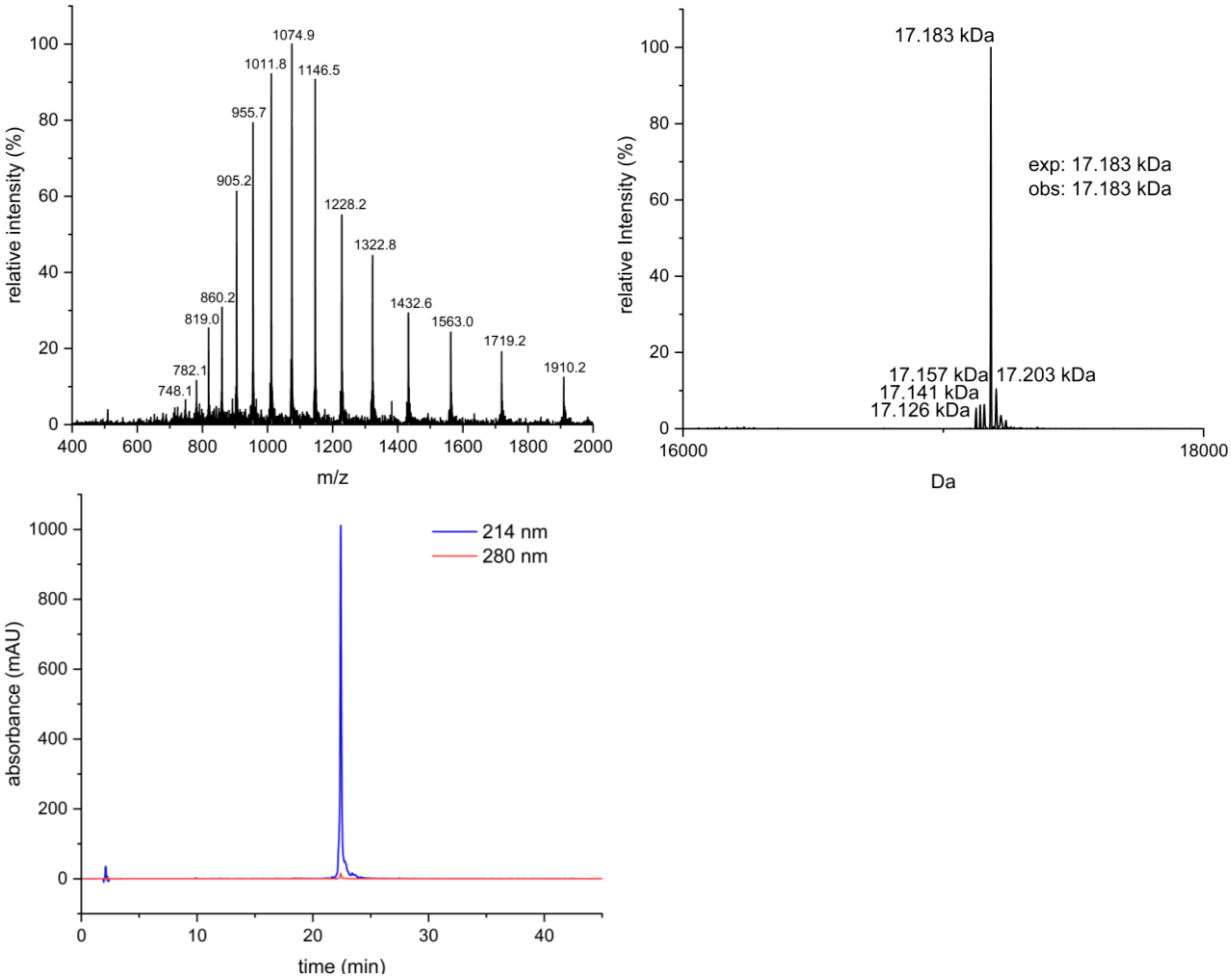

Figure 80 Characterization of isolated DiUb$^{wt\text{-}K48C}$AA. ESI-MS (left), deconvoluted mass spectrum (right), analytical RP-HPLC (bottom).

Figure 80 shows ESI-MS, deconvoluted mass spectrum and analytical RP-HPLC of isolated DiUb$^{wt\text{-}K48C}$AA. Different minor impurities of other modified diubiquitins result from the impurities of the respective hydrazide, as shown in Figure 67.

4.10 Generation of Tri- and TetraUb chains

The purified diubiquitins from sections 4.6-4.9 were used to build the final Tri- and TetraUbiquitin chains.

For all those reactions, the reaction mixture was frozen directly after the coupling reaction. An RP-HPLC chromatogram was then performed to check how good separated of the desired protein and the starting material elute. The reaction mixture was then purified directly.

3.10.1 TriUb$^{wt\text{-}K48C\text{-}K48C}$NHNH$_2$

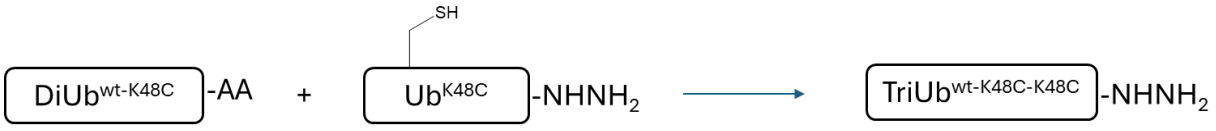

Figure 81 Reaction scheme for the TEC reaction between DiUb$^{wt\text{-}K48C}$AA with Ub^{K48C}NHNH$_2$.

To generate TriUb$^{wt\text{-}K48C\text{-}K48C}$NHNH$_2$, Ub$^{wt\text{-}K48C}$AA from section 4.9 was coupled with Ub^{K48C}NHNH$_2$.

This reaction was carried out under standard conditions (6 mM $Ub^{wt\text{-}K48C}AA$, 7.5 mM $Ub^{K48C}NHNH_2$, 5 mM LAP, 1.5 mM TCEP).

RP-HPLC chromatogram, ESI-MS and deconvoluted mass spectrum of the reaction is shown in Figure 82. A peak of triubiquitin is visible in the RP-HPLC chromatogram, the mass in the deconvoluted spectrum is in accordance with the calculated mass of the desired triubiquitin.

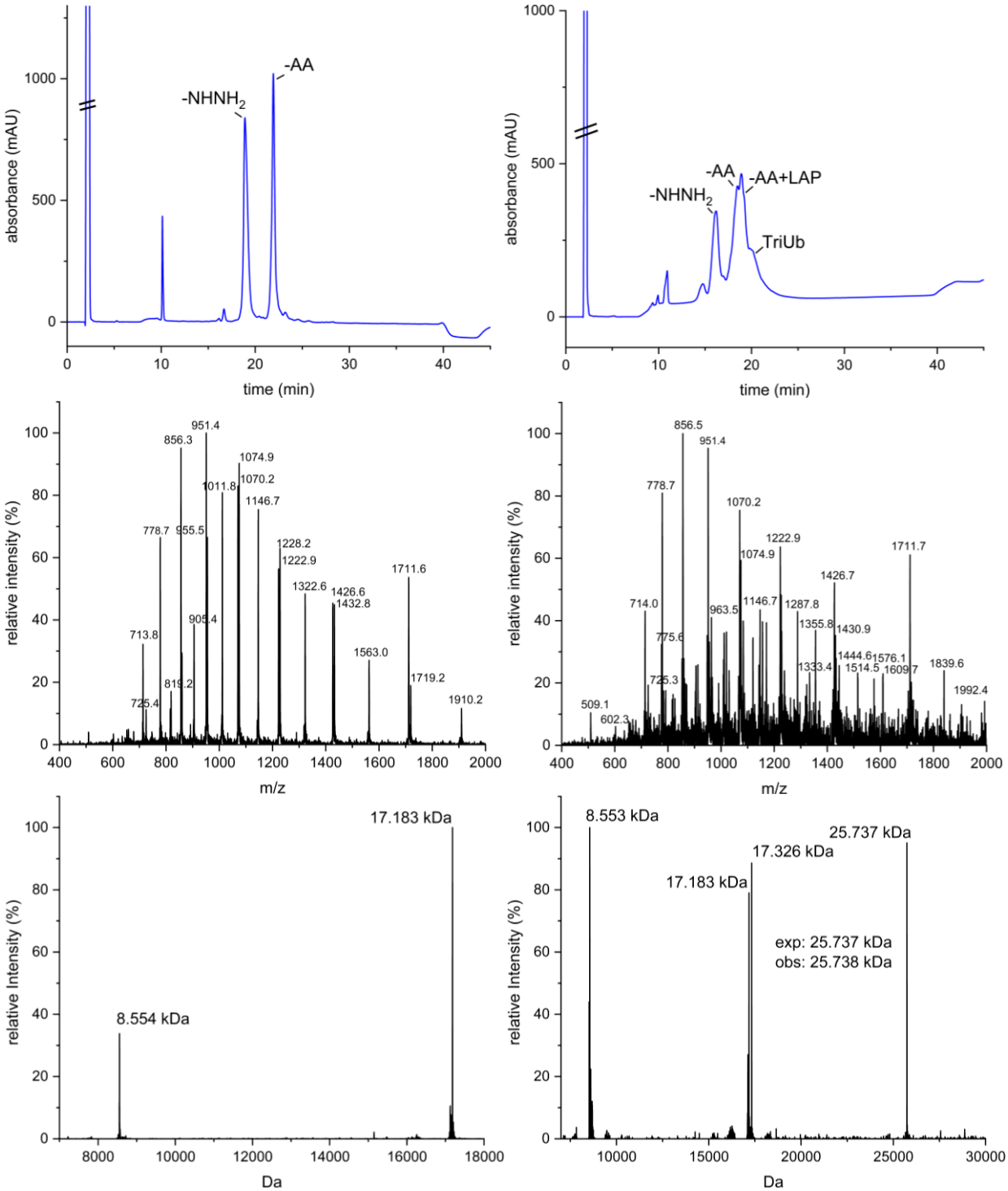

Figure 82 Photoinitiated TEC between $Ub^{wt\text{-}K48C}AA$ and $Ub^{K48C}NHNH_2$. Characterization of the crude reaction mixture before (left) and after (right) irradiation. Analytical RP-HPLC (top), ESI-MS (middle) and deconvoluted mass spectrum (bottom).

After purification, an analytical RP-HPLC and an ESI-MS were performed. Furthermore, an SDS-PAGE of all final ubiquitin chains (Figure 91) was performed.

Characterization of isolated TriUb$^{wt\text{-}K48C\text{-}K48C}$NHNH$_2$ with a yield of 1.5 mg (16 %) is shown in Figure 83. Also 0.8 mg of a pool with considerable amount and another pool of 3 mg with little amount of the desired protein was gained.

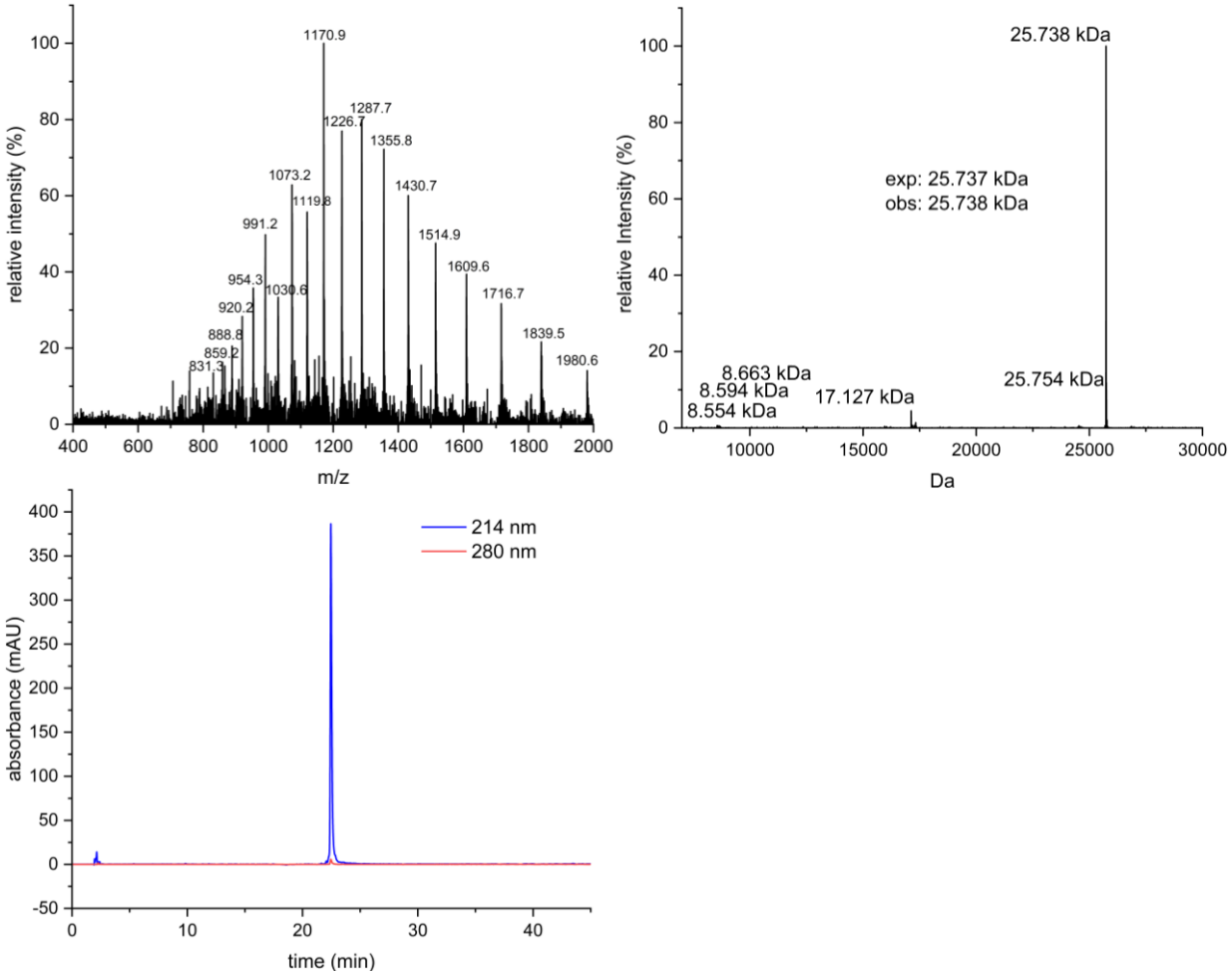

Figure 83 Characterization of isolated TriUb$^{wt\text{-}K48C\text{-}K48C}$NHNH$_2$. ESI-MS (left), deconvoluted mass spectrum (right), analytical RP-HPLC (bottom).

Figure 83 shows ESI-MS, deconvoluted mass spectrum and analytical RP-HPLC of isolated TriUb$^{wt\text{-}K48C\text{-}K48C}$NHNH$_2$.

4.10.2 TriUb$^{wt\text{-}K29C\text{-}K63C}$NHNH$_2$

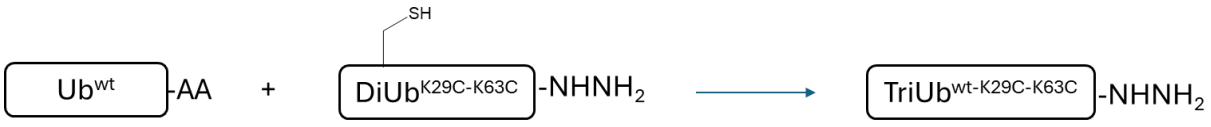

Figure 84 Reaction scheme for the TEC reaction between Ub^{wt}AA and DiUb$^{K29C\text{-}K63C}$NHNH$_2$.

To generate TriUb$^{wt\text{-}K29C\text{-}K63C}$NHNH$_2$, Ub$^{K29C\text{-}K63C}$NHNH$_2$ from section 4.7.1 was coupled with Ub^{wt}AA.

Due to the challenges in purification (see section 4.8) of the PAc-deprotected diubiquitins, it was not possible to obtain enough sufficiently pure DiUb$^{K29C\text{-}K63C}$NHNH$_2$ for the standard

conditions of the TEC. As a result, the concentrations of the proteins were reduced to 4.75 mM (AA) and 6.10 mM ($NHNH_2$). The concentrations of LAP (5 mM) and TCEP (1.5 mM) were not changed.

RP-HPLC, ESI-MS and deconvoluted spectrum of the reaction is shown in Figure 85. A peak of triubiquitin is visible in the RP-HPLC chromatogram, the mass in the deconvoluted mass spectrum is in accordance with the calculated mass of the desired triubiquitin.

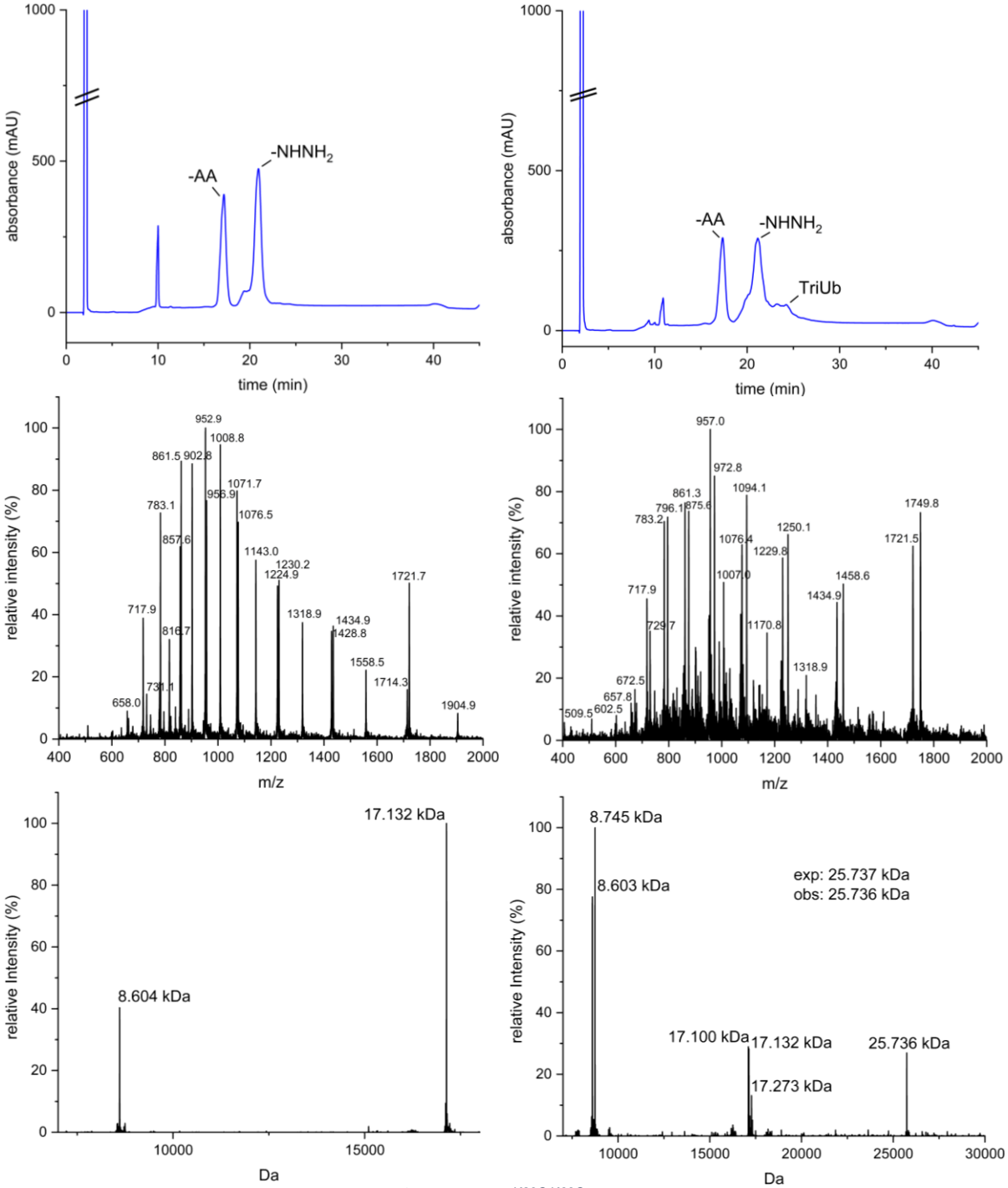

Figure 85 Photoinitiated TEC between $Ub^{wt}AA$ and $Ub^{K29C\text{-}K63C}NHNH_2$. Characterization of the crude reaction mixture before (left) and after (right) irradiation. Analytical RP-HPLC (top), ESI-MS (middle) and deconvoluted mass spectrum (bottom).

Furthermore, an SDS-PAGE of all final ubiquitin chains (Figure 91) was performed.

Characterization of isolated TriUb$^{wt\text{-}K29C\text{-}K63C}$NHNH$_2$ with a yield of 1.39 mg (18 %) is shown in Figure 86. Also 2.08 mg of another pool with little amount of desired protein was gained.

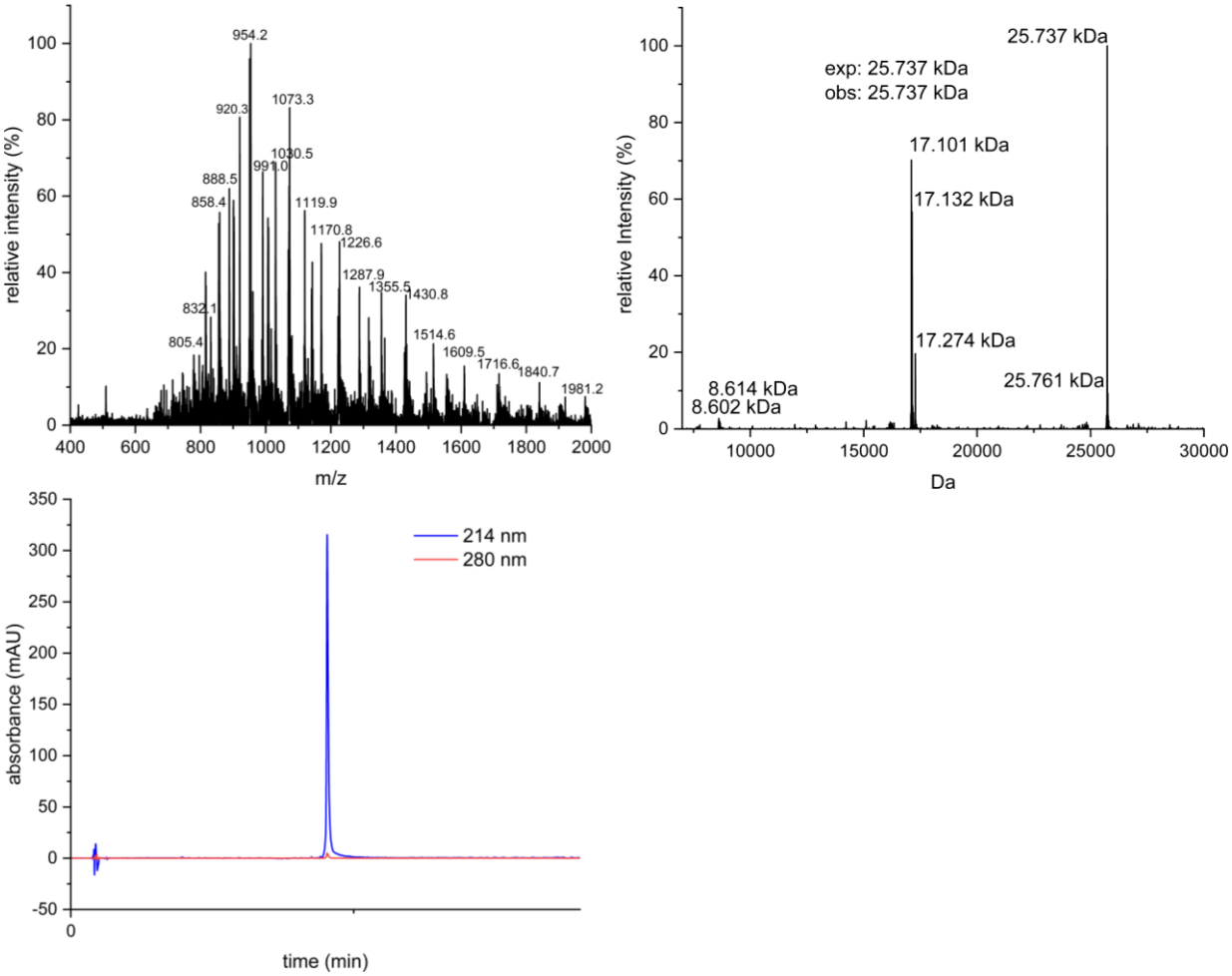

Figure 86 Characterization of isolated TriUb$^{wt\text{-}K29C\text{-}K63C}$NHNH$_2$. ESI-MS (left), deconvoluted mass spectrum (right), analytical RP-HPLC (bottom).

Figure 86, Figure 9 shows ESI-MS, deconvoluted mass spectrum and analytical RP-HPLC of isolated TriUb$^{wt\text{-}K29C\text{-}K63C}$NHNH$_2$.

4.10.3 TetraUb$^{wt\text{-}K48C\text{-}K48C\text{-}K48C}$NHNH$_2$

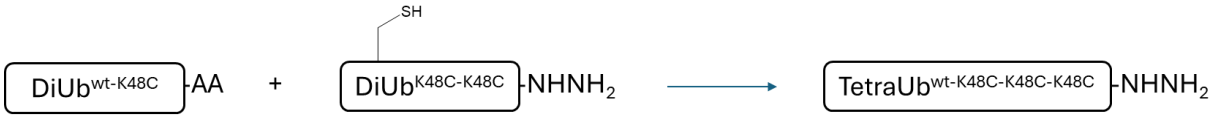

Figure 87 Reaction scheme for the TEC reaction between DiUb$^{wt\text{-}K48C}$AA and DiUb$^{K48C\text{-}K48C}$NHNH$_2$.

To generate TetraUb$^{wt\text{-}K48C\text{-}K48C\text{-}K48C}$NHNH$_2$, Ub$^{K48C\text{-}K48C}$NHNH$_2$ from section 4.7.2 was coupled with Ub$^{wt\text{-}K48C}$AA from section 4.8.

Due to the challenges in purification (see section 4.8) of the PAc-deprotected diubiquitins, it was not possible to obtain sufficient amounts of pure DiUb$^{K48C\text{-}K48C}$NHNH$_2$ for the standard conditions of the TEC. As a result, the concentrations of the proteins used were reduced to 3.71mM (AA) and 4.67 mM (NHNH$_2$). The concentrations of LAP (3.11 mM) and TCEP (0.93 mM) were lowered.

RP-HPLC, ESI-MS and deconvoluted mass spectrum of the reaction is shown in Figure 88. A peak of tetraubiquitin is clearly visible in the RP-HPLC chromatogram, the mass in the deconvoluted spectrum is in accordance with the calculated mass of the desired tetraubiquitin.

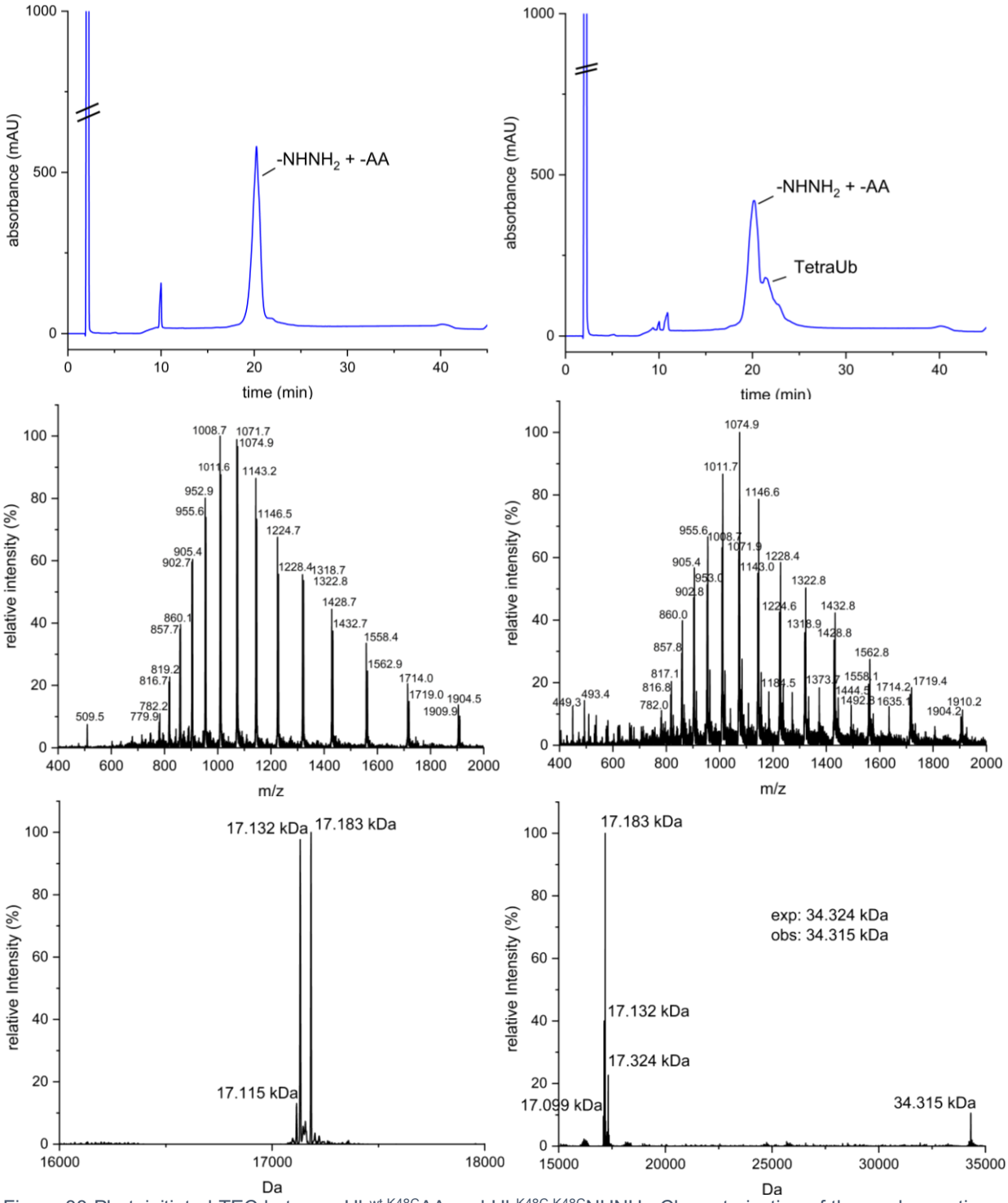

Figure 88 Photoinitiated TEC between $Ub^{wt\text{-}K48C}AA$ and $Ub^{K48C\text{-}K48C}NHNH_2$. Characterization of the crude reaction mixture before (left) and after (right) irradiation. Analytical RP-HPLC (top), ESI-MS (middle) and deconvoluted mass spectrum (bottom).

After purification, an analytical RP-HPLC and an ESI-MS were performed as characterization, like for the mono-ubiquitins. Furthermore, an SDS-PAGE of all final products (Figure 91) was performed.

Characterization of isolated TriUb$^{wt\text{-}K48C\text{-}K48C\text{-}K48C}$NHNH$_2$ with a yield of 0.51 mg (6 %) is shown in Figure 89. Also 0.83 mg of another pool with little amount of desired protein was gained.

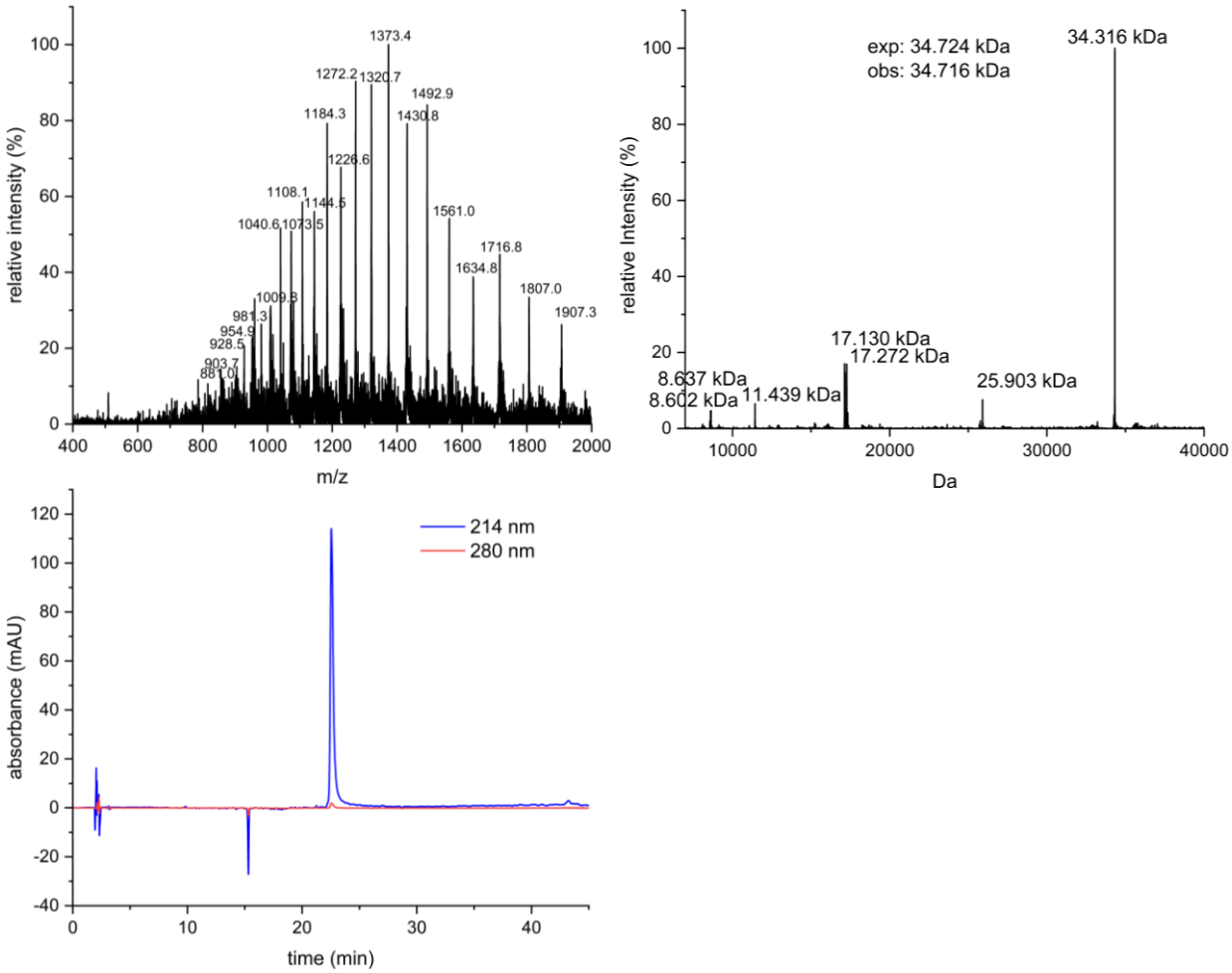

Figure 89 Characterization of isolated TetraUb$^{wt\text{-}K48C\text{-}K48C\text{-}K48C}$NHNH$_2$. ESI-MS (left), deconvoluted mass spectrum (right), analytical RP-HPLC (bottom).

Figure 89 shows ESI-MS, deconvoluted mass spectrum and analytical RP-HPLC of isolated TetraUb$^{wt\text{-}K48C\text{-}K48C}$NHNH$_2$.

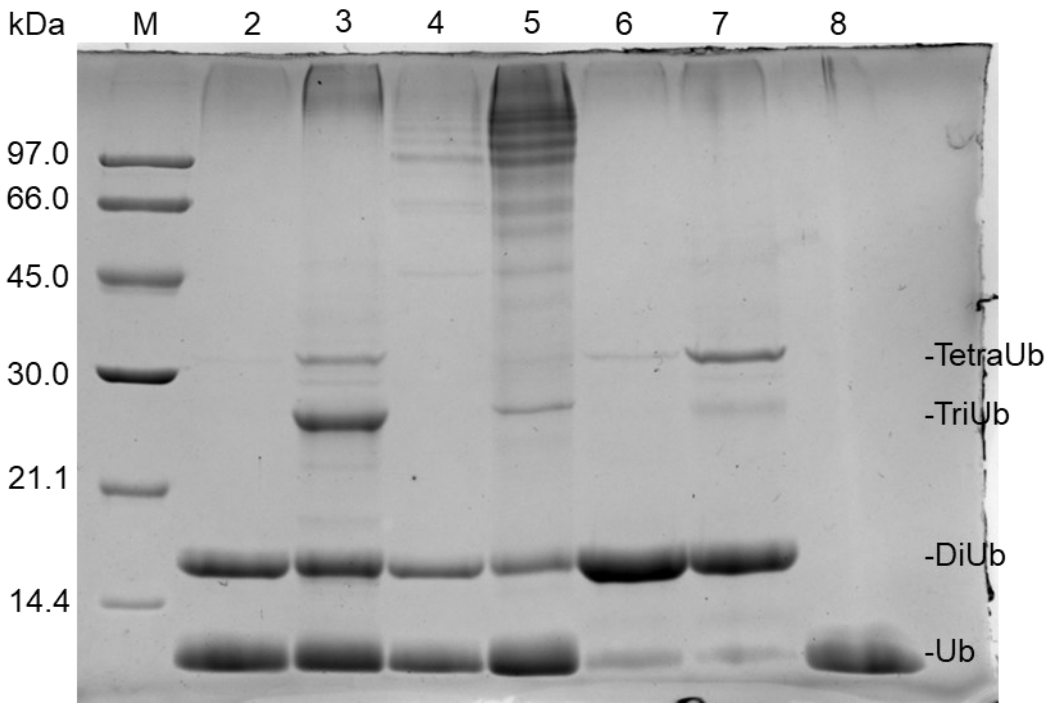

Figure 90 SDS PAGE of TECs of final ubiquitin chains. Lane 1 Marker, Lane 2 TEC TriUb$^{wt\text{-}K48C\text{-}K48C}$NHNH$_2$ t_0, Lane 3 TEC TriUb$^{wt\text{-}K48C\text{-}K48C}$NHNH$_2$ (25.737 kDa) t_1, Lane 4 TEC TriUb$^{wt\text{-}K29C\text{-}K63C}$NHNH$_2$ t_0, Lane 5 TEC TriUb$^{wt\text{-}K29C\text{-}K63C}$NHNH$_2$ (25.737 kDa) t_1, Lane 6 TEC TetraUb$^{wt\text{-}K48C\text{-}K48C\text{-}K48C}$NHNH$_2$ t_0, Lane 7 TetraUb$^{wt\text{-}K48C\text{-}K48C\text{-}K48C}$NHNH$_2$ (34.324 kDa) t_1, Lane 8 Ub^{wt}AA (~6.500 kDa).

The TEC reactions towards TriUb and TetraUb were additionally analyzed by SDS-PAGE (Figure 90). The bands of the mono-, di-, tri- and tetraubiquitin are clearly visible. In the respective time points for the formation of the two triubiquitins before the reaction, the building blocks used are recognizable as the main bands. For the tetraubiquitin besides the two diubiquitins coupled, mono-ubiquitin is still clearly recognizable on the gel. This illustrates the difficulties in the separation of the diubiquitin from its monomeric building blocks. After the reaction, the band of the respective coupling product is recognizable. In the reaction for TriUb$^{wt\text{-}K29C\text{-}K63C}$NHNH$_2$ (Lane 5), even though the building blocks were used in a slightly reduced concentration the difference in intensity of the desired triubiquitin is barely recognizable compared to the starting material.

Coupling of TetraUb$^{wt\text{-}K48C\text{-}K48C\text{-}K48C}$NHNH$_2$ (Lane 7) worked better. Furthermore, TriUb is also recognizable in this band, which was probably formed as a by-product from coupling of a DiUb with contaminated Ub.

Bands indicating higher molecular weight species are recognizable in all samples after the reaction. These bands are typical for TEC without protection of Cys, as described in the literature.[66] In this work those bands probably occur due to building blocks still containing mono-ubiquitin species.

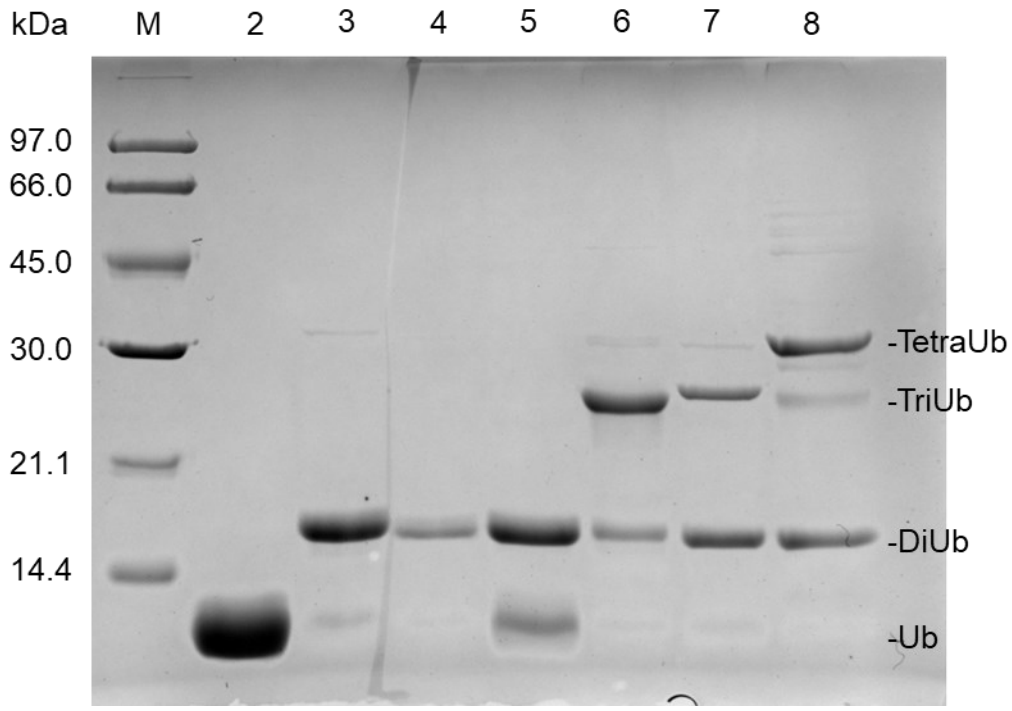

Figure 91 SDS PAGE of final ubiquitin chains. Lane 1 Marker, Lane 2 $Ub^{wt}AA$, Lane 3 $DiUb^{wt\text{-}K48C}AA$, Lane 4 $DiUb^{K29C\text{-}K63C}NHNH_2$, Lane 5 $DiUb^{K48C\text{-}K48C}NHNH_2$, Lane 6 $TriUb^{wt\text{-}K48C\text{-}K48C}NHNH_2$, Lane 7 $TriUb^{wt\text{-}K29C\text{-}K63C}NHNH_2$, Lane 8 $TetraUb^{wt\text{-}K48C\text{-}K48C\text{-}K48C}NHNH_2$.

Furthermore, an SDS-PAGE of all the isolated DiUb, TriUb and TetraUb (fractions with the highest purity) was performed, next to $Ub^{wt}AA$ as representative monomeric building block. The gel shows that all samples are still contaminated with monoubiquitin. Furthermore, both $TriUb^{wt\text{-}K48C\text{-}K48C}NHNH_2$ and $TriUb^{wt\text{-}K29C\text{-}K63C}NHNH_2$ still contain diubiquitin, $TetraUb^{wt\text{-}K48C\text{-}K48C\text{-}K48C}NHNH_2$ additionally contains triubiquitin. Comparing the band of $TriUb^{wt\text{-}K48C\text{-}K48C}NHNH_2$ (Lane 6) with the corresponding spectra from the characterization of this protein in Figure 83 reveals a lot more impurities than indicated by the RP-HPLC chromatogram and MS spectra.

4.12 Discussion of TEC and deprotection

In PAc deprotection, longer reaction times correlated with the formation of an unidentified byproduct. They could be reduced to 1 h by using a stirring bar and diluting the concentration of the product mixture, thus minimizing the amount of unidentified by-product. PAc deprotection after TEC could alternatively be carried out in MPAA (15 % v/v in 6M GndHCl) instead of acetic acid as described for the semisynthesis of Hsp27[65], For Prp (90-231), the reaction in MPAA was described as sluggish. For ubiquitin this would be a possibility to prevent the formation of the by-product which is possibly DiUbCOOH.

It was possible to generate small amounts of all three desired ubiquitin chains $TriUb^{wt\text{-}K48C\text{-}K48C}NHNH_2$, $TriUb^{wt\text{-}K29C\text{-}K63C}NHNH_2$ and $TetraUb^{wt\text{-}K48C\text{-}K48C\text{-}K48C}NHNH_2$ in the final reactions and to obtain suitable spectra for each of those.

In general, it is difficult to separate ubiquitin chains from the building blocks by RP-HPLC. Other purification methods used in the following paragraph to isolate ubiquitin chains are size exclusion and cation exchange chromatography. A low reaction turnover and the additional

deprotection of the cysteine mutants render this even more challenging. All of the above, as well as the randomly set fractions during purification (Figure 76), strongly influence the quantity and exact purity of isolated ubiquitin chains.

In this study[36], up to TetraUb chains K48-linked and K63-linked were built up enzymatically and then purified using cation exchange chromatography. A yield of 88 % is reported for diubiquitin, which is significantly higher than that reported in this work. In[66], up to HeptaUbiquitin chains of 6-, 48- and 63-linked oligomers were constructed using TEC and purified using size exclusion in a milligram scale. TEC was performed here in 100 µL with 2 mM building blocks and 0.5 mM LAP, but without TCEP and GndHCl. Compared to this work, the pools obtained were significantly purer. Both purification methods mentioned here would be possible alternatives to obtain pure tri- or tetraubiquitin after TEC.

5. Conclusion

During this thesis, four different Ub Lyc-to-Cys mutants (K11C, K29C, K48C, K63C) were generated carrying either a C-terminal hydrazide or allylamide. For Ub^{K29C}, Ub^{K48C} and Ub^{K63C} suitable plasmids were already available. For Ub^{K11C}, a plasmid and E. coli expression strain was produced via site-directed mutagenesis. Different diubiquitins were generated by TEC: $DiUb^{wt\text{-}K29C}NHNH_2$, $DiUb^{wt\text{-}K48C}NHNH_2$, $DiUb^{wt\text{-}K63C}NHNH_2$, $DiUb^{K29C\text{-}K63C}NHNH_2$, $DiUb^{K48C\text{-}K63C}NHNH_2$ and $DiUb^{K63C\text{-}K29C}NHNH_2$. Various attempts of coupling $Ub^{K11C}NHNH_2$ to $Ub^{wt}AA$ could not generate the desired diubiquitin. This could indicate a different accessibility or reactivity compared to the other cysteine mutants, even though PAc protection of $Ub^{K11C}SR$ was successful. During deprotection auf PAc, conditions were continously changed to improve yield. A by-product of this reaction, which coelutes with the desired protein and challenges purification was measured by HR-MS and revealed a mass difference of 14 Da, which indicates an exchange of the C-terminal hydrazide to a carboxylic acid. Finally, $TriUb^{wt\text{-}K48C\text{-}K48C}NHNH_2$, $TriUb^{wt\text{-}K29C\text{-}K63C}NHNH_2$ and $TetraUb^{wt\text{-}K48C\text{-}K48C\text{-}K48C}NHNH_2$ were produced via TEC and purified sufficiently enough for characterization, but further optimization is needed regarding yield and purification of the pure proteins from TEC.

6. References

(1) Walsh, C. T.; Garneau-Tsodikova, S.; Gatto, G. J. Protein Posttranslational Modifications: The Chemistry of Proteome Diversifications. *Angew. Chem. Int. Ed.* **2005**, *44* (45), 7342–7372. https://doi.org/10.1002/anie.200501023.

(2) Song, L.; Luo, Z.-Q. Post-Translational Regulation of Ubiquitin Signaling. *J. Cell Biol.* **2019**, *218* (6), 1776–1786. https://doi.org/10.1083/jcb.201902074.

(3) Popovic, D.; Vucic, D.; Dikic, I. Ubiquitination in Disease Pathogenesis and Treatment. *Nat. Med.* **2014**, *20* (11), 1242–1253. https://doi.org/10.1038/nm.3739.

(4) Hershko, A.; Ciechanover, A. THE UBIQUITIN SYSTEM. *Annu. Rev. Biochem.* **1998**, *67* (1), 425–479. https://doi.org/10.1146/annurev.biochem.67.1.425.

(5) Clague, M. J.; Heride, C.; Urbé, S. The Demographics of the Ubiquitin System. *Trends Cell Biol.* **2015**, *25* (7), 417–426. https://doi.org/10.1016/j.tcb.2015.03.002.

(6) Abeywardana, T.; Pratt, M. R. Using Chemistry to Investigate the Molecular Consequences of Protein Ubiquitylation. *ChemBioChem* **2014**, *15* (11), 1547–1554. https://doi.org/10.1002/cbic.201402117.

(7) Pickart, C. M.; Fushman, D. Polyubiquitin Chains: Polymeric Protein Signals. *Curr. Opin. Chem. Biol.* **2004**, *8* (6), 610–616. https://doi.org/10.1016/j.cbpa.2004.09.009.

(8) Sun, L.; Chen, Z. J. The Novel Functions of Ubiquitination in Signaling. *Curr. Opin. Cell Biol.* **2004**, *16* (2), 119–126. https://doi.org/10.1016/j.ceb.2004.02.005.

(9) Haglund, K.; Dikic, I. Ubiquitylation and Cell Signaling. *EMBO J.* **2005**, *24* (19), 3353–3359. https://doi.org/10.1038/sj.emboj.7600808.

(10) Kulathu, Y.; Komander, D. Atypical Ubiquitylation — the Unexplored World of Polyubiquitin beyond Lys48 and Lys63 Linkages. *Nat. Rev. Mol. Cell Biol.* **2012**, *13* (8), 508–523. https://doi.org/10.1038/nrm3394.

(11) Fan, J.-B.; Arimoto, K.; Motamedchaboki, K.; Yan, M.; Wolf, D. A.; Zhang, D.-E. Identification and Characterization of a Novel ISG15-Ubiquitin Mixed Chain and Its Role in Regulating Protein Homeostasis. *Sci. Rep.* **2015**, *5* (1), 12704. https://doi.org/10.1038/srep12704.

(12) Hendriks, I. A.; D'Souza, R. C. J.; Yang, B.; Verlaan-de Vries, M.; Mann, M.; Vertegaal, A. C. O. Uncovering Global SUMOylation Signaling Networks in a Site-Specific Manner. *Nat. Struct. Mol. Biol.* **2014**, *21* (10), 927–936. https://doi.org/10.1038/nsmb.2890.

(13) Goldknopf, I. L.; French, M. F.; Musso, R.; Busch, H. Presence of Protein A24 in Rat Liver Nucleosomes. *Proc. Natl. Acad. Sci.* **1977**, *74* (12), 5492–5495. https://doi.org/10.1073/pnas.74.12.5492.

(14) Fottner, M.; Weyh, M.; Gaussmann, S.; Schwarz, D.; Sattler, M.; Lang, K. A Modular Toolbox to Generate Complex Polymeric Ubiquitin Architectures Using Orthogonal Sortase Enzymes. *Nat. Commun.* **2021**, *12* (1), 6515. https://doi.org/10.1038/s41467-021-26812-9.

(15) Nakagawa, T.; Nakayama, K. Protein Monoubiquitylation: Targets and Diverse Functions. *Genes Cells* **2015**, *20* (7), 543–562. https://doi.org/10.1111/gtc.12250.

(16) Glickman, M. H.; Ciechanover, A. The Ubiquitin-Proteasome Proteolytic Pathway: Destruction for the Sake of Construction. *Physiol. Rev.* **2002**, *82* (2), 373–428. https://doi.org/10.1152/physrev.00027.2001.

(17) Chen, J.; Chen, Z. J. Regulation of NF-κB by Ubiquitination. *Curr. Opin. Immunol.* **2013**, *25* (1), 4–12. https://doi.org/10.1016/j.coi.2012.12.005.

(18) Chen, Z. J.; Sun, L. J. Nonproteolytic Functions of Ubiquitin in Cell Signaling. *Mol. Cell* **2009**, *33* (3), 275–286. https://doi.org/10.1016/j.molcel.2009.01.014.

(19) Swatek, K. N.; Komander, D. Ubiquitin Modifications. *Cell Res.* **2016**, *26* (4), 399–422. https://doi.org/10.1038/cr.2016.39.

(20) Yau, R. G.; Doerner, K.; Castellanos, E. R.; Haakonsen, D. L.; Werner, A.; Wang, N.; Yang, X. W.; Martinez-Martin, N.; Matsumoto, M. L.; Dixit, V. M.; Rape, M. Assembly and Function of Heterotypic Ubiquitin Chains in Cell-Cycle and Protein Quality Control. *Cell* **2017**, *171* (4), 918-933.e20. https://doi.org/10.1016/j.cell.2017.09.040.

(21) Haakonsen, D. L.; Rape, M. Branching Out: Improved Signaling by Heterotypic Ubiquitin Chains. *Trends Cell Biol.* **2019**, *29* (9), 704–716. https://doi.org/10.1016/j.tcb.2019.06.003.
(22) Gopinath, P.; Ohayon, S.; Nawatha, M.; Brik, A. Chemical and Semisynthetic Approaches to Study and Target Deubiquitinases. *Chem. Soc. Rev.* **2016**, *45* (15), 4171–4198. https://doi.org/10.1039/C6CS00083E.
(23) Mali, S. M.; Singh, S. K.; Eid, E.; Brik, A. Ubiquitin Signaling: Chemistry Comes to the Rescue. *J. Am. Chem. Soc.* **2017**, *139* (14), 4971–4986. https://doi.org/10.1021/jacs.7b00089.
(24) Merrifield, R. B. **Solid Phase Peptide Synthesis. I. The Synthesis of a Tetrapeptide**. *J. Am. Chem. Soc.* **1963**, *85* (14), 2149–2154. https://doi.org/10.1021/ja00897a025.
(25) Kent, S. B. H. Total Chemical Synthesis of Proteins. *Chem Soc Rev* **2009**, *38* (2), 338–351. https://doi.org/10.1039/B700141J.
(26) Conibear, A. C.; Watson, E. E.; Payne, R. J.; Becker, C. F. W. Native Chemical Ligation in Protein Synthesis and Semi-Synthesis. *Chem. Soc. Rev.* **2018**, *47* (24), 9046–9068. https://doi.org/10.1039/C8CS00573G.
(27) Francis, D. M.; Page, R. Strategies to Optimize Protein Expression in *E. Coli*. *Curr. Protoc. Protein Sci.* **2010**, *61* (1). https://doi.org/10.1002/0471140864.ps0524s61.
(28) Oberg, K.; Chrunyk, B. A.; Wetzel, R.; Fink, A. L. Native-like Secondary Structure in Interleukin-1.Beta. Inclusion Bodies by Attenuated Total Reflectance FTIR. *Biochemistry* **1994**, *33* (9), 2628–2634. https://doi.org/10.1021/bi00175a035.
(29) Yan, F.; Qian, M.; Yang, F.; Cai, F.; Yuan, Z.; Lai, S.; Zhao, X.; Gou, L.; Hu, Z.; Deng, H. A Novel Pro-Apoptosis Protein PNAS-4 from Xenopus Laevis: Cloning, Expression, Purification, and Polyclonal Antibody Production. *Biochem. Mosc.* **2007**, *72* (6), 664–671. https://doi.org/10.1134/S0006297907060107.
(30) Valax, P.; Georgiou, G. Molecular Characterization of β-Lactamase Inclusion Bodies Produced in *Escherichia Coli.* 1. Composition. *Biotechnol. Prog.* **1993**, *9* (5), 539–547. https://doi.org/10.1021/bp00023a014.
(31) Sharp, P. M.; Li, W.-H. The Codon Adaptation Index-a Measure of Directional Synonymous Codon Usage Bias, and Its Potential Applications. *Nucleic Acids Res.* **1987**, *15* (3), 1281–1295. https://doi.org/10.1093/nar/15.3.1281.
(32) Calderone, T. L.; Stevens, R. D.; Oas, T. G. High-Level Misincorporation of Lysine for Arginine at AGA Codons in a Fusion Protein Expressed inEscherichia Coli. *J. Mol. Biol.* **1996**, *262* (4), 407–412. https://doi.org/10.1006/jmbi.1996.0524.
(33) Hatfield, G. W.; Roth, D. A. Optimizing Scaleup Yield for Protein Production: Computationally Optimized DNA Assembly (CODA) and Translation Engineering™. In *Biotechnology Annual Review*; Elsevier, 2007; Vol. 13, pp 27–42. https://doi.org/10.1016/S1387-2656(07)13002-7.
(34) Wakagi, T.; Oshima, T.; Imamura, H.; Matsuzawa, H. Cloning of the Gene for Inorganic Pyrophosphatase from a Thermoacidophilic Archaeon, *Sulfolobus* Sp. Strain 7, and Overproduction of the Enzyme by Coexpression of tRNA for Arginine Rare Codon. *Biosci. Biotechnol. Biochem.* **1998**, *62* (12), 2408–2414. https://doi.org/10.1271/bbb.62.2408.
(35) Tegel, H.; Steen, J.; Konrad, A.; Nikdin, H.; Pettersson, K.; Stenvall, M.; Tourle, S.; Wrethagen, U.; Xu, L.; Yderland, L.; Uhlén, M.; Hober, S.; Ottosson, J. High-throughput Protein Production – Lessons from Scaling up from 10 to 288 Recombinant Proteins per Week. *Biotechnol. J.* **2009**, *4* (1), 51–57. https://doi.org/10.1002/biot.200800183.
(36) Pickart, C. M.; Raasi, S. Controlled Synthesis of Polyubiquitin Chains. In *Methods in Enzymology*; Elsevier, 2005; Vol. 399, pp 21–36. https://doi.org/10.1016/S0076-6879(05)99002-2.
(37) Chen, Z.; Pickart, C. M. A 25-Kilodalton Ubiquitin Carrier Protein (E2) Catalyzes Multi-Ubiquitin Chain Synthesis via Lysine 48 of Ubiquitin. *J. Biol. Chem.* **1990**, *265* (35), 21835–21842.
(38) Zhou, Y.; Xie, Q.; Wang, H.; Sun, H. Chemical Approaches for the Preparation of Ubiquitinated Proteins via Natural Linkages. *J. Pept. Sci.* **2022**, *28* (3), e3367. https://doi.org/10.1002/psc.3367.

(39) Sui, X.; Wang, Y.; Du, Y.-X.; Liang, L.-J.; Zheng, Q.; Li, Y.-M.; Liu, L. Development and Application of Ubiquitin-Based Chemical Probes. *Chem. Sci.* **2020**, *11* (47), 12633–12646. https://doi.org/10.1039/D0SC03295F.
(40) Pellois, J.; Muir, T. W. A Ligation and Photorelease Strategy for the Temporal and Spatial Control of Protein Function in Living Cells. *Angew. Chem. Int. Ed.* **2005**, *44* (35), 5713–5717. https://doi.org/10.1002/anie.200501244.
(41) Chatterjee, C.; McGinty, R. K.; Pellois, J.; Muir, T. W. Auxiliary-Mediated Site-Specific Peptide Ubiquitylation. *Angew. Chem. Int. Ed.* **2007**, *46* (16), 2814–2818. https://doi.org/10.1002/anie.200605155.
(42) McGinty, R. K.; Kim, J.; Chatterjee, C.; Roeder, R. G.; Muir, T. W. Chemically Ubiquitylated Histone H2B Stimulates hDot1L-Mediated Intranucleosomal Methylation. *Nature* **2008**, *453* (7196), 812–816. https://doi.org/10.1038/nature06906.
(43) Weller, C. E.; Huang, W.; Chatterjee, C. Facile Synthesis of Native and Protease-Resistant Ubiquitylated Peptides. *ChemBioChem* **2014**, *15* (9), 1263–1267. https://doi.org/10.1002/cbic.201402135.
(44) Weller, C. E.; Dhall, A.; Ding, F.; Linares, E.; Whedon, S. D.; Senger, N. A.; Tyson, E. L.; Bagert, J. D.; Li, X.; Augusto, O.; Chatterjee, C. Aromatic Thiol-Mediated Cleavage of N–O Bonds Enables Chemical Ubiquitylation of Folded Proteins. *Nat. Commun.* **2016**, *7* (1), 12979. https://doi.org/10.1038/ncomms12979.
(45) Pan, M.; Zheng, Q.; Ding, S.; Zhang, L.; Qu, Q.; Wang, T.; Hong, D.; Ren, Y.; Liang, L.; Chen, C.; Mei, Z.; Liu, L. Chemical Protein Synthesis Enabled Mechanistic Studies on the Molecular Recognition of K27-linked Ubiquitin Chains. *Angew. Chem. Int. Ed.* **2019**, *58* (9), 2627–2631. https://doi.org/10.1002/anie.201810814.
(46) Gao, S.; Pan, M.; Zheng, Y.; Huang, Y.; Zheng, Q.; Sun, D.; Lu, L.; Tan, X.; Tan, X.; Lan, H.; Wang, J.; Wang, T.; Wang, J.; Liu, L. Monomer/Oligomer Quasi-Racemic Protein Crystallography. *J. Am. Chem. Soc.* **2016**, *138* (43), 14497–14502. https://doi.org/10.1021/jacs.6b09545.
(47) Pan, M.; Gao, S.; Zheng, Y.; Tan, X.; Lan, H.; Tan, X.; Sun, D.; Lu, L.; Wang, T.; Zheng, Q.; Huang, Y.; Wang, J.; Liu, L. Quasi-Racemic X-Ray Structures of K27-Linked Ubiquitin Chains Prepared by Total Chemical Synthesis. *J. Am. Chem. Soc.* **2016**, *138* (23), 7429–7435. https://doi.org/10.1021/jacs.6b04031.
(48) Pan, M.; Zheng, Q.; Gao, S.; Qu, Q.; Yu, Y.; Wu, M.; Lan, H.; Li, Y.; Liu, S.; Li, J.; Sun, D.; Lu, L.; Wang, T.; Zhang, W.; Wang, J.; Li, Y.; Hu, H.-G.; Tian, C.; Liu, L. Chemical Synthesis of Structurally Defined Phosphorylated Ubiquitins Suggests Impaired Parkin Activation by Phosphorylated Ubiquitins with a Non-Phosphorylated Distal Unit. *CCS Chem.* **2019**, *1* (5), 476–489. https://doi.org/10.31635/ccschem.019.20190001.
(49) Kumar, K. S. A.; Bavikar, S. N.; Spasser, L.; Moyal, T.; Ohayon, S.; Brik, A. Total Chemical Synthesis of a 304 Amino Acid K48-Linked Tetraubiquitin Protein. *Angew. Chem. Int. Ed.* **2011**, *50* (27), 6137–6141. https://doi.org/10.1002/anie.201101920.
(50) Wan, Q.; Danishefsky, S. J. Free-Radical-Based, Specific Desulfurization of Cysteine: A Powerful Advance in the Synthesis of Polypeptides and Glycopolypeptides. *Angew. Chem. Int. Ed.* **2007**, *46* (48), 9248–9252. https://doi.org/10.1002/anie.200704195.
(51) Haj-Yahya, M.; Ajish Kumar, K. S.; Erlich, L. A.; Brik, A. Protecting Group Variations of Δ-mercaptolysine Useful in Chemical Ubiquitylation. *Pept. Sci.* **2010**, *94* (4), 504–510. https://doi.org/10.1002/bip.21384.
(52) Ajish Kumar, K. S.; Haj-Yahya, M.; Olschewski, D.; Lashuel, H. A.; Brik, A. Highly Efficient and Chemoselective Peptide Ubiquitylation. *Angew. Chem. Int. Ed.* **2009**, *48* (43), 8090–8094. https://doi.org/10.1002/anie.200902936.
(53) Kumar, K. S. A.; Spasser, L.; Erlich, L. A.; Bavikar, S. N.; Brik, A. Total Chemical Synthesis of Di-ubiquitin Chains. *Angew. Chem. Int. Ed.* **2010**, *49* (48), 9126–9131. https://doi.org/10.1002/anie.201003763.
(54) Hejjaoui, M.; Haj-Yahya, M.; Kumar, K. S. A.; Brik, A.; Lashuel, H. A. Towards Elucidation of the Role of Ubiquitination in the Pathogenesis of Parkinson's Disease with Semisynthetic

Ubiquitinated α-Synuclein. *Angew. Chem. Int. Ed.* **2011**, *50* (2), 405–409. https://doi.org/10.1002/anie.201005546.

(55) Bavikar, S. N.; Spasser, L.; Haj-Yahya, M.; Karthikeyan, S. V.; Moyal, T.; Ajish Kumar, K. S.; Brik, A. Chemical Synthesis of Ubiquitinated Peptides with Varying Lengths and Types of Ubiquitin Chains to Explore the Activity of Deubiquitinases. *Angew. Chem. Int. Ed.* **2012**, *51* (3), 758–763. https://doi.org/10.1002/anie.201106430.

(56) Haj-Yahya, M.; Eltarteer, N.; Ohayon, S.; Shema, E.; Kotler, E.; Oren, M.; Brik, A. N-Methylation of Isopeptide Bond as a Strategy to Resist Deubiquitinases. *Angew. Chem. Int. Ed.* **2012**, *51* (46), 11535–11539. https://doi.org/10.1002/anie.201205771.

(57) Kumar, K. S. A.; Spasser, L.; Ohayon, S.; Erlich, L. A.; Brik, A. Expeditious Chemical Synthesis of Ubiquitinated Peptides Employing Orthogonal Protection and Native Chemical Ligation. *Bioconjug. Chem.* **2011**, *22* (2), 137–143. https://doi.org/10.1021/bc1004735.

(58) Sun, H.; Meledin, R.; Mali, S. M.; Brik, A. Total Chemical Synthesis of Ester-Linked Ubiquitinated Proteins Unravels Their Behavior with Deubiquitinases. *Chem. Sci.* **2018**, *9* (6), 1661–1665. https://doi.org/10.1039/C7SC04518B.

(59) Qu, Q.; Pan, M.; Gao, S.; Zheng, Q.; Yu, Y.; Su, J.; Li, X.; Hu, H. A Highly Efficient Synthesis of Polyubiquitin Chains. *Adv. Sci.* **2018**, *5* (7), 1800234. https://doi.org/10.1002/advs.201800234.

(60) Tang, S.; Liang, L.; Si, Y.; Gao, S.; Wang, J.; Liang, J.; Mei, Z.; Zheng, J.; Liu, L. Practical Chemical Synthesis of Atypical Ubiquitin Chains by Using an Isopeptide-Linked Ub Isomer. *Angew. Chem. Int. Ed.* **2017**, *56* (43), 13333–13337. https://doi.org/10.1002/anie.201708067.

(61) Valkevich, E. M.; Guenette, R. G.; Sanchez, N. A.; Chen, Y.; Ge, Y.; Strieter, E. R. Forging Isopeptide Bonds Using Thiol–Ene Chemistry: Site-Specific Coupling of Ubiquitin Molecules for Studying the Activity of Isopeptidases. *J. Am. Chem. Soc.* **2012**, *134* (16), 6916–6919. https://doi.org/10.1021/ja300500a.

(62) Hoyle, C. E.; Bowman, C. N. Thiol–Ene Click Chemistry. *Angew. Chem. Int. Ed.* **2010**, *49* (9), 1540–1573. https://doi.org/10.1002/anie.200903924.

(63) Posner, T. Beiträge Zur Kenntniss Der Ungesättigten Verbindungen. II. Ueber Die Addition von Mercaptanen an Ungesättigte Kohlenwasserstoffe., 1905.

(64) Chong, S.; Montello, G. E.; Zhang, A.; Cantor, E. J.; Liao, W.; Xu, M.-Q.; Benner, J. Utilizing the C-Terminal Cleavage Activity of a Protein Splicing Element to Purify Recombinant Proteins in a Single Chromatographic Step. *Nucleic Acids Res.* **1998**, *26* (22), 5109–5115. https://doi.org/10.1093/nar/26.22.5109.

(65) Matveenko, M.; Hackl, S.; Becker, C. F. W. Utility of the Phenacyl Protecting Group in Traceless Protein Semisynthesis through Ligation–Desulfurization Chemistry. *ChemistryOpen* **2018**, *7* (1), 106–110. https://doi.org/10.1002/open.201700180.

(66) Trang, V. H.; Valkevich, E. M.; Minami, S.; Chen, Y.; Ge, Y.; Strieter, E. R. Nonenzymatic Polymerization of Ubiquitin: Single-Step Synthesis and Isolation of Discrete Ubiquitin Oligomers. *Angew. Chem. Int. Ed.* **2012**, *51* (52), 13085–13088. https://doi.org/10.1002/anie.201207171.

7. Appendix

Figure A 1 Plasmid encoding for Ub^{wt} – intein fusion construct.

UbK11C_for: TCT GAC TTG CAC CAT CAC TC

UbK11C_rev: GTC TTC ACG AAG ATC TGC

Figure A 2 Primer for site directed mutagenesis of Ub^{K11C} fusion construct.

>UbK11C cl1_T7
GAAATAATTTTGTTTAACTTTAAGAAGGAGATATACATATGCAGATCTTCGTGAAGACTCTGACTGGTTGC
ACCATCACTCTCGAAGTGGAGCCGAGTGACACCATTGAGAATGTCAAGGCAAAGATCCAAGACAAGGAAGG
CATCCCTCCTGACCAGCAGAGGTTGATCTTTGCTGGGAAACAGCTGGAAGATGGACGCACCCTGTCTGACT
ACAACATCCAGAAAGAGTCCACCCTGCACCTGGTACTCCGTCTCAGAGGTGGTTGCATCACGGGAGATGCA
CTAGTTGCCCTACCCGAGGGCGAGTCGGTACGCATCGCCGACATCGTGCCGGGTGCGCGGCCCAACAGTGA
CAACGCCATCGACCTGAAAGTCCTTGACCGGCATGGCAATCCCGTGCTCGCCGACCGGCTGTTCCACTCCG
GCGAGCATCCGGTGTACACGGTGCGTACGGTCGAAGGTCTGCGTGTGACGGGCACCGCGAACCACCCGTTG
TTGTGTTTGGTCGACGTCGCCGGGGTGCCGACCCTGCTGTGGAAGCTGATCGACGAAATCAAGCCGGGCGA
TTACGCGGTGATTCAACGCAGCGCATTCAGCGTCGACTGTGCAGGTTTTGCCCGCGGGAAACCCGAATTTG
CGCCCACAACCTACACAGTCGGCGTCCCTGGACTGGTGCGTTTCTTGGAAGCACACCACCGAGACCCGGAC
GCCCAAGCTATCGCCGACGAGCTGACCGACGGGCGGTTCTACTACGCGAAAGTCGCCAGTGTCACCGACGC
CGGCGTGCAGCCGGTGTATAGCCTTCGTGTCGACACGGCAGACCACGCGTTTATCACGAACGGGTTCGTCA
GCCACGCTACTGGCCTCACCGGAATTCACCACCACCACCACCACCACTCCGGTCTGAACTCAGGCCTCACG
ACAAATCCTGGTGTATCCGCTTGGCAGGTCAACACAGCTTATACTGCGGGACAATTGGTCACATATAACGG
CAAGACGTATAAATGTTTGCAGCCCCACACCTCCTTGGCAGGATGGGAACCATCCAACGTTCCTGCCTTGT
GGCAGCTTCAATGACTGCAGGAAGGGGATCCGGCTGCTAACAAAGCC
Figure A 3 Sequencing results of clone 1, forward.

>UbK11C cl1_T7term
NNTTTCGGGCTTTGTTAGCAGCCGGATCCCCTTCCTGCAGTCATTGAAGCTGCCACAAGGCAGGAACGTTG
GATGGTTCCCATCCTGCCAAGGAGGTGTGGGGCTGCAAACATTTATACGTCTTGCCGTTATATGTGACCAA
TTGTCCCGCAGTATAAGCTGTGTTGACCTGCCAAGCGGATACACCAGGATTTGTCGTGAGGCCTGAGTTCA
GACCGGAGTGGTGGTGGTGGTGGTGGTGAATTCCGGTGAGGCCAGTAGCGTGGCTGACGAACCCGTTCGTG
ATAAACGCGTGGTCTGCCGTGTCGACACGAAGGCTATACACCGGCTGCACGCCGGCGTCGGTGACACTGGC
GACTTTCGCGTAGTAGAACCGCCCGTCGGTCAGCTCGTCGGCGATAGCTTGGGCGTCCGGGTCTCGGTGGT
GTGCTTCCAAGAAACGCACCAGTCCAGGGACGCCGACTGTGTAGGTTGTGGGCGCAAATTCGGGTTTCCCG
CGGGCAAAACCTGCACAGTCGACGCTGAATGCGCTGCGTTGAATCACCGCGTAATCGCCCGGCTTGATTTC
GTCGATCAGCTTCCACAGCAGGGTCGGCACCCCGGCGACGTCGACCAAACACAACAACGGGTGGTTCGCGG
TGCCCGTCACACGCAGACCTTCGACCGTACGCACCGTGTACACCGGATGCTCGCCGGAGTGGAACAGCCGG
TCGGCGAGCACGGGATTGCCATGCCGGTCAAGGACTTTCAGGTCGATGGCGTTGTCACTGTTGGGCCGCGC
ACCCGGCACGATGTCGGCGATGCGTACCGACTCGCCCTCGGGTAGGGCAACTAGTGCATCTCCCGTGATGC
AACCACCTCTGAGACGGAGTACCAGGTGCAGGGTGGACTCTTTCTGGATGTTGTAGTCAGACAGGGTGCGT
CCATCTTCCAGCTGTTTCCCAGCAAAGATCAACCTCTGCTGGTCAGGAGGGATGCCTTCCTTGTCTTGGAT
CTTTGCCTTGACATTCTCAATGGTGTCACTCGGCTCCACTTCGAGAGTGATGGTGCAACCAGTCAGAGTCT
TCMCGAAGAATCTGCATATGTWWWTCYCCTTCTTAAAGTTAAACAAAATTWTTT
Figure A 4 Sequencing results of clone 1, reverse.

>UbK11C cl2_T7
AAATAATTTTGTTTAACTTTAAGAAGGAGATATACATATGCAGATCTTCGTGAAGACTCTGACTGGTTGCA
CCATCACTCTCGAAGTGGAGCCGAGTGACACCATTGAGAATGTCAAGGCAAAGATCCAAGACAAGGAAGGC
ATCCCTCCTGACCAGCAGAGGTTGATCTTTGCTGGGAAACAGCTGGAAGATGGACGCACCCTGTCTGACTA
CAACWTCCAGAAAGAGTCCACCCTGCWCCTGGTACTCCGTCTCAGAGGTGGTTGCATCACGGGAGATGCAC
TAGTTGCCCTACCCGAGGGCGAGTCGGTACGCATCGCCGACATCGTGCCGGGTGCGCGGCCCAACAGTGAC
AACGCCATCGACCTGAAAGTCCTTGACCGGCATGGCAATCCCGTGCTCGCCGACCGGCTGTTCCACTCCGG
CGAGCATCCGGTGTACACGGTGCGTACGGTCGAAGGTCTGCGTGTGACGGGCACCGCGAACCACCCGTTGT
TGTGTTTGGTCGACGTCGCCGGGGTGCCGACCCTGCTGTGGAAGCTGATCGACGAAATCAWGCCGGGCGAT
TACRCGGTGATTCAACGCAGCGCATTCAGCGTCGACTGTGCAGGTTTTGCCCGCGGGAAACCCGAATTTGC
GCCCACAACCTACACAGTCGGCGTCCCTGGACTGGTGCGTTTCTTGGAAGCACACCACCGAGACCCGGACG
CCCAAGCTATCGCCRACGAGCTGACCGACGGGCGGTTCTACTACGCGAAAGTCGCCAGTGTCACCGACGCC
GGCGTGCAGCCGGTGTATAGCCTTCGTGTCGACACGGCAGACCACGCGTTTATCACGAACGGGTTCGTCAG
CCACGCTACTGGCCTCACCGGAATTCACCACCACCACCACCACCACTCCGGTCTGAACTCAGGCCTCACGA
CAAATCCTGGTGTATCCGCTTGGCAGGTCAACACAGCTTATACTGCGGGACAATTGGTCACATATAACGGC
AAGACGTATAAATGTTTGCAGCCCCACACCTCCTTGGCAGGATGGGAACCATCCAACGTTCCTGCCTTGTG
GCAGCTTCAATGACTGCAGGAAGGGGATCCGGCTGCTAT
Figure A 5 Sequencing results of clone 2, forward.

>UbK11C cl2_T7term
TTTCGGGCTTTGTTAGCAGCCGGATCCCCTTCCTGCAGTCATTGAAGCTGCCACAAGGCAGGAACGTTGGA
TGGTTCCCATCCTGCCAAGGAGGTGTGGGGCTGCAAACATTTATACGTCTTGCCGTTATATGTGACCAATT
GTCCCGCAGTATAAGCTGTGTTGACCTGCCAAGCGGATACACCAGGATTTGTCGTGAGGCCTGAGTTCAGA
CCGGAGTGGTGGTGGTGGTGGTGGTGAATTCCGGTGAGGCCAGTAGCGTGGCTGACGAACCCGTTCGTGAT
AAACGCGTGGTCTGCCGTGTCGACACGAAGGCTATACACCGGCTGCACGCCGGCGTCGGTGACACTGGCGA
CTTTCGCGTAGTAGAACCGCCCGTCGGTCAGCTCGTCGGCGATAGCTTGGGCGTCCGGGTCTCGGTGGTGT
GCTTCCAAGAAACGCACCAGTCCAGGGACGCCGACTGTGTAGGTTGTGGGCGCAAATTCGGGTTTCCCGCG
GGCAAAACCTGCACAGTCGACGCTGAATGCGCTGCGTTGAATCACCGCGTAATCGCCCGGCTTGATTTCGT
CGATCAGCTTCCACAGCAGGGTCGGCACCCCGGCGACGTCGACCAAACACAACAACGGGTGGTTCGCGGTG
CCCGTCACACGCAGACCTTCGACCGTACGCACCGTGTACACCGGATGCTCGCCGGAGTGGAACAGCCGGTC
GGCGAGCACGGGATTGCCATGCCGGTCAAGGACTTTCAGGTCGATGGCGTTGTCACTGTTGGGCCGCGCAC
CCGGCACGATGTCGGCGATGCGTACCGACTCGCCCTCGGGTAGGGCAACTAGTGCATCTCCCGTGATGCAA
CCACCTCTGAGACGGAGTACCAGGTGCAGGGTGGACTCTTTCTGGATGTTGTAGTCAGACAGGGTGCGTCC
ATCTTCCAGCTGTTTCCCAGCAAAGATCAACCTCTGCTGGTCAGGAGGGATGCCTTCCTTGTCTTGGATCT
TTGCCTTGACATTCTCAATGGTGTCACTCGGCTCCACTTCGAGAGTGATGGTGCAACCAGTCAAAAGTCTT
CCNAAAGATCTGCATATGWATATCTCCTTCTTAAAGTTAAACCAAAATTATT
Figure A 6 Sequencing results of clone 2, reverse.

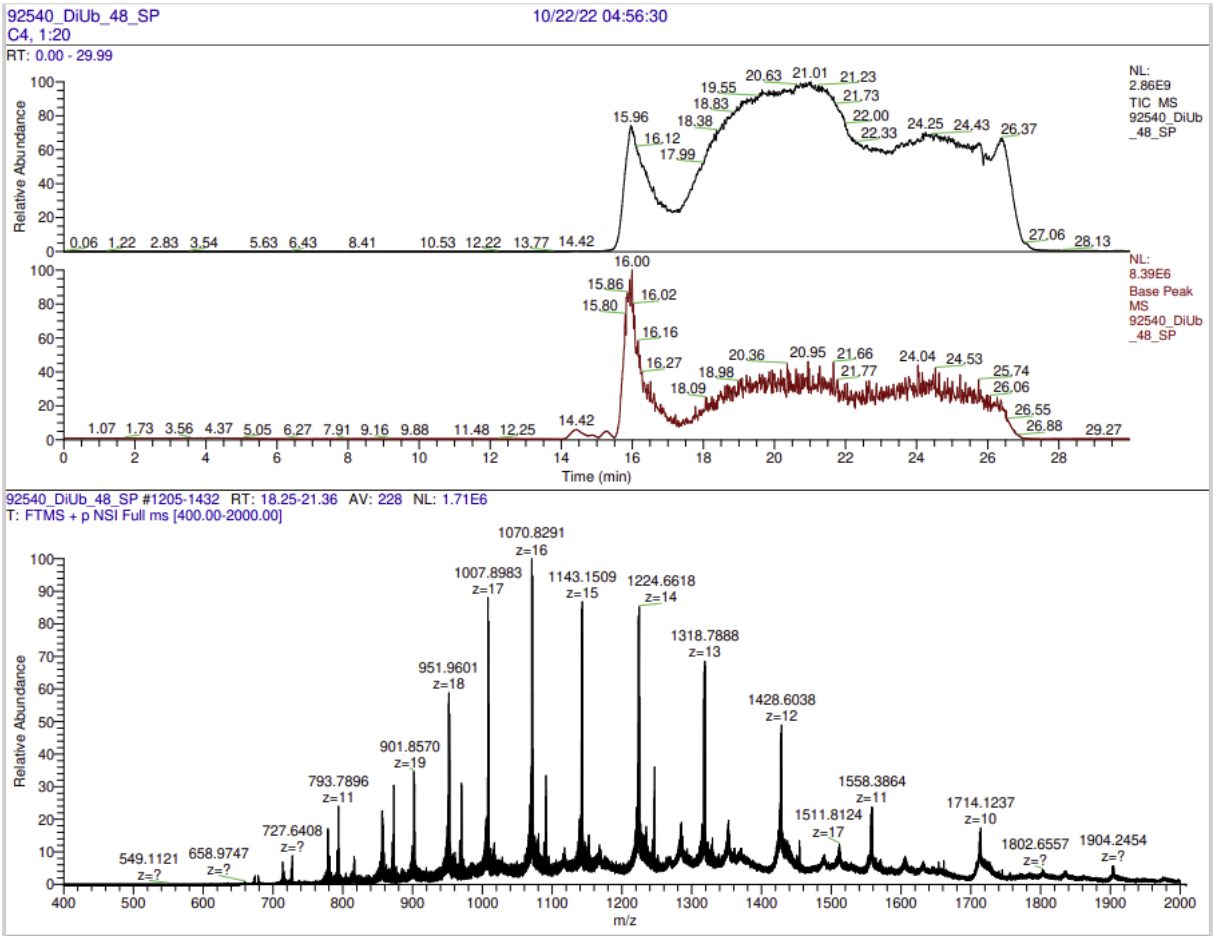

Figure A 7 HR LC-MS and mass spectrum of the by-product during PAc deprotection.

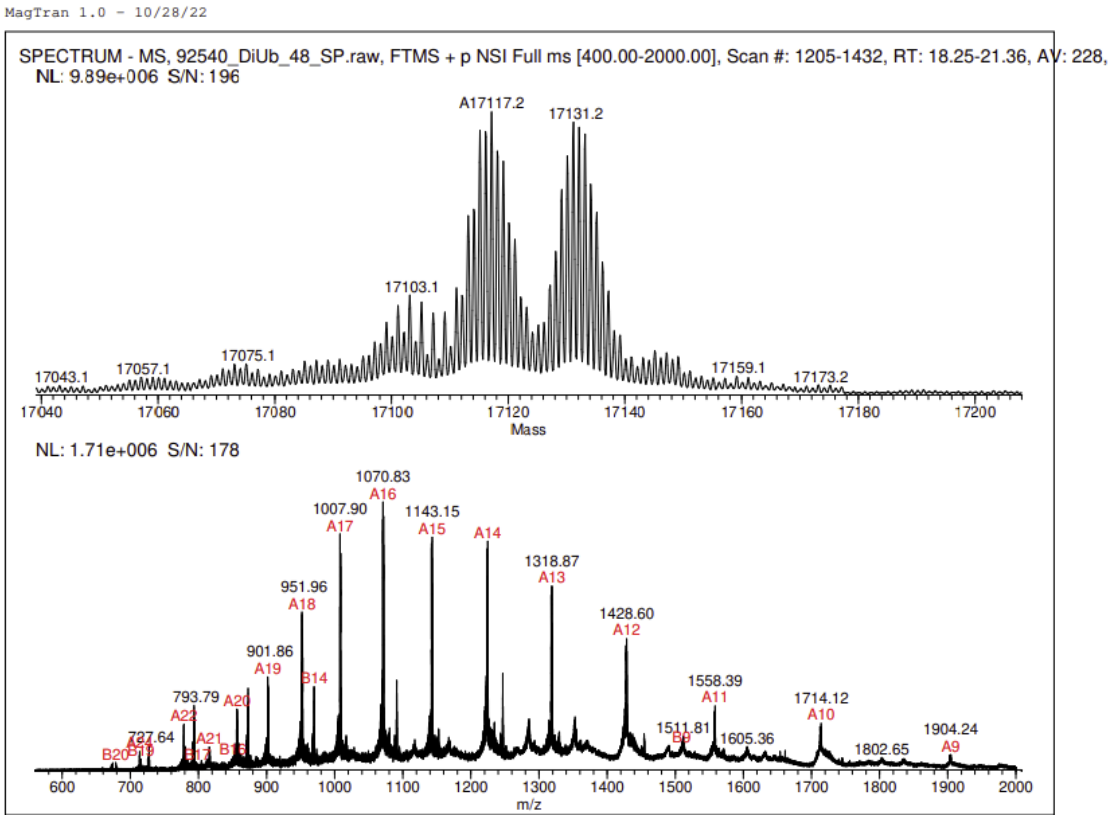

Figure A 8 HR mass spectrum and deconvoluted mass spectrum of the by-product during PAc deprotection.

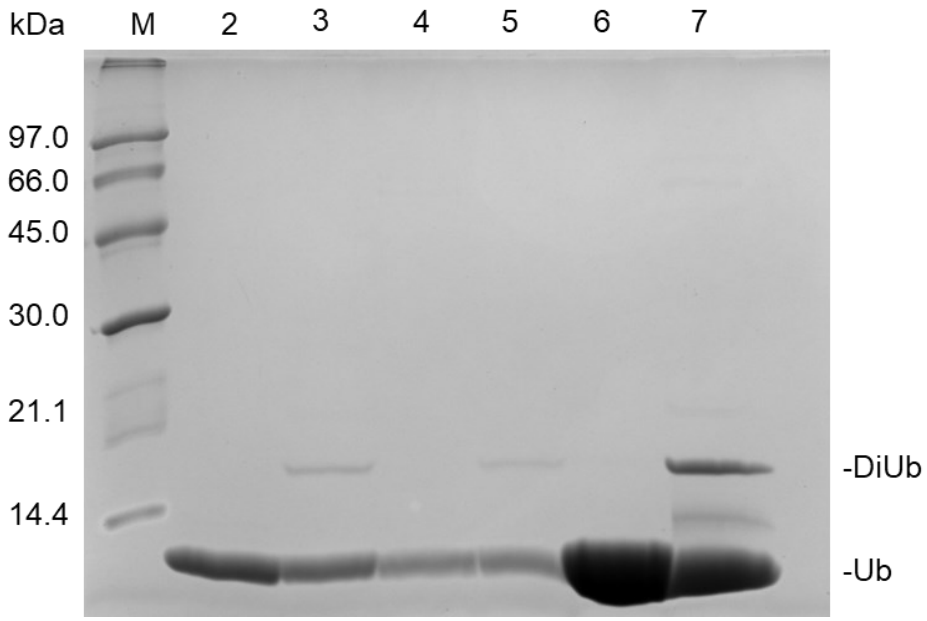

Figure A 9 SDS PAGE of TECs. Lane 1 Marker, Lane 2 TEC $DiUb^{wt\text{-}K11C}NHNH_2$ t_0, Lane 3 TEC $DiUb^{wt\text{-}K11C}NHNH2$ t_1, Lane 4 TEC $DiUb^{wt\text{-}K11C}NHNH_2$ t_0, Lane 5 TEC $DiUb^{wt\text{-}K11C}NHNH_2$ t_1, Lane 6 $Ub^{wt}AA$ (~8.500 kDa), Lane 7 $Ub^{K11C}NHNH_2$.

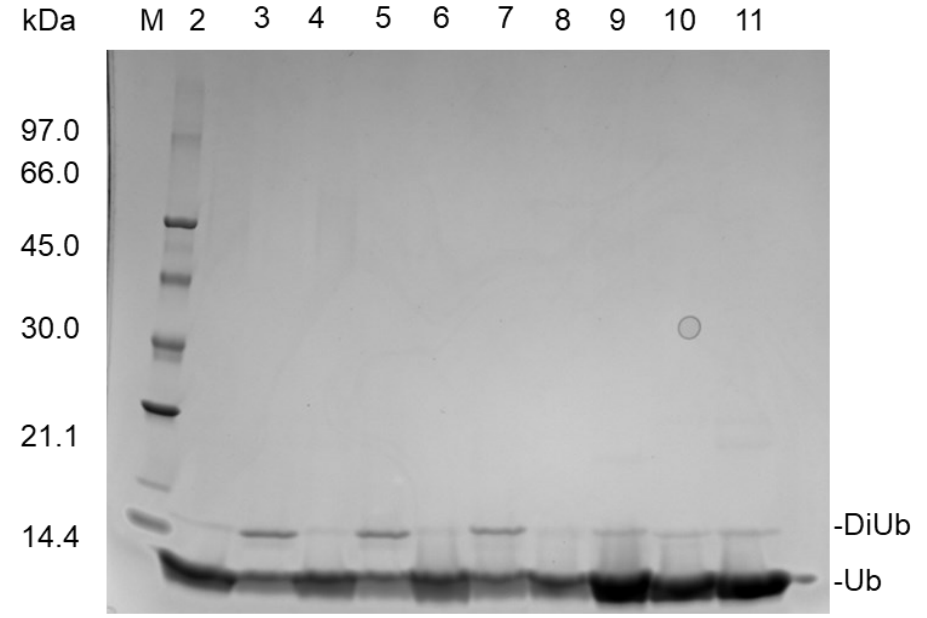

Figure A 10 SDS PAGE of TECs. Lane 1 Marker, Lane 2 TEC $DiUb^{K63C\text{-}K29C}NHNH_2$ t_0, Lane 3 TEC $DiUb^{K63C\text{-}K29C}NHNH_2$ t_1, Lane 4 TEC $DiUb^{K63C\text{-}K29C}NHNH_2$ t_0, Lane 5 TEC $DiUb^{K63C\text{-}K29C}NHNH_2$ t_1, Lane 6 TEC $DiUb_{K29C\text{-}K63C}NHNH_2$ t_0, Lane 7 $DiUb^{K29C\text{-}K63C}NHNH_2$ t_1, Lane 8 $Ub^{K63C}{}_{pac}AA$ (~8.500 kDa).

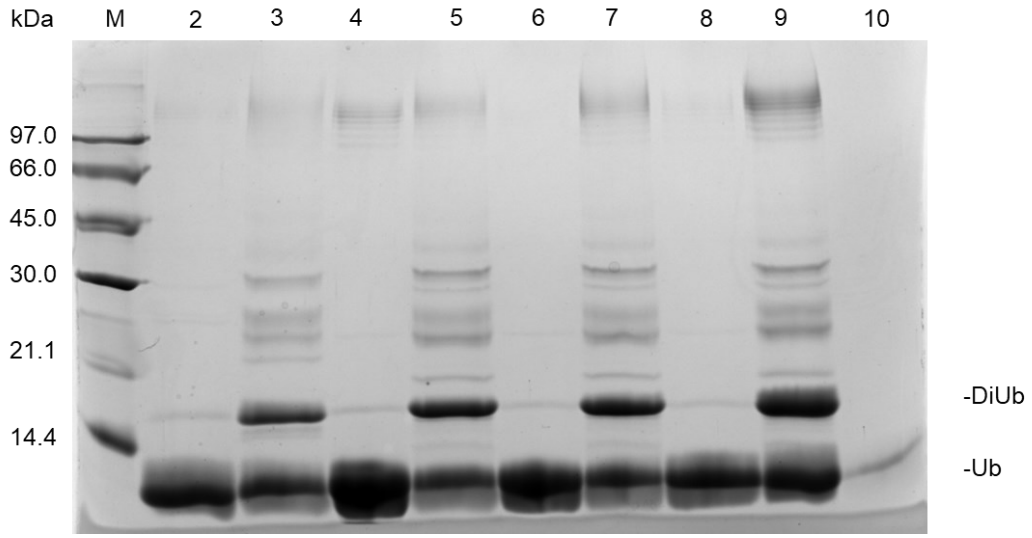

Figure A 11 SDS PAGE of TECs. Lane 1 Marker, Lane 2 TEC $DiUb^{wt\text{-}K29C}NHNH_2$ t_0, Lane 3 TEC $DiUb^{wt\text{-}K29C}NHNH_2$ t_1, Lane 4 TEC $DiUb^{wt\text{-}K48C}NHNH_2$ t_0, Lane 5 TEC $DiUb^{wt\text{-}K48C}NHNH_2$ t_1, Lane 6 TEC $DiUb^{wt\text{-}K48C}NHNH_2$ t_0, Lane 7 $DiUb^{wt\text{-}K48C}NHNH_2$ t_1, Lane 8 TEC $DiUb^{wt\text{-}K48C}NHNH_2$ t_0, Lane 9 $DiUb^{wt\text{-}K48C}NHNH_2$ t_1 Lane 10 $Ub^{wt}AA$ (~8.500 kDa).

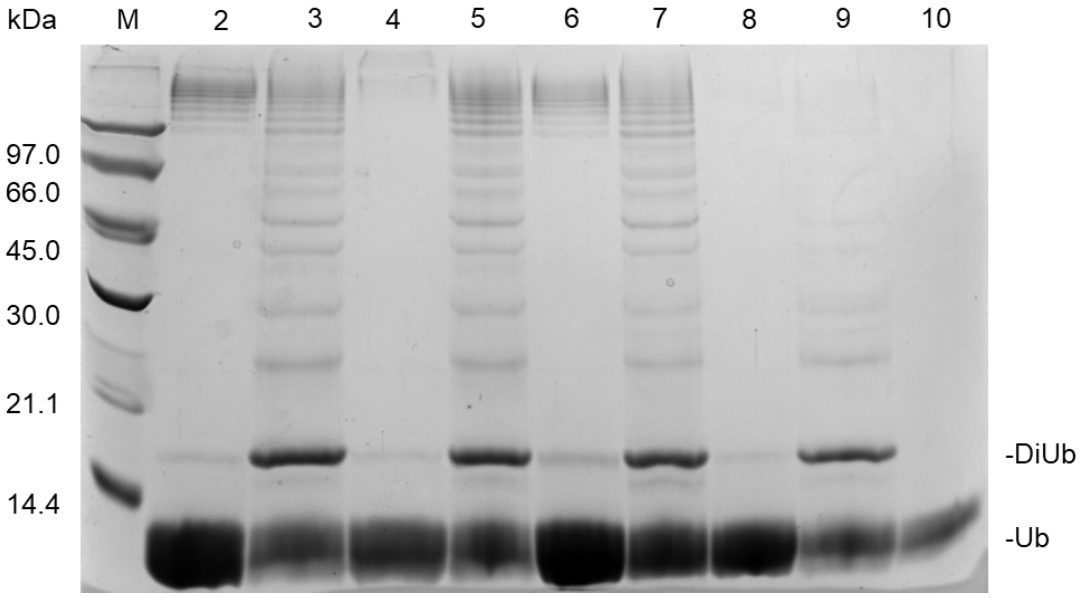

Figure A 12 SDS PAGE of TECs. Lane 1 Marker, Lane 2 TEC $DiUb^{wt\text{-}K63C}NHNH_2$ t_0, Lane 3 TEC $DiUb^{wt\text{-}K63C}NHNH_2$ t_1, Lane 4 TEC $DiUb^{wt\text{-}K63C}NHNH_2$ t_0, Lane 5 TEC $DiUb^{wt\text{-}K63C}NHNH_2$ t_1, Lane 6 TEC $DiUb^{K29C\text{-}K63C}NHNH_2$ t_0, Lane 7 $DiUb^{K29C\text{-}K63C}NHNH_2$ t_1, Lane 8 TEC $DiUb^{K29C\text{-}K63C}NHNH_2$ t_0, Lane 9 $DiUb^{K29C\text{-}K63C}NHNH_2$ t_1 Lane 10 $Ub^{wt}AA$ (~8.500 kDa).

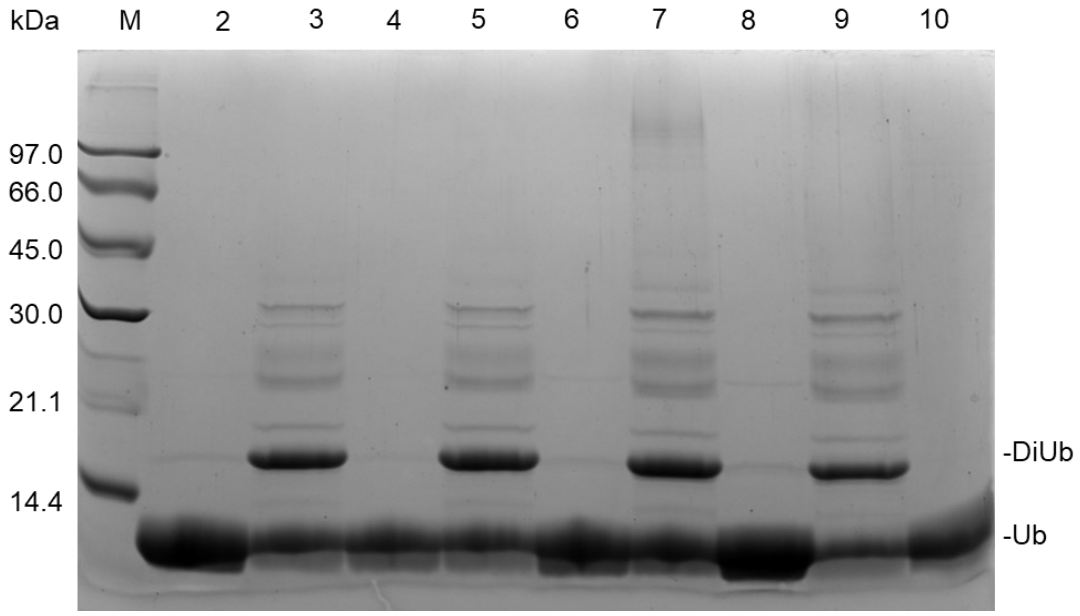

Figure A 13 SDS PAGE of TECs. Lane 1 Marker, Lane 2 TEC $DiUb^{wt\text{-}K48C}NHNH_2$ t_0, Lane 3 TEC $DiUb^{wt\text{-}K48C}NHNH_2$ t_1, Lane 4 TEC $DiUb^{wt\text{-}K48C}NHNH_2$ t_0, Lane 5 TEC $DiUb^{wt\text{-}K48C}NHNH_2$ t_1, Lane 6 TEC $DiUb^{K48C\text{-}K48C}NHNH_2$ t_0, Lane 7 $DiUb^{K48C\text{-}K48C}NHNH_2$ t_1, Lane 8 TEC $DiUb^{K48C\text{-}K48C}NHNH_2$ t_0, Lane 9 $DiUb^{K48C\text{-}K48C}NHNH_2$ t_1 Lane 10 $Ub^{wt}AA$ (~8.500 kDa).

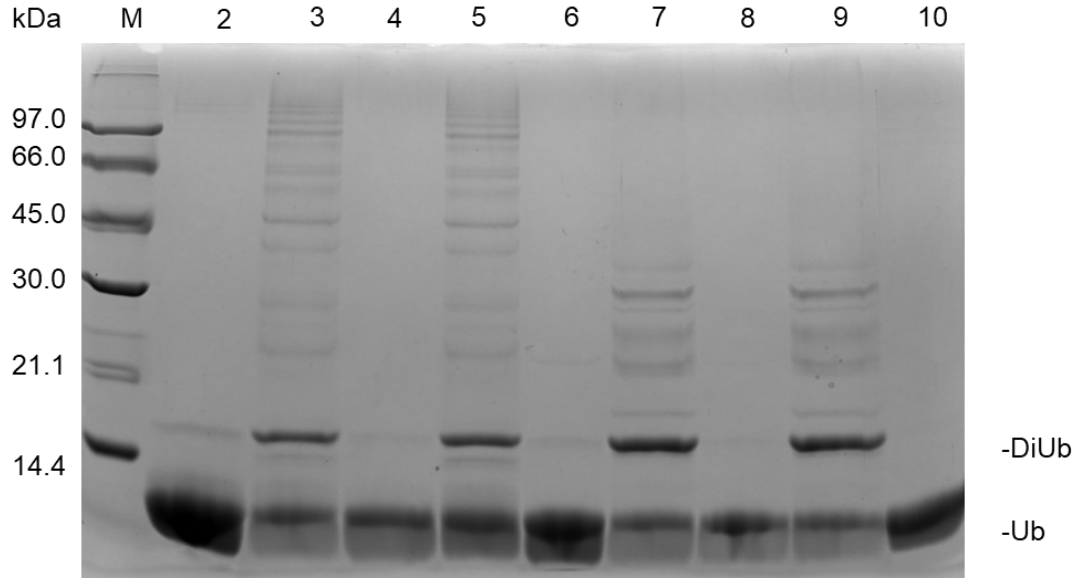

Figure A 14 SDS PAGE of TECs. Lane 1 Marker, Lane 2 TEC $DiUb^{K29C\text{-}K63C}NHNH_2$ t_0, Lane 3 TEC $DiUb^{K29C\text{-}K63C}NHNH_2$ t_1, Lane 4 TEC $DiUb^{K29C\text{-}K63C}NHNH_2$ t_0, Lane 5 TEC $DiUb^{K29C\text{-}K63C}NHNH_2$ t_1, Lane 6 TEC $DiUb^{K48C\text{-}K48C}NHNH_2$ t_0, Lane 7 $DiUb^{K48C\text{-}K48C}NHNH_2$ t_1, Lane 8 TEC $DiUb^{K48C\text{-}K48C}NHNH_2$ t_0, Lane 9 $DiUb^{K48C\text{-}K48C}NHNH_2$ t_1 Lane 10 $Ub^{wt}AA$ (~8.500 kDa).

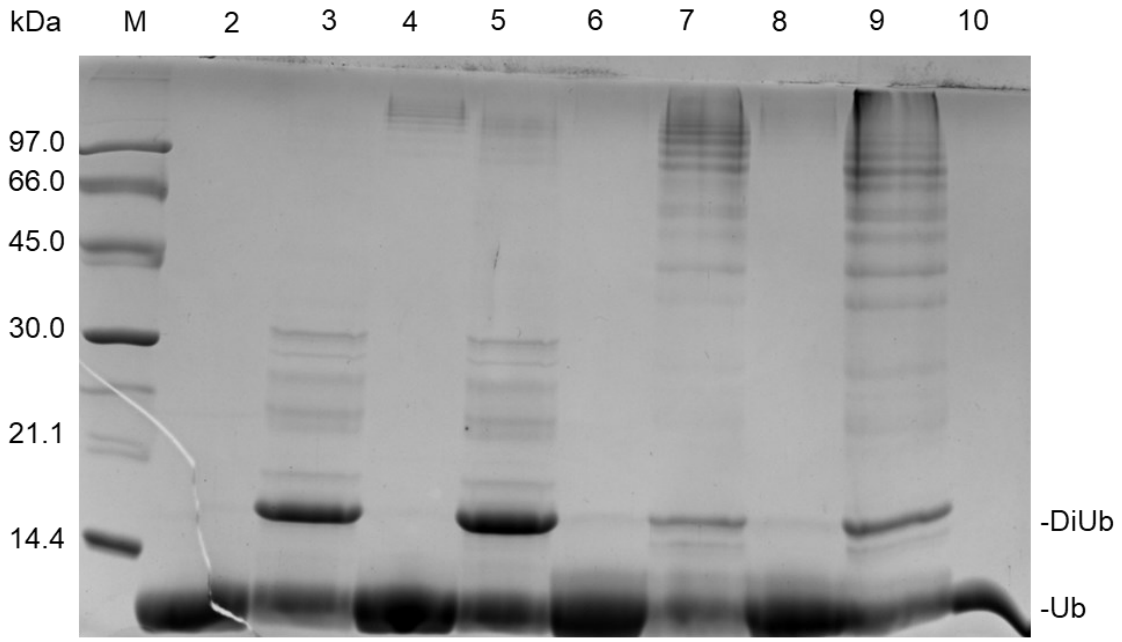

Figure A 15 SDS PAGE of TECs. Lane 1 Marker, Lane 2 TEC $DiUb^{wt\text{-}K48C}NHNH_2$ t_0, Lane 3 TEC $DiUb^{wt\text{-}K48C}NHNH_2$ t_1, Lane 4 TEC $DiUb^{wt\text{-}K48C}NHNH_2$ t_0, Lane 5 TEC $DiUb^{wt\text{-}K48C}NHNH_2$ t_1, Lane 6 TEC $DiUb^{K29C\text{-}K63C}NHNH_2$ t_0, Lane 7 $DiUb^{K29C\text{-}K63C}NHNH_2$ t_1, Lane 8 TEC $DiUb^{K29C\text{-}K63C}NHNH_2$ t_0, Lane 9 $DiUb^{K29C\text{-}K63C}NHNH_2$ t_1 Lane 10 $Ub^{wt}AA$ (~8.500 kDa).

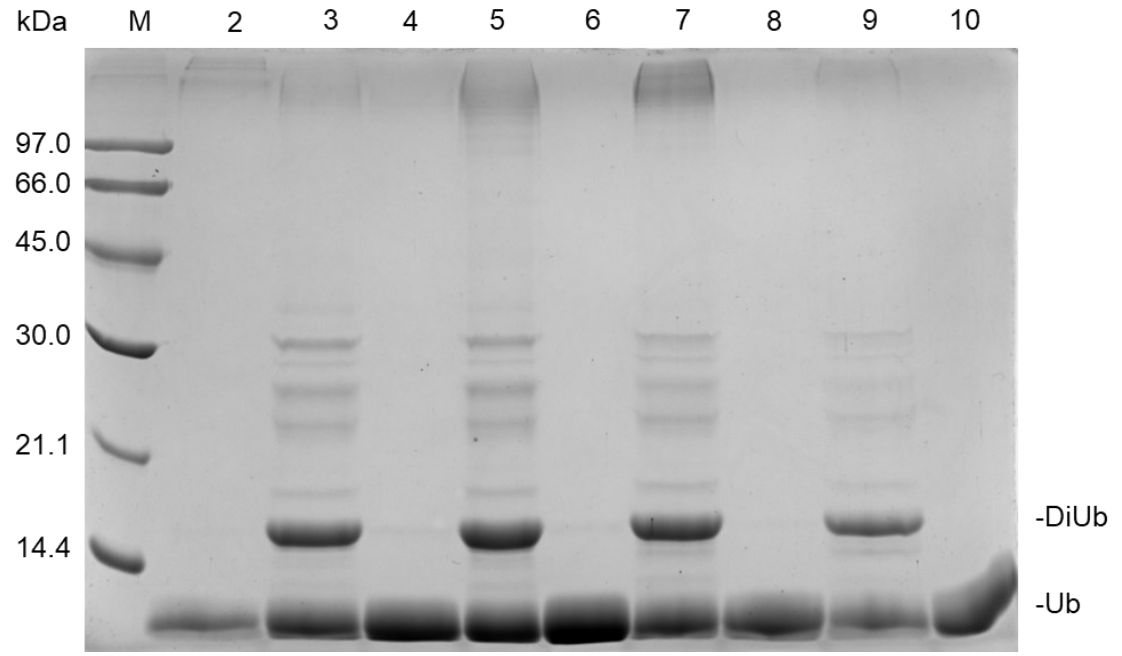

Figure A 16 SDS PAGE of TECs. Lane 1 Marker, Lane 2 TEC $DiUb^{K48C\text{-}K48C}NHNH_2$ t_0, Lane 3 TEC $DiUb^{K48C\text{-}K48C}NHNH_2$ t_1, Lane 4 TEC $DiUb^{K48C\text{-}K48C}NHNH_2$ t_0, Lane 5 TEC $DiUb^{K48C\text{-}K48C}NHNH_2$ t_1, Lane 6 TEC $DiUb^{wt\text{-}K48C}NHNH_2$ t_0, Lane 7 $DiUb^{wt\text{-}K48C}NHNH_2$ t_1, Lane 8 TEC $DiUb^{wt\text{-}K48C}NHNH_2$ t_0, Lane 9 $DiUb^{wt\text{-}K48C}NHNH_2$ t_1 Lane 10 $Ub^{wt}AA$ (~8.500 kDa).

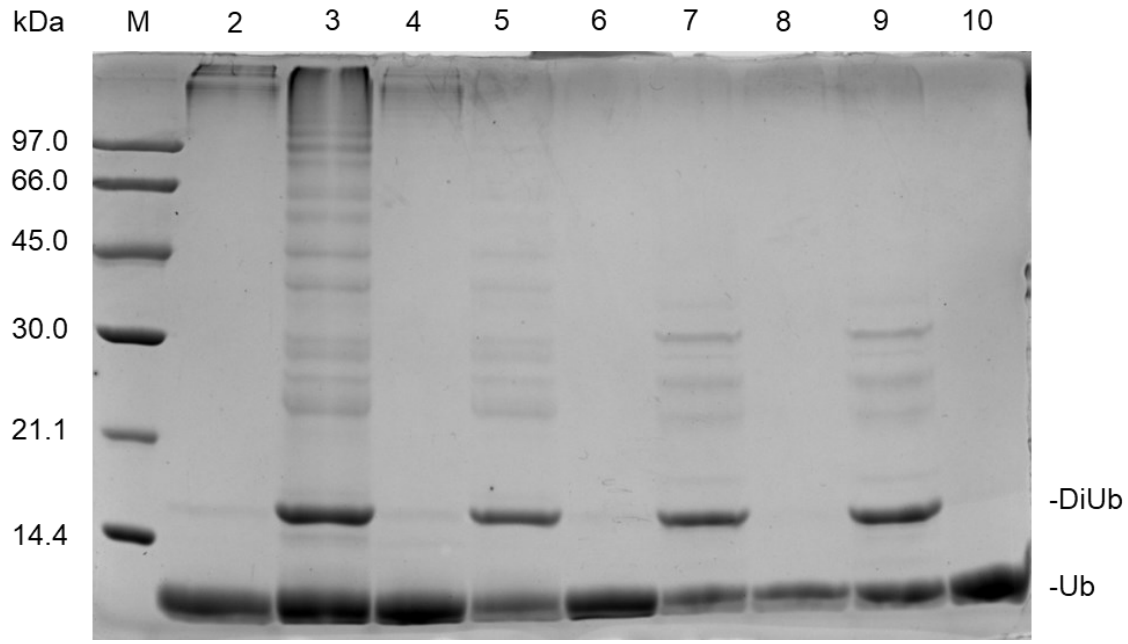

Figure A 17 SDS PAGE of TECs. Lane 1 Marker, Lane 2 TEC $DiUb^{K29C\text{-}K63C}NHNH_2\ t_0$, Lane 3 TEC $DiUb^{K29C\text{-}K63C}NHNH_2\ t_1$, Lane 4 TEC $DiUb^{K29C\text{-}K63C}NHNH_2\ t_0$, Lane 5 TEC $DiUb^{K29C\text{-}K63C}NHNH_2\ t_1$, Lane 6 TEC $DiUb^{K48C\text{-}K48C}NHNH_2\ t_0$, Lane 7 $DiUb^{K48C\text{-}K48C}NHNH_2\ t_1$, Lane 8 TEC $DiUb^{K48C\text{-}K48C}NHNH_2\ t_0$, Lane 9 $DiUb^{K48C\text{-}K48C}NHNH_2\ t_1$ Lane 10 $Ub^{wt}AA$ (~8.500 kDa).